USGS
science for a changing world

Response of Currents and Water Quality to Changes in Dam Operations in Hoover Reservoir, Columbus, Ohio, August 24–28, 2015

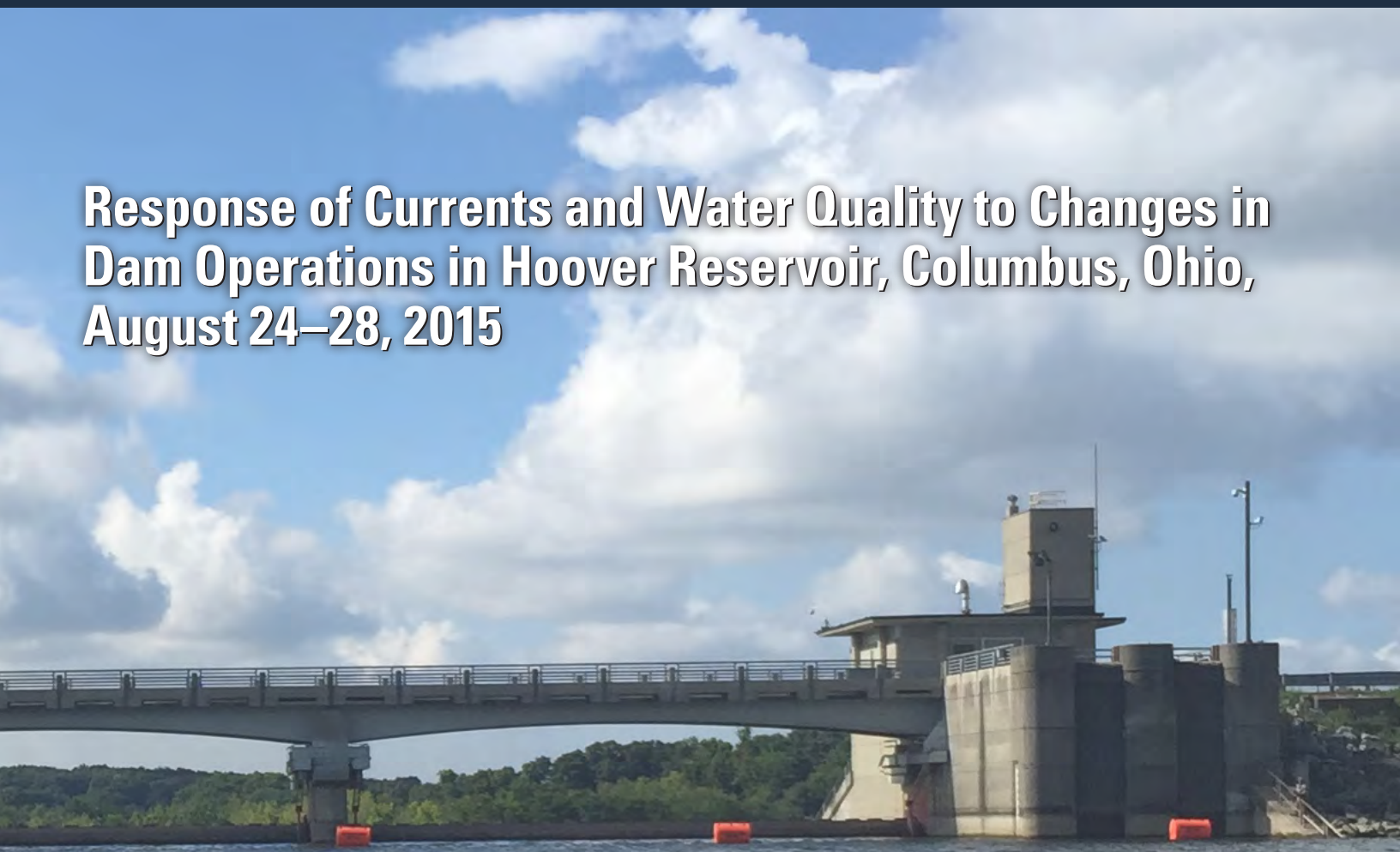

Scientific Investigations Report 2017–5027

U.S. Department of the Interior
U.S. Geological Survey

Cover. Hoover Reservoir Dam, Columbus Ohio, August 25, 2015, taken by Branden L. Vonins, U.S. Geological Survey.

Response of Currents and Water Quality to Changes in Dam Operations in Hoover Reservoir, Columbus, Ohio, August 24–28, 2015

By Branden L. Vonins and P. Ryan Jackson

Scientific Investigations Report 2017–5027

U.S. Department of the Interior
U.S. Geological Survey

U.S. Department of the Interior
RYAN K. ZINKE, Secretary

U.S. Geological Survey
William H. Werkheiser, Acting Director

U.S. Geological Survey, Reston, Virginia: 2017

Suggested citation:
Vonins, B.L., and Jackson, P.R., 2017, Response of currents and water quality to changes in dam operations in Hoover Reservoir, Columbus, Ohio, August 24–28, 2015: U.S. Geological Survey Scientific Investigations Report 2017–5027, 62 p., https://doi.org/10.3133/sir20175027.

ISSN 2328-0328 (online)

Contents

Figures

Tables

Conversion Factors

U.S. customary units to International System of Units

Multiply	By	To obtain
	Length	
inch (in.)	2.54	centimeter (cm)
inch (in.)	25.4	millimeter (mm)
foot (ft)	0.3048	meter (m)
mile (mi)	1.609	kilometer (km)
	Area	
acre	4,047	square meter (m^2)
acre	0.4047	hectare (ha)
acre	0.4047	square hectometer (hm^2)
acre	0.004047	square kilometer (km^2)
square foot (ft^2)	929.0	square centimeter (cm^2)
square foot (ft^2)	0.09290	square meter (m^2)
square mile (mi^2)	259.0	hectare (ha)
square mile (mi^2)	2.590	square kilometer (km^2)
	Volume	
acre-foot (acre-ft)	1,233	cubic meter (m^3)
acre-foot (acre-ft)	0.001233	cubic hectometer (hm^3)
	Flow rate	
foot per second (ft/s)	0.3048	meter per second (m/s)
cubic foot per second (ft^3/s)	0.02832	cubic meter per second (m^3/s)
gallon per day (gal/d)	0.003785	cubic meter per day (m^3/d)
mile per hour (mi/h)	1.609	kilometer per hour (km/h)

Temperature in degrees Celsius (°C) may be converted to degrees Fahrenheit (°F) as follows:

$$°F = (1.8 \times °C) + 32.$$

Datum

Vertical coordinate information is referenced to the National Geodetic Vertical Datum of 1929 (NGVD29).

Supplemental Information

Specific conductance is given in microsiemens per centimeter at 25 degrees Celsius (µS/cm at 25 °C).

Concentrations of chemical constituents in water are given in either milligrams per liter (mg/L) or micrograms per liter (µg/L).

Response of Currents and Water Quality to Changes in Dam Operations in Hoover Reservoir, Columbus, Ohio, August 24–28, 2015

By Branden L. Vonins and P. Ryan Jackson

Abstract

Hoover Reservoir, an important drinking water supply for the City of Columbus, Ohio, has been the source of a series of taste and odor problems in treated drinking water during the past few years. These taste and odor problems were caused by the compounds geosmin and 2-methylisoborneol, which are thought to have been related to cyanobacteria blooms. In an effort to reduce the phosphorus available for cyanobacteria blooms at fall turnover, the City of Columbus began experimenting with the dam's selective withdrawal system to remove excess phosphorus in the hypolimnion, which is released from bottom sediments during summer anoxic conditions.

The U.S. Geological Survey completed two synoptic survey campaigns to assess distributions of water quality and water velocity in the lower part of Hoover Reservoir to provide information on the changes to reservoir dynamics caused by changing dam operations. One campaign (campaign 1) was done while water was being withdrawn from the reservoir through the dam's middle gate and the other (campaign 2) while water was being withdrawn through the dam's lower gate. Velocities were measured using an acoustic Doppler current profiler, and water-quality parameters were measured using an autonomous underwater vehicle equipped with water-quality sensors. Along with the water-quality and water-velocity data, meteorological, inflow and outflow discharges, and independent water-quality data were compiled to monitor changes in other parameters that affect reservoir behavior. Monthly nutrient data, collected by the City of Columbus, were also analyzed for trends in concentration during periods of expected stratification.

Based on the results of the two campaigns, when compared to withdrawing water through the middle gate, withdrawing water through the lower gate seemed to increase shear-driven mixing across the thermocline, which resulted in an increase in the depth of the epilimnion throughout the lower part of Hoover Reservoir. The observations from this study, if repeatable and driven primarily by changes in gate operations, can inform nutrient management strategies for Hoover Reservoir. Increased mixing across the thermocline may potentially supply nutrients from the hypolimnion to algae in the epilimnion. Although operation of the lower gate has the potential to export nutrients from the hypolimnion (where the concentrations of nutrients have typically been higher during summer months) through two mechanisms (direct withdrawal and mixing into the epilimnion), supply of nutrients to the epilimnion through enhanced mixing could lead to a short-term increase in algal populations. Therefore, further study is recommended to (1) test the repeatability of the results of gate changes on water-quality distributions and circulation patterns in lower Hoover Reservoir, (2) identify the immediate effect of gate changes on nutrient concentrations in the water column, and (3) identify the best management practices to reduce the nutrient storage in the hypolimnion of Hoover Reservoir without increasing the potential for nutrient transport to the highly productive epilimnion.

Introduction

The City of Columbus, Ohio, relies on nearby Hoover Reservoir as one of several sources of drinking water (fig. 1). Beginning in late 2013 and lasting into February 2014, treated drinking water sourced from Hoover Reservoir developed a taste and odor (TO) issue (Hunt, 2014). The issue reoccurred in the summer of 2015 (Arenschield, 2015). The TO problems were caused by two compounds, geosmin and 2-methylisoborneol (MIB), both known to be produced by certain species of cyanobacteria (American Water Works Association, 2010). The 2013 TO problems resulted in more than 1,700 consumer complaints and required special treatment at a substantial cost to the City of Columbus (Hunt, 2014).

The 2013/2014 TO problems were of particular concern because they began late in fall 2013 and lasted into February 2014 (Narciso, 2014), which is later than typical for cyanobacteria blooms (Graham and others, 2008). City of Columbus officials hypothesized that this bloom was partly caused by high nutrient concentrations near the bottom, which form during summer stratification, mixing throughout the water column when the reservoir turned over in the fall—a process in which

colder air temperatures cause the surface water to cool and sink, causing the water column to mix (Horne and Goldman, 1994). City of Columbus officials further hypothesized that this unusually late TO problem may have been exacerbated by nutrients adsorbed by sediment or decaying plants settling to the bottom of the reservoir while it was stratified and then becoming resuspended during the fall turnover, which added to the supply of nutrients for the late season bloom.

The dam at Hoover Reservoir is equipped with a selective withdrawal system that allows the City of Columbus to choose from three locations in the water column where water will be released downstream. This withdrawal system consists of three intake gate structures located approximately 600 feet (ft) from the western shore with upper (elevation = 880 ft), middle (865 ft), and lower (842 ft) gates, which the City of Columbus can use to release water downstream (gate elevations referenced to the National Geodetic Vertical Datum of 1929 [NGVD29]). Since the onset of TO issues in Hoover Reservoir, the City of Columbus has been experimenting with different withdrawal configurations in an attempt to reduce the concentration of nutrients within the hypolimnion (the part of a stratified body of water below the thermocline) during summer stratification. By doing so, the City of Columbus hoped to reduce the supply of nutrients that are released from the sediment during stratification and mixed throughout the water column during fall turnover; however, the effectiveness of these practices was largely unknown.

Previous studies have worked to evaluate the effectiveness of such practices to reduce nutrient concentrations and have found a wide range of results. In a study of 48 lakes, Nürnberg (2007) determined that hypolimnetic withdrawal could increase total phosphorus export from anywhere between 2 and 38 fold. He suggested these differences in efficiencies depend on a few factors, such as reservoir size and shape, withdrawal depth, and the reservoir's hydrology. Further study was required to better understand how these factors would combine to influence the effectiveness of hypolimnetic withdrawal at Hoover Reservoir.

With the goal of gathering information on the changes to reservoir dynamics caused by changing dam operations, the U.S. Geological Survey (USGS), in cooperation with the City of Columbus, completed two synoptic survey campaigns to assess distributions of water quality and water velocity in the lower part of Hoover Reservoir in August 2015. The first campaign (campaign 1) was taken while the City of Columbus was withdrawing water from the middle gate and the second campaign (campaign 2) was taken while the City of Columbus was withdrawing water from the lower gate. The data from these campaigns were supplemented with meteorological, flow, and independent water-quality data from the period, as well as monthly nutrient profiles collected by the City of Columbus. These supplementary data are essential for understanding how factors other than gate changes may have affected reservoir dynamics and water-quality distributions during this study. This report presents the methods used during the survey, compares the results of the two campaigns to identify potential effects of gate changes on the reservoir, considers influences of other factors beyond gate changes and how they may confound study results, and discusses the results in the context of the broader TO selective withdrawal management strategies being implemented by the City of Columbus. Although this study provides a better understanding of the response of the reservoir to operational gate changes, observed changes in the reservoir cannot be wholly attributed to gate changes. Conclusive recommendations for use in development of a selective withdrawal management strategy will require further study.

Purpose and Scope

The purpose of this report is to present the results of two synoptic survey campaigns of the lower part of Hoover Reservoir conducted by the USGS during August 24–28, 2015. This report will attempt to identify changes to circulation, mixing, and velocity characteristics in the lower part of the reservoir related to changes in gate operations at the Hoover Reservoir dam.

The scope is limited to analysis of two synoptic survey campaigns, one collected when water was being withdrawn through the mid-level gate and the other collected when water was being withdrawn through the low-level gate, as well as the analysis of supplemental meteorological, flow, and water-quality data.

Study Area

In 1955, a dam was built on Big Walnut Creek approximately 12 miles (mi) northeast of downtown Columbus, Ohio, near the town of Westerville (fig. 1). The dam formed the impoundment known today as Hoover Reservoir. The reservoir is long and narrow (approximately 8 mi long with a maximum width of approximately 5,000 ft) and has a predominantly north-south orientation. The reservoir has a surface area of approximately 2,800 acres (Ohio Department of Natural Resources, 2010) and can impound more than 1,900 acre-feet of water (City of Columbus Public Utilities, 2016).

This study focused on a 1.6-mi long part of lower Hoover Reservoir, which contained the reach of reservoir from the dam to just north of the Delaware-Franklin County line (fig. 1).

Parts of Franklin County, Licking County, Knox County, Morrow County (not shown), and Delaware County, constituting an area of about 190 square miles (mi^2), drain to the reservoir (U.S. Geological Survey, 2016). The land that drains to Hoover Reservoir consists mainly of row crops and forest (Ohio Environmental Protection Agency, 2001).

Water taken from below Hoover Reservoir is transferred to the Hap Cremean Water Plant (HCWP) for treatment and is then distributed to customers in the greater north Columbus area (City of Columbus Water Protection, 2016). The plant

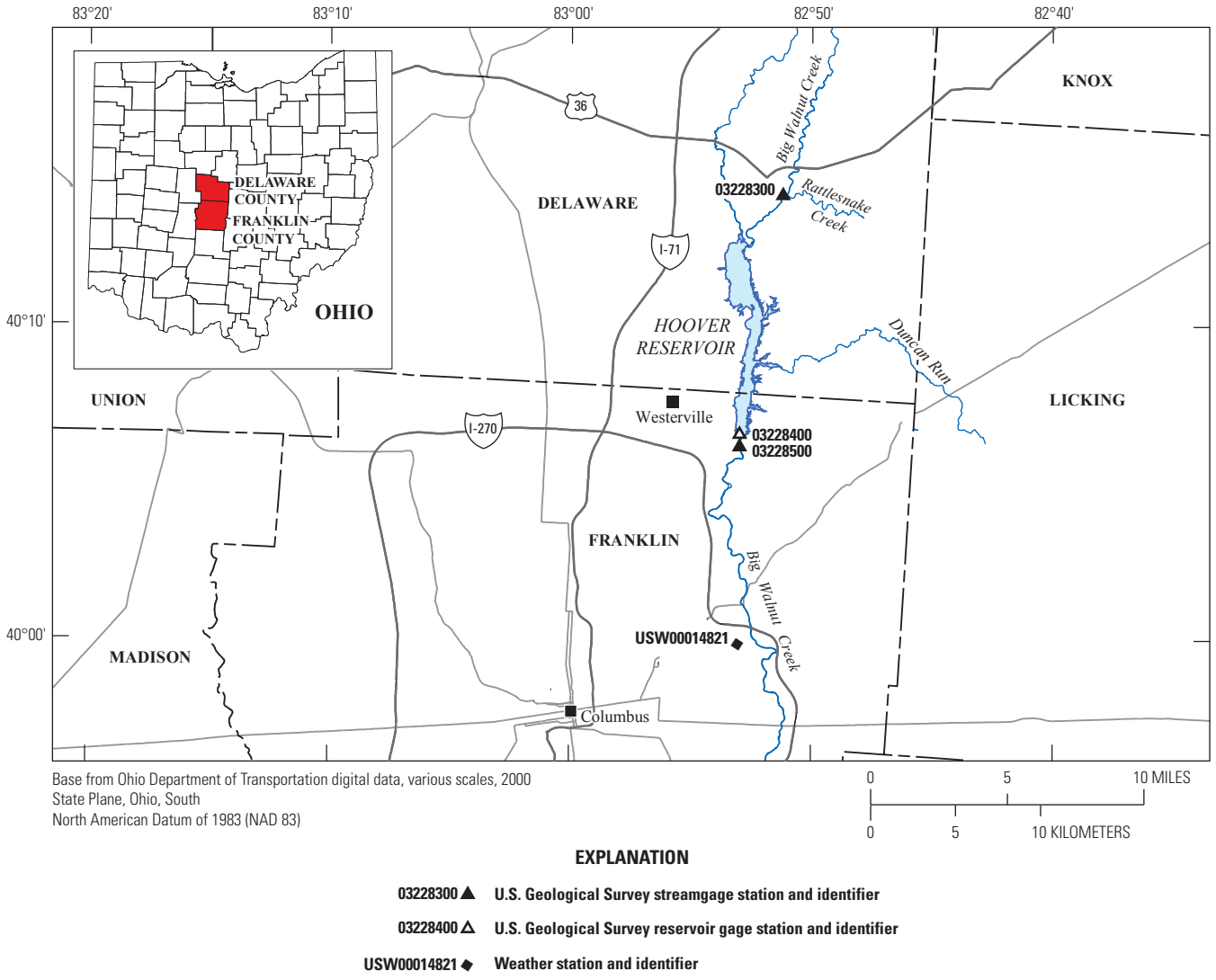

Figure 1. Hoover Reservoir and surrounding area including the locations of U.S. Geological Survey streamgage Big Walnut Creek at Sunbury (03228300), U.S. Geological Survey streamgage Big Walnut Creek at Central College (03228500), U.S. Geological Survey Reservoir Gage Hoover Reservoir at Central College (03228400), and National Oceanic and Atmospheric Administration weather station Port Columbus International Airport (USW00014821).

has a treatment capacity of 125 million gallons per day and in 2014 supplied approximately 49 percent of Columbus' water (Blevins, 2014).

Data Sources, Collection, and Processing

This section describes the data sources (for non-USGS data) and the instruments and methods used to collect and process the data presented in this report. These data include nutrient data, meteorological data, inflow and outflow data (flow data), reservoir water-surface elevation data (reservoir elevation data), floating water-quality profiler data (profiler data), water-velocity distributions (velocity data), and water-quality distributions (water-quality data). Analysis and interpretation of the processes in the reservoir during operation of the two different gates are based on the spatiotemporal variations observed in this dataset.

Meteorological Data

Air temperature and wind data, for the week leading up to and through the survey period, were obtained from the National Oceanic and Atmospheric Association's (NOAA) weather station at Port Columbus International Airport (station USW00014821; National Oceanic and Atmospheric Administration, 2016). This weather station is located about 8 miles south of the study area (fig. 1). The data obtained were in the

form of daily statistics. All meteorological data were processed with custom scripts written in R (R Core Team, 2016). The data underwent basic statistical analysis (such as the computation of range, maximum, and minimums). R's graphical functions were then used to visualize the data to facilitate interpretation.

Flow Data and Reservoir Elevation Data

Data from the streamgage on Big Walnut Creek at Sunbury (03228300) (U.S. Geological Survey, 2015a) were used to assess inflow to the reservoir. The streamgage is located about 9 miles upstream from the dam and has a drainage area of 101 mi^2, which is considerably smaller than the dam's 190 mi^2 (fig. 1). Discharge data were available at 15-minute intervals.

Data from the streamgage on Big Walnut Creek at Central College (03228500) (U.S. Geological Survey, 2015c) were used to assess outflow from the reservoir. The streamgage is located approximately 1,800 ft downstream from the dam and has a negligible difference in drainage area when compared to the dam (fig. 1). Therefore, the flow computed for the USGS streamgage on Big Walnut Creek at Central College can be considered to be equal to the flow released from the dam. Discharge data were available at 15-minute intervals.

Water-surface elevation data for the reservoir were obtained from the USGS streamgage on Hoover Reservoir at Central College (03228400) (U.S. Geological Survey, 2015b). The streamgage is located at the dam and recorded water-surface elevations every hour (fig. 1).

Discharge and reservoir elevation data were processed with custom scripts written in R. The scripts were used for basic statistical analysis and visualization of the data to facilitate interpretation.

Profiler Data

The City of Columbus operates a Yellow Springs Instrument (YSI) model 6951 pontoon vertical water-quality profiling system equipped with a YSI 6600 V2-4 multiparameter sonde. The sonde periodically measures vertical profiles of temperature, specific conductance, pH, dissolved oxygen, turbidity, total chlorophyll, and phycocyanin (blue-green algae). The water-quality sensor suite includes a YSI 6560 temperature/conductivity probe, YSI 6561 pH sensor, YSI 6150 ROX optical dissolved oxygen sensor, YSI 6136 turbidity sensor, YSI 6025 chlorophyll sensor, and YSI 6131 BGA-PC phycocyanin (blue-green algae) sensor. This suite of sensors is nearly identical to those used by the USGS during the survey, with only the pH sensor being different (the USGS used a YSI 6589 pH sensor). Also, with the exception of the total chlorophyll, all sensors were calibrated in the same manner to the USGS instrument (the City of Columbus performed a two-point calibration for total chlorophyll using deionized water and 110 micrograms per liter [µg/L] of rhodamine WT dye solution, whereas the USGS performed a single-point calibration in deionized water).

The profiler is located on a buoy about 400 ft north of the dam and approximately 700 ft from the western shore (fig. 2). Every 4 hours the profiler takes readings at 3.28 ft depth intervals, starting at a depth of 3.28 ft and ending at 45.9 ft depth (Benjamin Ellsesser, City of Columbus, written commun., January 14, 2016). The total time to complete a profile is approximately 20 minutes. The water-quality data collected by the City of Columbus with the automated profiler provide an independent water-quality dataset for comparison to water-quality data collected in this study. Profiler data were provided by the City of Columbus in a spreadsheet and used without further checks or modification by the USGS (Benjamin Ellsesser, City of Columbus, unpub. data, January 14, 2016).

Nutrient Data

The City of Columbus supplied nutrient data collected at various locations on Hoover Reservoir for summer and early fall of 2014, 2015, and 2016. These data included concentrations of nitrate, ammonia, total phosphate, and orthophosphate. Samples were collected from a boat and sampling procedures followed these certified monitoring methods: SM-4500-NO_3-F, SM-4500-NH_3, and SM-4500-P-F (Benjamin Ellsesser, City of Columbus, written commun., September 23, 2016; Standard Methods Online, 2016). During most sampling trips, samples were obtained at the surface, at approximately mid-depth, and near the bottom; however, there were times when only one or two of these depths were sampled. If two samples were collected during a trip, the data were included in the analysis; however, if only one depth was sampled on a trip, that sample was omitted from analysis because a nutrient profile could not be generated from the single point. When multiple samples were taken at a particular depth during the same trip, the parameter concentrations for each sample were averaged together to yield a single concentration for each parameter at that particular depth for that day. Finally, scripts were written in R to produce graphical representations of the nutrient profiles.

Survey Data

Two synoptic survey campaigns to map the distributions of water velocity and water quality were completed during August 24–28, 2015. The first (campaign 1) was done on August 24–25, 2015, while the City of Columbus was releasing water through the dam's middle gate (approximately 26 ft below the water surface). After the first campaign was completed on the evening of August 25, 2015, the City of Columbus closed the dam's middle gate and opened the lower gate. No data were collected on August 26, 2015, in an attempt to allow reservoir conditions to equilibrate to the gate change before beginning the second campaign. The second campaign (campaign 2) was then done on August 27–28, 2015. The two

Figure 2. Lower Hoover Reservoir including the locations of survey cross sections, the location of the withdrawal gates, the location of the City of Columbus's profiler, and the location of the line that all cross sections were plotted in reference to.

campaigns yielded velocity and water-quality datasets that were used for analysis. The USGS velocity data presented in this report are published as a data release through the USGS ScienceBase data portal in Vonins (2016), whereas the USGS water-quality data are published through the USGS ScienceBase data portal in Jackson and Dupre (2016).

Velocity Data

Velocity data were collected with a Teledyne RDI 600 kilohertz Rio Grande® acoustic Doppler current profiler (ADCP) that was connected to a Hemisphere A101 Smart Antenna differential global positioning system (GPS) for georeferencing. The ADCP was mounted to the starboard side (right-hand side, facing forward) of an aluminum jon boat with the GPS antenna mounted directly above the ADCP. Velocity data for each campaign were measured at 11 cross sections (fig. 2; table 1). Each cross section consisted of four transects, where a transect is defined as one transit from a starting bank to the opposite bank. Slow boat speeds were maintained to try to ensure the highest-quality data were being collected while also allowing time to complete the survey.

The ADCP, with a few exceptions, was configured using the same settings throughout data collection (table 1). A smaller depth-cell size was used in campaign 1 at cross section 1 before the range of depths in the reservoir was known. The two cross-section measurements where the transducer depth was set deeper than the norm (due to an error in deployment) had negligible effects on the collected data. The effects were considered negligible for two reasons: (1) because the changes were accounted for in the ADCP's processing software and (2) because the change in depth of the transducer was small compared to the depth of the reservoir. To ensure accurate headings, the ADCP's compass was calibrated and evaluated during each survey before measurements at cross sections 1, 4, 6, 8, and 11.

Post-processing of the data collected with the ADCP was completed using WinRiver II (Teledyne RD Instruments, 2014) and the Velocity Mapping Toolbox (VMT) (Parsons and others, 2013), and R. WinRiver II was used to correct the changes in transducer depths and to apply sample averaging prior to exporting the velocity data for further processing in the VMT. The averaging parameters applied to the velocity data and the associated post-processing programs are shown in table 2. The VMT was used to determine mean velocity distributions by averaging together results from the transects measured at each cross section (table 2). This multitransect averaging process helps reduce the instrument's electronic noise often present in single transect velocity data. The velocity data were further averaged using the VMT's spatial-averaging capabilities (table 2). The VMT was then used to prepare plots of the velocity data in plan view. Finally, the VMT was used to output the mean velocity distributions from each cross section in comma separated values (CSV) format for further analysis in R.

Scripts in R were used to prepare plots of cross-section views. R was used to create these plots rather than the VMT, because the VMT resets the origin for each cross section. In order to allow easy comparison of distances and depths between cross sections as well as to help visualize reservoir layout, the scripts written in R were designed so each cross-section plot had the same horizontal and vertical scale and

Table 1. Configuration of the acoustic Doppler current profiler used throughout data collection.

Campaign	Date	Cross section	Cell size, in centimeters	Transducer depth, in centimeters	Magnetic variance , in degrees	Water mode	Bottom track mode
1	08/24/15	1	23	49	-7.1	12	5
1	08/24/15	2	50	49	-7.1	12	5
1	08/24/15	3	50	49	-7.1	12	5
1	08/24/15	4	50	49	-7.1	12	5
1	08/24/15	5	50	49	-7.1	12	5
1	08/25/15	6	50	49	-7.1	12	5
1	08/25/15	7	50	49	-7.1	12	5
1	08/25/15	8	50	49	-7.1	12	5
1	08/25/15	9	50	49	-7.1	12	5
1	08/25/15	10	50	61	-7.1	12	5
1	08/25/15	11	50	61	-7.1	12	5
2	08/27/15	1	50	49	-7.1	12	5
2	08/27/15	2	50	49	-7.1	12	5
2	08/27/15	3	50	49	-7.1	12	5
2	08/27/15	4	50	49	-7.1	12	5
2	08/27/15	5	50	49	-7.1	12	5
2	08/27/15	6	50	49	-7.1	12	5
2	08/27/15	7	50	49	-7.1	12	5
2	08/27/15	8	50	49	-7.1	12	5
2	08/27/15	9	50	49	-7.1	12	5
2	08/27/15	10	50	49	-7.1	12	5
2	08/28/15	11	50	49	-7.1	12	5

Table 2. Velocity data averaging parameters and the software used.

[VMT, Velocity Mapping Toolbox; N/A, not applicable]

Plot	Profile averaging in WinRiver II, in number of ensembles	Number of transects averaged in VMT	Depth/layer averaging in VMT	Horizontal averaging in VMT, in number of cells	Vertical averaging in R, in number of cells	Horizontal averaging in R, in number of cells
Plan view	3	4	Depth ranges shown in figures 6 though 11	5	N/A	N/A
Cross section	3	4	N/A	None	5	5

were plotted in relation to a constant bank reference line. Each cross section is plotted in relation to a line defined by the coordinates 40° 07’ 50.71” North, 82° 52’ 28.58” West and 40° 06’ 28.85” North, 82° 52’ 42.89” West (fig. 2).

Water-Quality Data

Water-quality data were collected with an autonomous underwater vehicle (AUV) along three approximately 8,000 ft survey lines longitudinally spanning the lower part of Hoover Reservoir from the dam to the Smothers Road Bridge (fig. 3). A total of 14 water-quality surveys (where a survey consisted of water-quality measurements made along one of the survey lines) were completed during the two campaigns (table 3). The AUV was used to measure the spatial distributions of selected water-quality parameters and bathymetry. In addition, the AUV collected side-scan sonar imagery along survey lines C, E, and W (not presented in this report). The water-quality parameters measured by the instrument include temperature, specific conductance, pH, dissolved oxygen, turbidity, total chlorophyll, and phycocyanin (yields blue-green algae concentrations). A manned boat was used to deploy and recover the AUV.

To provide three-dimensional water-quality data, the AUV was programmed to collect data in an undulating dive pattern in which the AUV moved between the water surface and 6 ft above the reservoir bed as it traversed the survey line at a speed of 2 knots (3.4 feet per second [ft/s]). The undulating dive pattern used a 15-degree dive angle and resulted in approximately 30 profiles of the water column over an 8,000-ft survey line (resulting in measurements at a given depth occurring about 270 ft apart).

The AUV used in the surveys had a length of 63.6 inches (in.), a diameter of 5.8 in., weighed approximately 60 pounds (lb) in air (fig. 4), and was built by YSI, Inc. and OceanServer Technology, Inc. (EcoMapper® AUV). The AUV consisted of a carbon-fiber hull with aluminum nose and tail sections. The nose of the AUV houses a 6600 V2-4 YSI multiparameter sonde bulkhead with four optical ports and temperature/conductivity and pH ports. The water-quality sensor suite consists of a YSI 6600 V2-4 bulkhead equipped with a YSI 6560FR fast response temperature/conductivity probe, YSI 6589FR fast response pH sensor, YSI 6150 ROX optical dissolved oxygen sensor, YSI 6136 turbidity sensor, YSI 6025 chlorophyll sensor, and YSI 6131 BGA-PC phycocyanin (blue-green algae) sensor. Manufacturer’s specifications for each of the probes are shown in table 4. All water-quality sensors are sampled at a rate of 1 hertz. A pressure sensor also is integrated into the sonde bulkhead for measurement of the sample depth.

Near the water-quality sensor suite (on the nose of the vehicle) is the Doppler velocimetry log (DVL) instrument. The DVL is a six-beam system for underwater navigation (bottom tracking) and includes vertical beams (uplooking and downlooking) for altitude and depth measurement. Additionally, the DVL provides current-profiling capabilities below the instrument. Located on the top of the vehicle (near the tail section) is the antennae mast, which houses a differential GPS antenna (Wide Area Augmentation System corrected), a 2.4-gigahertz 802.11g wireless radio antenna, navigation lights, and an external power plug for vehicle charging. Directly below the antennae mast on both sides of the vehicle are the side-scan sonar transducers. The tail consists of four independent control fins and a three-blade propeller. More detailed information on the DVL and side-scan sonar systems, calibration procedures for the AUV, instrument operation, handling of data files, and data-processing routines is in Jackson (2013).

Instrument calibration, data file management, operation, and methods used to process the AUV data, including computation of water density from measurements of temperature and specific conductance, are discussed in detail in appendix 1 of Jackson (2013). Data processing routines include manual screening of data from each sensor to remove outliers, application of a moving-average filter to reduce noise in optical sensors (when necessary), correction for sensor response time for each parameter, computation of vertical profiles of each water-quality parameter (constructed from the median value of each parameter for discrete depth intervals), and contouring of point data to produce longitudinal sections of each water-quality parameter along a survey line. If insufficient data exist due to a partial dive of the AUV before surfacing to make a turn or correct for drift off line, a blank area may be present in

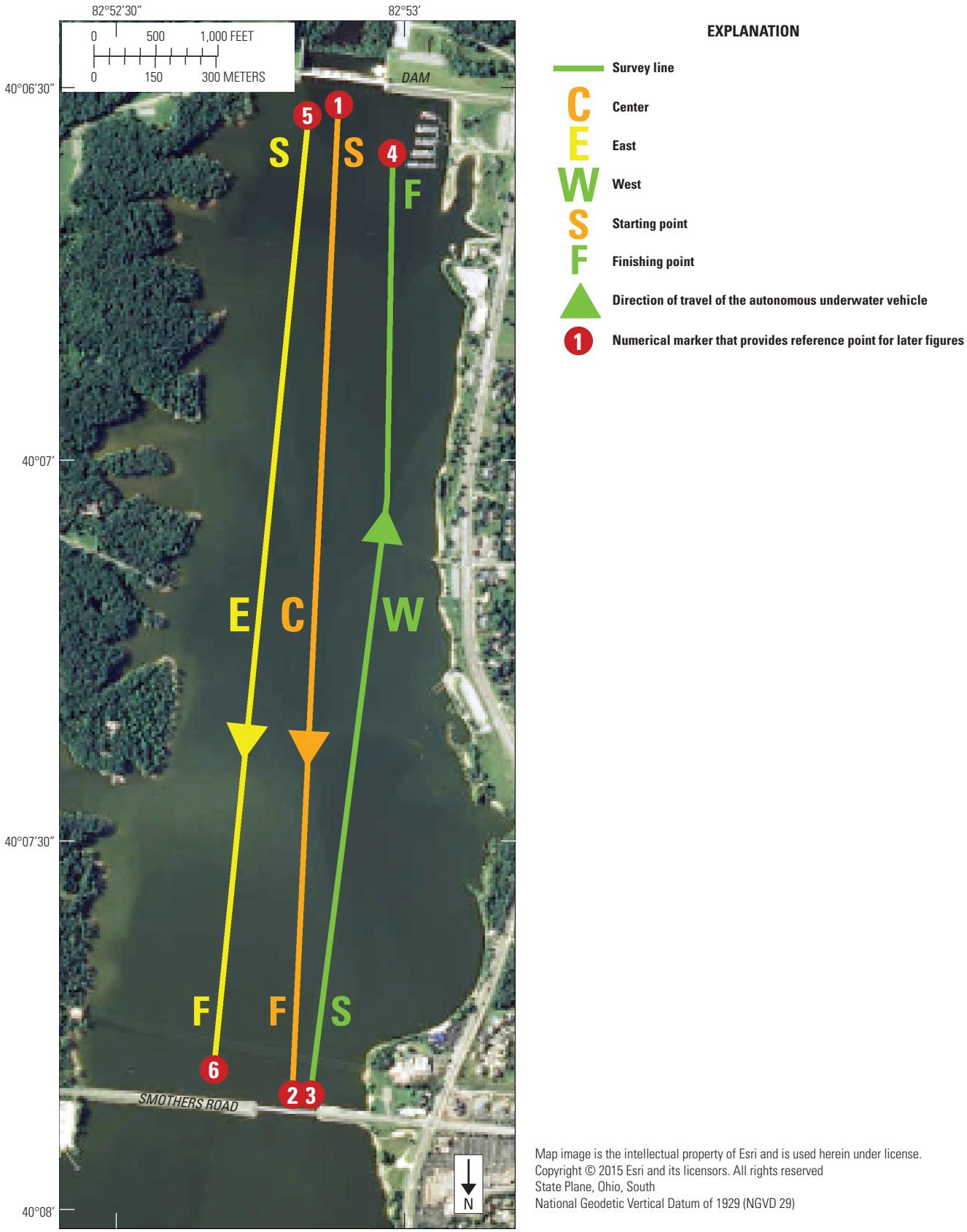

State Plane, Ohio, South
National Geodetic Vertical Datum of 1929 (NGVD 29)

Figure 3. Autonomous underwater vehicle survey lines in the lower part of Hoover Reservoir, Ohio.

Table 3. Summary of water-quality surveys during the two campaigns.

[EDT, Eastern daylight time; surveys in bold were used for water-quality comparison plots]

Campaign	Date	Survey number	Dam gate configuration	Survey line	Start time (EDT)	End time (EDT)	Duration (minutes)	Mean time (EDT)
1	**08/25/15**	**1**	**Middle**	**C**	**9:45**	**10:30**	**45**	**10:07**
1	08/25/15	2	Middle	C	10:48	11:36	48	11:12
1	**08/25/15**	**3**	**Middle**	**C**	**11:57**	**12:46**	**49**	**12:21**
1	08/25/15	4	Middle	W	14:43	15:25	42	15:04
1	08/25/15	5	Middle	E	15:28	16:13	45	15:50
2	**08/27/15**	**6**	**Lower**	**C**	**7:39**	**8:25**	**46**	**8:02**
2	08/27/15	7	Lower	W	8:28	9:11	43	8:49
2	08/27/15	8	Lower	E	9:13	10:00	47	9:36
2	08/27/15	9	Lower	C	10:27	11:13	46	10:50
2	08/27/15	10	Lower	C	11:24	12:12	48	11:48
2	08/27/15	11	Lower	W	12:16	12:57	41	12:36
2	08/27/15	12	Lower	E	13:00	13:51	51	13:25
2	08/27/15	13	Lower	C	14:01	14:48	47	14:24
2	**08/27/15**	**14**	**Lower**	**C**	**15:03**	**15:49**	**46**	**15:26**

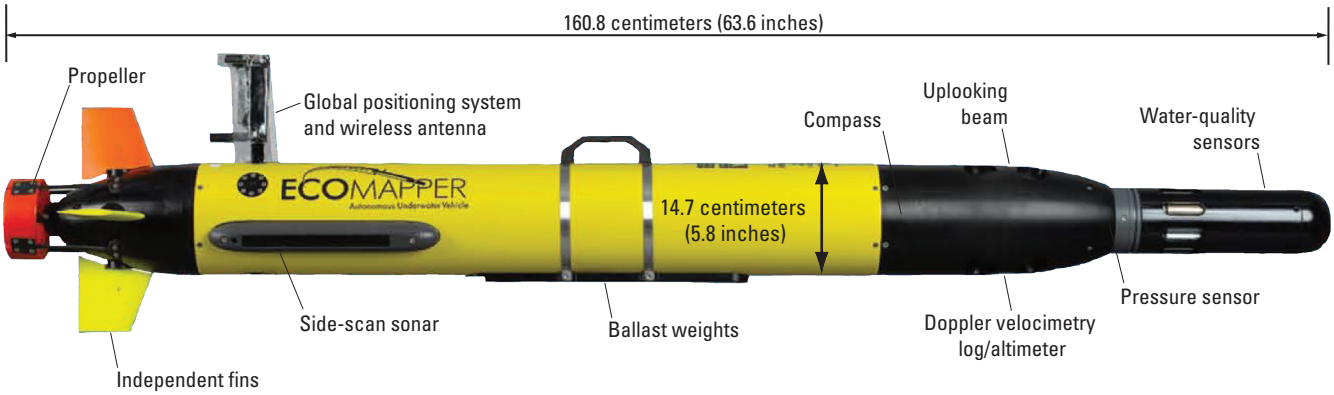

Figure 4. Schematic of the autonomous underwater vehicle.

Table 4. Manufacturer's specifications for the water-quality sensors aboard the autonomous underwater vehicle.

[µS/cm, microsiemens per centimeter at 25 degrees Celsius; --, not specified; ±, plus or minus; %, percent; °C, degrees Celsius; ft, foot; m, meter; N/A, not applicable; ppt, parts per thousand; mg/L, milligrams per liter; NTU, nephelometric turbidity units; µg/L, micrograms per liter; R^2, coefficient of determination; >, greater than; cells/mL, cells per milliliter]

Sensor	Sensor model number	Range	Detection limit	Resolution	Accuracy	Linearity	Estimated lag, in seconds
Conductivity	YSI 6560FR	0 to 100,000 µS/cm	--	1 to 100 µS/cm	±0.5% + 1 µS/cm	--	0.5
Temperature	YSI 6560FR	−5 to 50 ºC	--	0.01 ºC	±0.15 ºC	--	2.1
Depth	Deep	0 to 656 ft (200 m)	--	0.001 ft (0.001 m)	±1 ft (±0.3 m)	--	--
Salinity	N/A	0 to 70 ppt	--	0.01 ppt	±1% or 0.1 ppt	--	--
pH	YSI 6589FR	0 to 14 units	--	0.01 units	±0.2 units	--	*7.1
Dissolved oxygen	YSI 6150	0 to 50 mg/L	--	0.01 mg/L	±0.1 mg/L or 1%	--	>10
Turbidity	YSI 6136	0 to 1,000 NTU	--	0.01 NTU	±2% or 0.3 NTU	--	2.1
Chlorophyll	YSI 6025	0 to 400 µg/L	0.1 µg/L	0.1 µg/L	--	$R^2 > 0.9999$	2.1
Blue-green algae (phycocyanin)	YSI 6131	0 to 280,000 cells/mL	220 cells/mL	1 cell/mL	--	$R^2 > 0.9999$	2.1

*Can vary with age of sensor.

the contoured data. Because the AUV undulation patterns and paths are slightly different between each survey on the same line, some contoured survey data may have such blank areas while other surveys may not. In addition, AUV surveys on the same line can have slightly different paths due to underwater drift of the AUV off the survey line (generally less than 15 ft), which can result in slightly different reservoir bed profiles for the same survey line, especially in areas where the bed topography is highly variable.

Response of Currents and Water Quality to Changes in Dam Operations

The following sections present and discuss the meteorological, nutrient, hydrodynamic, and water-quality data that were collected during the surveys. Standard terminology from limnology is used in the discussion to reference the various regions (or strata) of the stratified water column in this reservoir. The thermocline (also referred to as the metalimnion) is defined as the region with the greatest temperature gradient, marked by a layer above (the epilimnion) and below (the hypolimnion) in which the water masses are at different temperatures. In many lakes and reservoirs, the epilimnion is well-mixed for many water-quality parameters including temperature, whereas the hypolimnion often exhibits some stratification as the summer progresses (Wetzel, 2001). When stratification is present in the hypolimnion, it is typically weaker (has a smaller temperature gradient) than the primary thermocline. The initial temperature of the hypolimnion is usually defined by the final temperature of the water during the spring turnover, and stratification of the hypolimnion results from direct solar heating (during clear water conditions where light can penetrate below the thermocline), variable density inflows, and episodic mixing in the epilimnion during wind and storm events, which drives turbulent conduction of heat across the thermocline and into the hypolimnion (Wetzel, 2001). A more extensive discussion of lake and reservoir stratification is in Hutchinson (1957).

Meteorological and Flow Data

The average daily high air temperature at Port Columbus during August 2015 was 27.7 degrees Celsius (°C) (National Weather Service, 2015), which is 1 °C cooler than the mean August high observed from 1981 to 2010. The week of the survey was also relatively cool, with temperatures only reaching 26 °C on August 28, 2015, and 20 °C on August 25 and 26 (fig. 5*A*). The nights leading up to and including the study period also were cooler than normal with low air temperatures below 14 °C on three of the nights of data collection (fig. 5*A*), almost 4 °C cooler than the mean August low from 1981 to 2010 (National Weather Service, 2015).

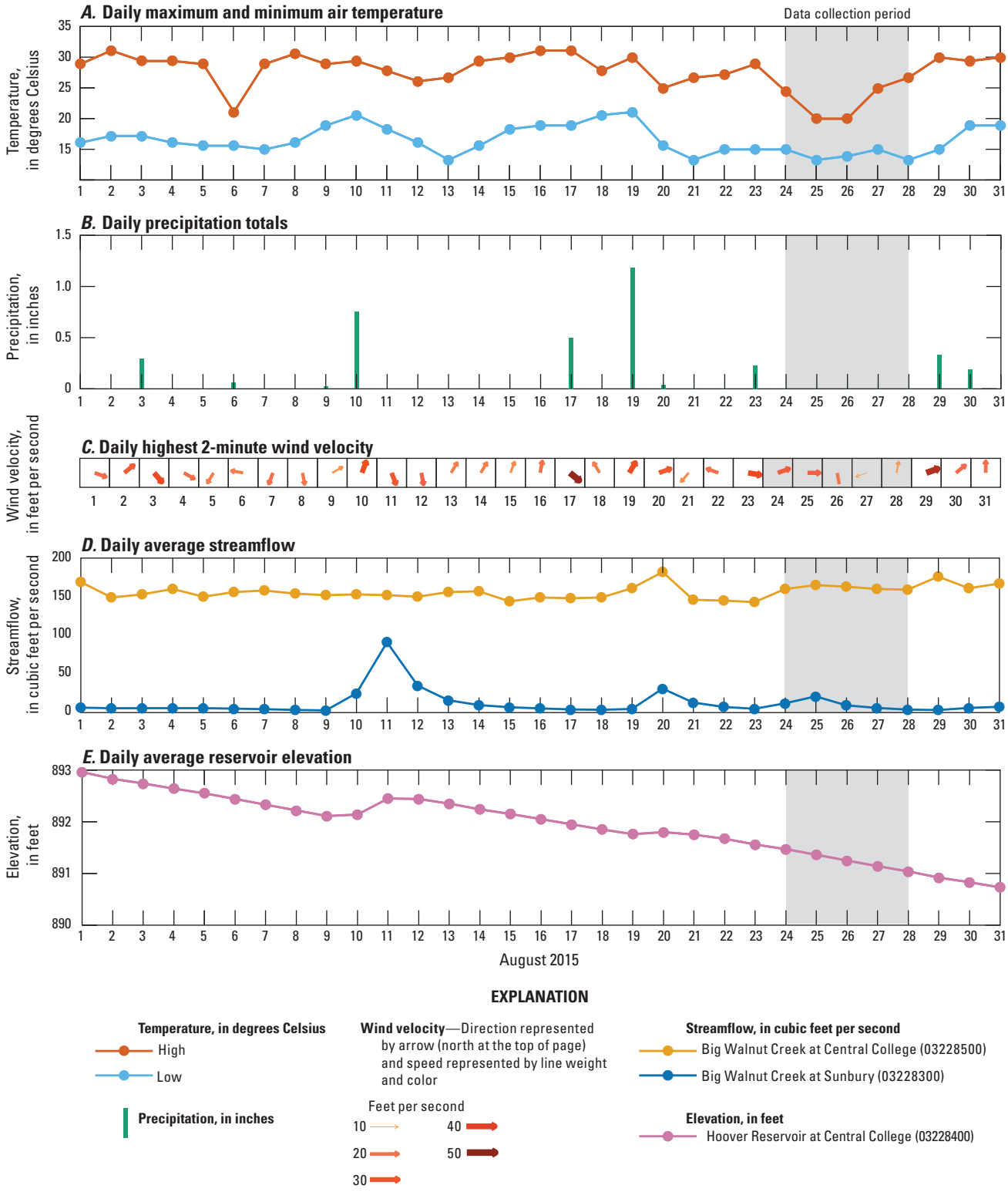

Figure 5. Meteorological, stream flow, and reservoir surface elevations for the month of August, 2015. *A*, Daily high and low air temperature as recorded at Port Columbus International Airport (station GHCND:USW00014821) by the National Atmospheric and Oceanic Administration (NOAA). *B*, Daily precipitation totals as recorded at Port Columbus International Airport (station GHCND:USW00014821) by NOAA. *C*, Daily highest 2-minute wind velocity as recorded at Port Columbus International Airport (station GHCND: USW0014821) by NOAA. *D*, Daily streamflow averages at two U.S. Geological Survey (USGS) streamgages, Big Walnut Creek at Central College (03228500) and Big Walnut Creek at Sunbury (03228300). *E*, Hoover Reservoir's surface elevation recorded by the USGS streamgage, Hoover Reservoir at Central College (03228400).

August 2015 was wetter than the 1981 to 2010 mean, receiving 3.59 in. of rain, more than a quarter of an inch above average. Of the 3.59 in. that fell in August 2015, about 40 percent (1.45 in.) fell within 1 week of the start of data collection (1.18 in. fell on August 19) (fig. 5*B*).

Winds for the week of data collection were variable. During August 23–25, winds were predominately from the west, during August 26–27 winds blew predominately from the north, and on August 28 winds blew predominately from the south. The wind gusts were strongest (37 ft/s) the day before data collection started (August 23) and then winds calmed as the week progressed until gusts fell to 10–12 ft/s on August 27–28 (fig. 5*C*).

The flow at the Big Walnut Creek at Sunbury streamgage does not equal the inflow to Hoover Reservoir because other streams, such as Little Walnut Creek, also drain to the reservoir. Consequently, the flow at the streamgage was used only to show the timing of inflow events and it is likely that inflow to the reservoir during these events was substantially larger than what was reported by the streamgage. As seen in figure 5*D*, there were three increases in daily mean streamflow at the Big Walnut Creek at Sunbury streamgage during the month of August 2015. Of the three peaks, one was approximately 4 days prior to data collection and another was on the second day of data collection.

During the month of August, daily average outflow from the reservoir ranged from 143 to 182 cubic feet per second (ft^3/s) and averaged 156 ft^3/s (fig. 5*D*). Outflow from the reservoir was held relatively constant during data collection; however, outflows were more variable during the week prior to data collection: a 13-percent rise, a 20-percent drop, and another 12-percent rise in outflow occurred the week before data collection—the three largest percent changes to daily flow during the month of August.

The pool elevation of the reservoir declined approximately 2 ft during August 2015 (fig. 5*E*); however, the pool elevation did rise twice during this period in response to the two largest precipitation events of the month. Despite the large drop in pool elevation during August 2015, the mean pool elevations for campaign 1 and 2 are 891.36 (standard deviation [SD]=0.01 ft) and 891.15 ft (SD=0.01 ft) (NGVD29), respectively; therefore, the pool elevation only dropped by 0.21 ft between campaign 1 and campaign 2. This change is approximately 0.4 percent of the mean depth of the lower part of Hoover Reservoir and is therefore a rather insignificant change in pool elevation between survey campaigns.

The variability in meteorology, inflow, and outflow before and during data collection confounds the ability to ascribe observed changes in reservoir dynamics to gate operations alone. Imberger and Hamblin (1982) described six broad forces that affect reservoir dynamics: wind-forced motion, free-wave motion, velocity concentration (resulting from something such as a contraction to flow), inflow, outflow, and reservoir heating. Of the six forces, wind-forced motion, reservoir heating, inflow, and outflow underwent changes before and during data collection.

The outflow data were also used to estimate an average velocity through the lower reach of the reservoir to give a rough idea of residence time within the study section. This calculation assumed that flow through each cross section was directed toward the dam with uniform velocity and that a representative average cross-sectional area can be obtained by averaging the areas in the measured cross sections. It should be noted that the measured cross-section areas do not include edge areas where it was too shallow to operate the ADCP. The estimated average cross-sectional area of the reservoir between Smothers Road and the dam was approximately 69,000 square feet (ft^2). Dividing the average outflow for the week of data collection (156 ft^3/s) by the average cross-sectional area in the lower reach (69,000 ft^2) results in a computed average water velocity of about 0.002 ft/s. Dividing the length of the reservoir from Smothers Road to the dam (about 8,448 ft) by the average velocity indicates that an approximate average residency time for a particle of water in the lower reservoir was about 49 days (assuming outflow and cross-section areas remain constant). It is likely that some particles of water will pass through the lower reach much faster and others will take even longer than 49 days; however, this approximation shows that the reservoir may require more time than was given to react to the changes in gates.

Velocity Data

In the following section, observed circulation patterns that may affect reservoir mixing and residency time are presented, described, and discussed.

Contiguous Paths of Flow

The depth-averaged velocity patterns were variable and complex during campaigns 1 and 2 (figs. 6–11); however, two possible preferred flow paths (paths of contiguous downstream flow) were identified for campaign 1. These paths were of interest because they are the most direct routes identified for water and particle transport through the study section. The first path was observed in the 10 to 20 ft depth range during campaign 1 (fig. 7) where flow came through the Smother's Road bridge and followed the west bank before moving toward the center of the reservoir in the middle of the reach, and finally spread across the width of the reservoir as it approached the dam.

The second path identified in campaign 1 follows the zone of maximum downstream velocity as it shifts to adjacent depth ranges when moving from cross section to cross section (fig. 12). In the upper part of the study reach (where the reservoir was shallowest) the highest downstream velocities were in the 0 to 10 ft depth range (fig. 12). As the reservoir deepened the highest velocities shifted to a deeper range (10 to 20 ft). At the deepest section of the reservoir, the highest velocities were in the 20 to 26 ft depth range. Finally, just upstream from the dam, the highest velocities were in the 26 to 33 ft depth range,

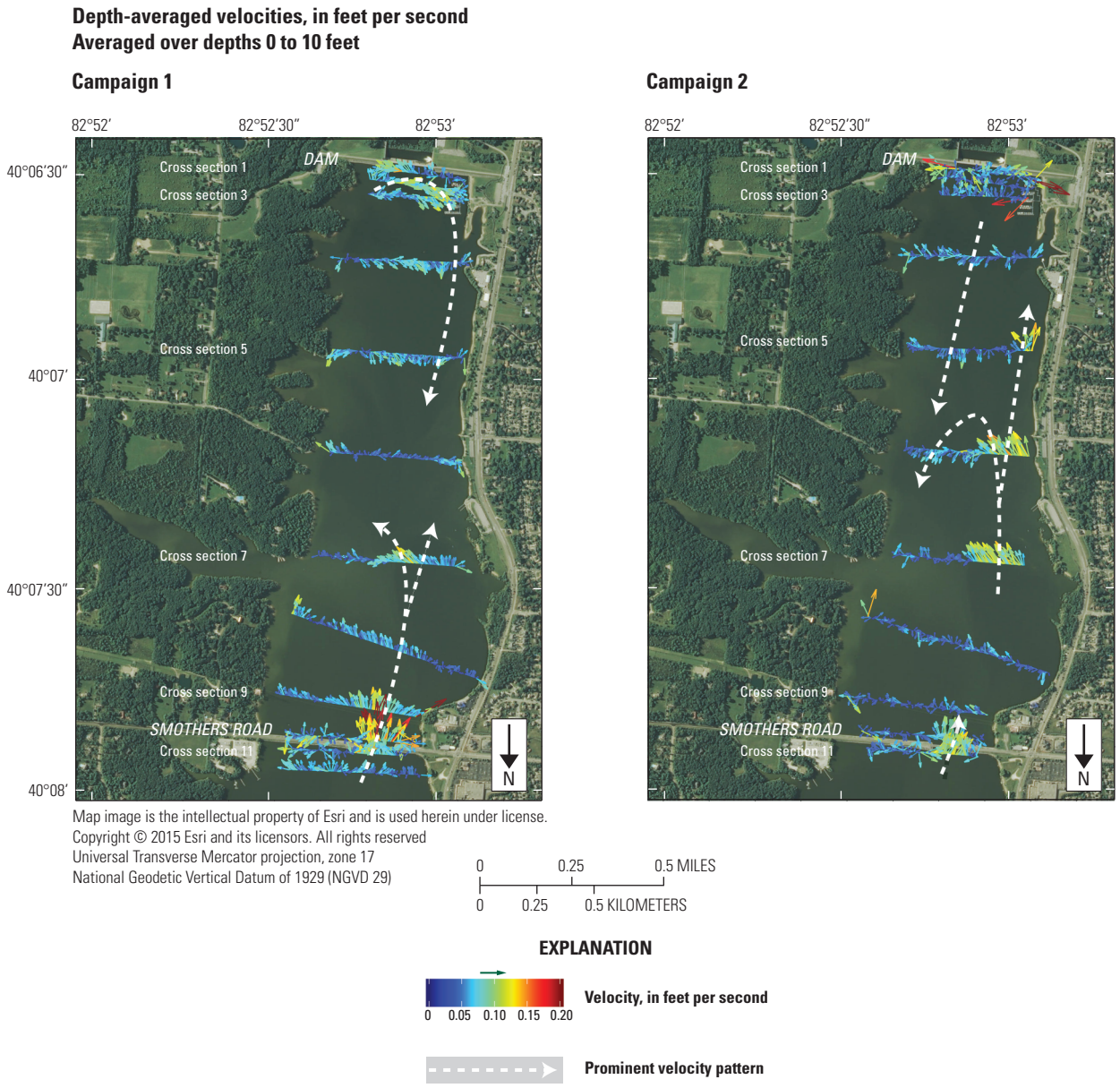

Figure 6. Comparison of campaign 1 and campaign 2 depth-averaged velocities for a depth of 0 to 10 feet with major circulation paths. In campaign 1, primarily downstream flow was observed from the bridge to approximately cross section 6, whereas strong upstream flow was observed from the dam to about cross section 6. In campaign 2, strong downstream flow through the bridge was observed but then velocities drop to near zero. Toward the middle of the study section in campaign 2, strong downstream velocities were present along the west bank and then recirculated back upstream along the east bank. Mean pool elevations for campaign 1 and 2 are 891.36 and 891.15 feet (National Geodetic Vertical Datum of 1929), respectively.

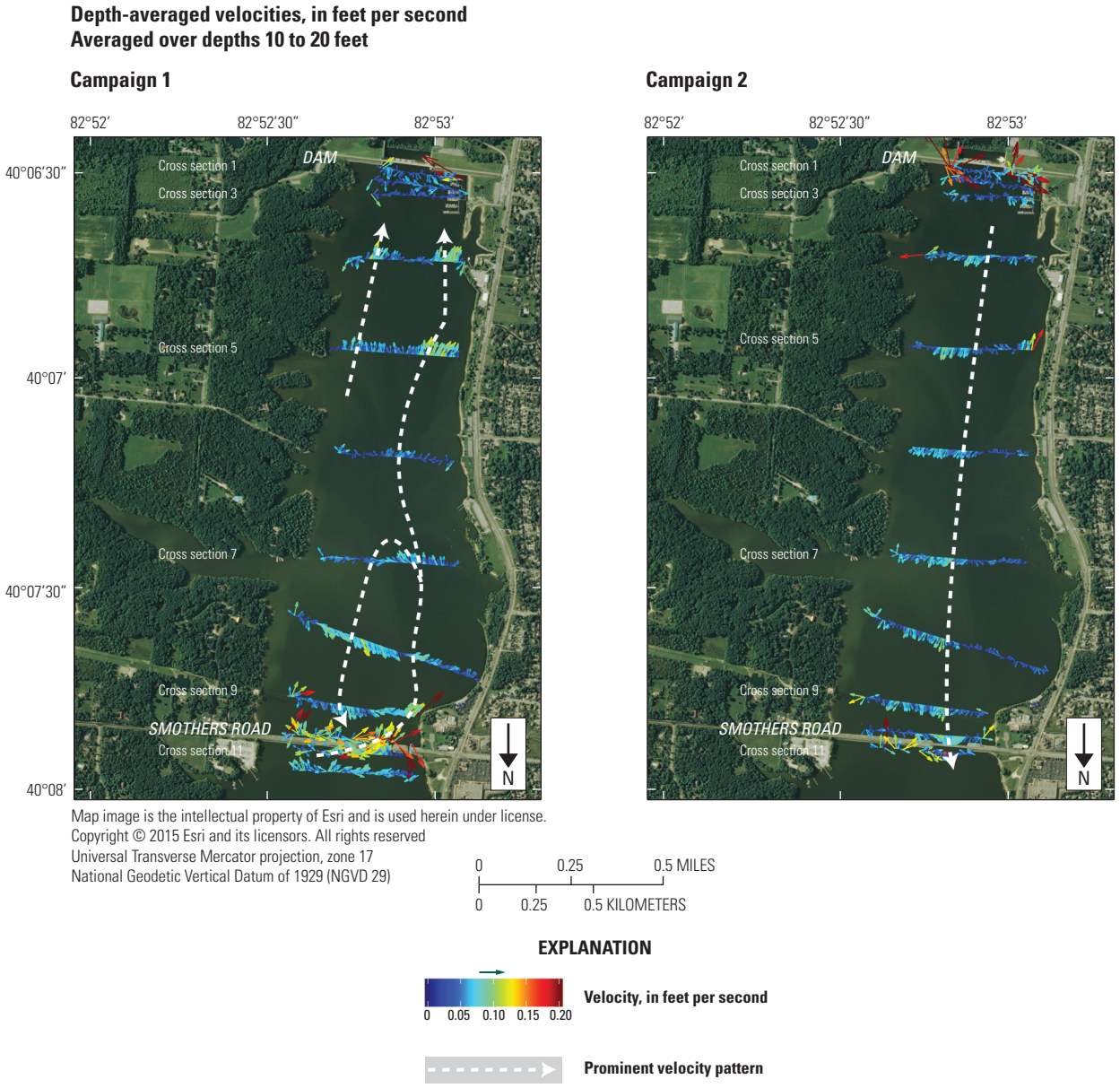

Figure 7. Comparison of campaign 1 and campaign 2 depth-averaged velocities for a depth of 10 to 20 feet with major circulation paths. In campaign 1, downstream velocities were observed along the west bank from the bridge to approximately cross section 6, with upstream velocities observed along the east bank. Below cross section 6, velocities were primarily downstream until reaching the dam, where little velocity was observed. Campaign 2 showed consistent upstream flow along the east bank with very little downstream flow anywhere. Mean pool elevations for campaign 1 and 2 are 891.36 and 891.15 feet (National Geodetic Vertical Datum of 1929), respectively.

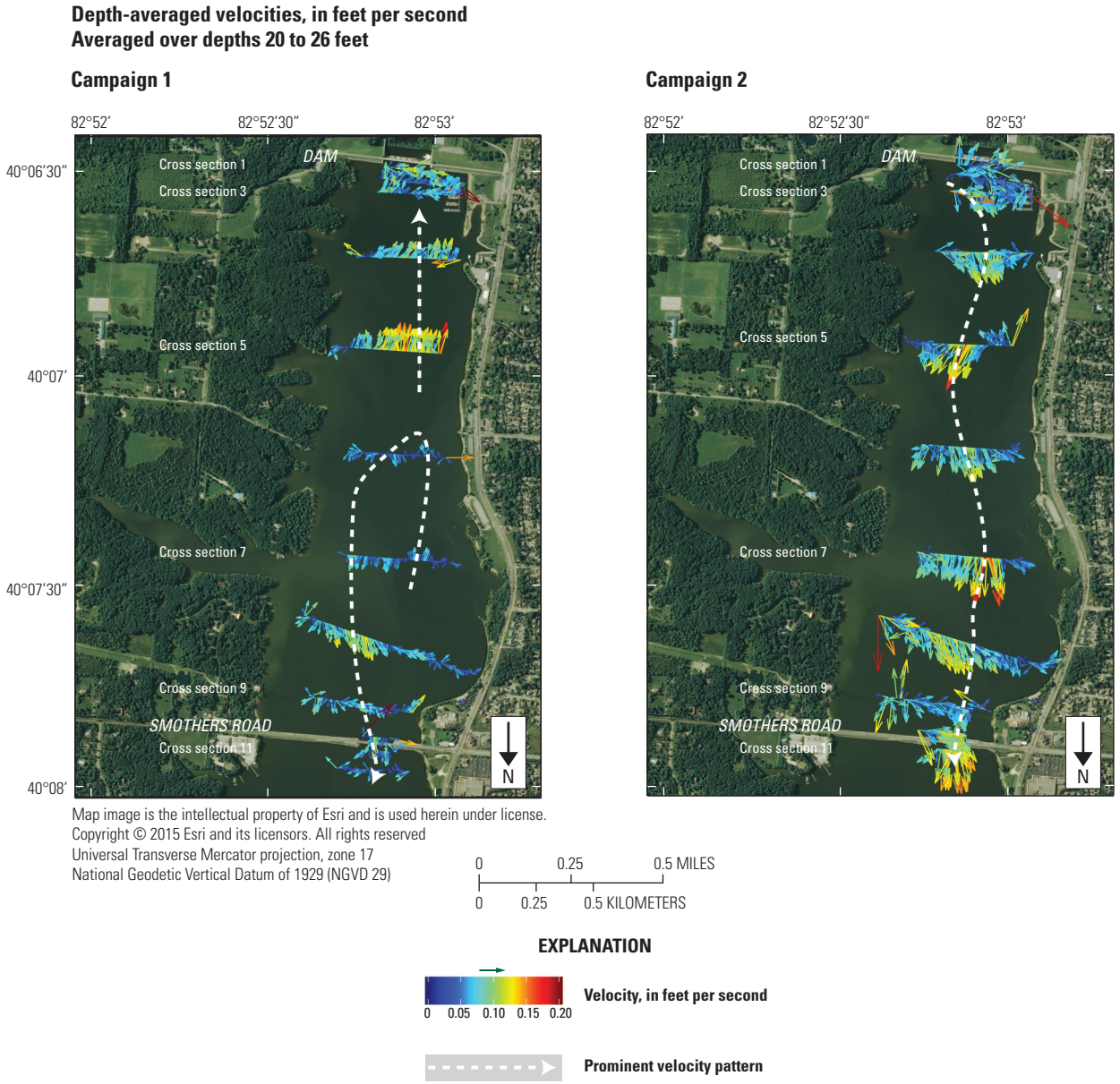

Figure 8. Comparison of campaign 1 and campaign 2 depth-averaged velocities for a depth of 20 to 26 feet with major circulation paths. In campaign 1, the upper part of the study section had upstream velocities along the east bank and slow water speeds along the west bank. There was little velocity at cross section 6. Strong downstream velocities were observed in the lower part of the study section. In campaign 2, strong upstream velocities were observed throughout the study section. Mean pool elevations for campaign 1 and 2 are 891.36 and 891.15 feet (National Geodetic Vertical Datum of 1929), respectively.

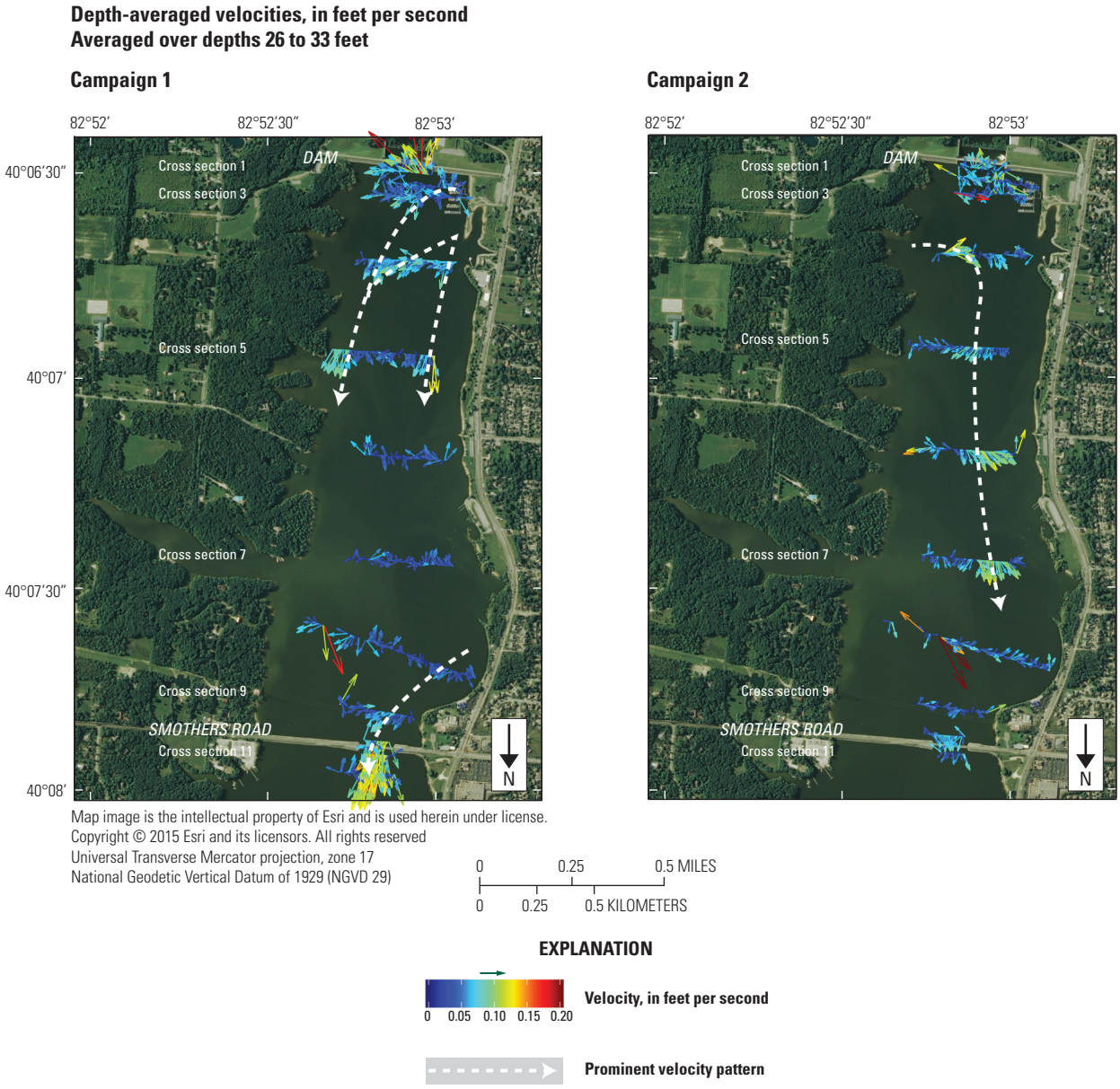

Figure 9. Comparison of campaign 1 and campaign 2 depth-averaged velocities for a depth of 26 to 33 feet with major circulation paths. In campaign 1, high downstream velocities were observed at the dam with upstream velocities in the rest of the lower to middle part of the study section. There were slow velocities through the middle to upper part of the study section until the bridge, which had strong upstream velocities. In campaign 2, there were slow velocities near the dam. Some moderate upstream velocities from cross section 4 through cross section 7. The upper study section had slow and mixed direction velocities except for some upstream flow through the bridge opening. Mean pool elevations for campaign 1 and 2 are 891.36 and 891.15 feet (National Geodetic Vertical Datum of 1929), respectively.

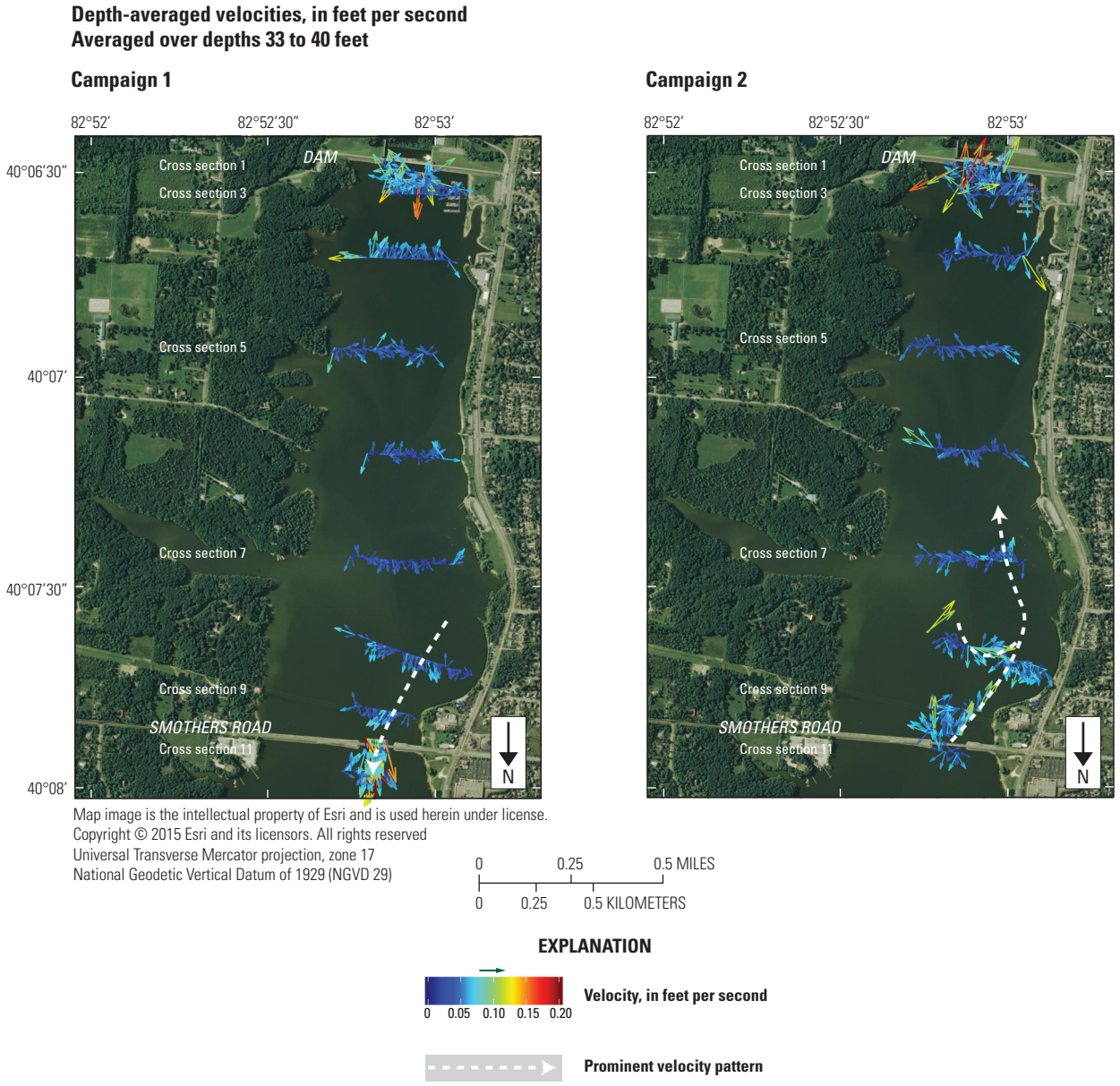

Figure 10. Comparison of campaign 1 and campaign 2 depth-averaged velocities for a depth of 33 to 40 feet with major circulation paths. In campaign 1, low velocities were seen throughout the study section except for some strong upstream velocities through the bridge. In campaign 2, slow velocities were observed throughout the study section; however, a series of downstream velocities were observed in the upper part of the study section. Mean pool elevations for campaign 1 and 2 are 891.36 and 891.15 feet (National Geodetic Vertical Datum of 1929), respectively.

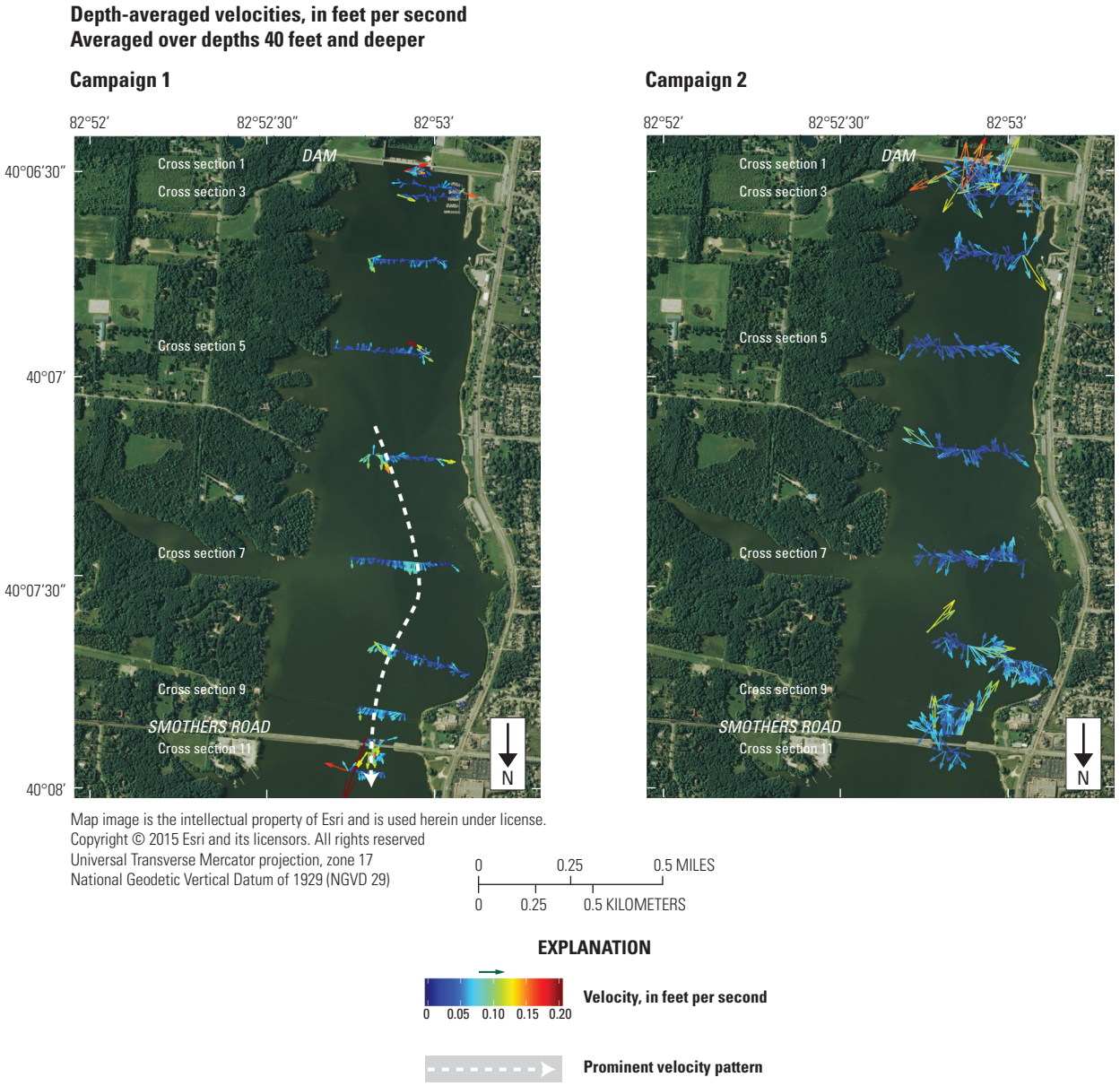

Figure 11. Comparison of campaign 1 and campaign 2 depth-averaged velocities for a depth of 40 feet to the bottom of the reservoir with major circulation paths. In campaign 1, the lower part of the study section had mostly slow velocities, whereas the upper part had primary upstream velocities. In campaign 2, slow velocities were present throughout the study section. Mean pool elevations for campaign 1 and 2 are 891.36 and 891.15 feet (National Geodetic Vertical Datum of 1929), respectively.

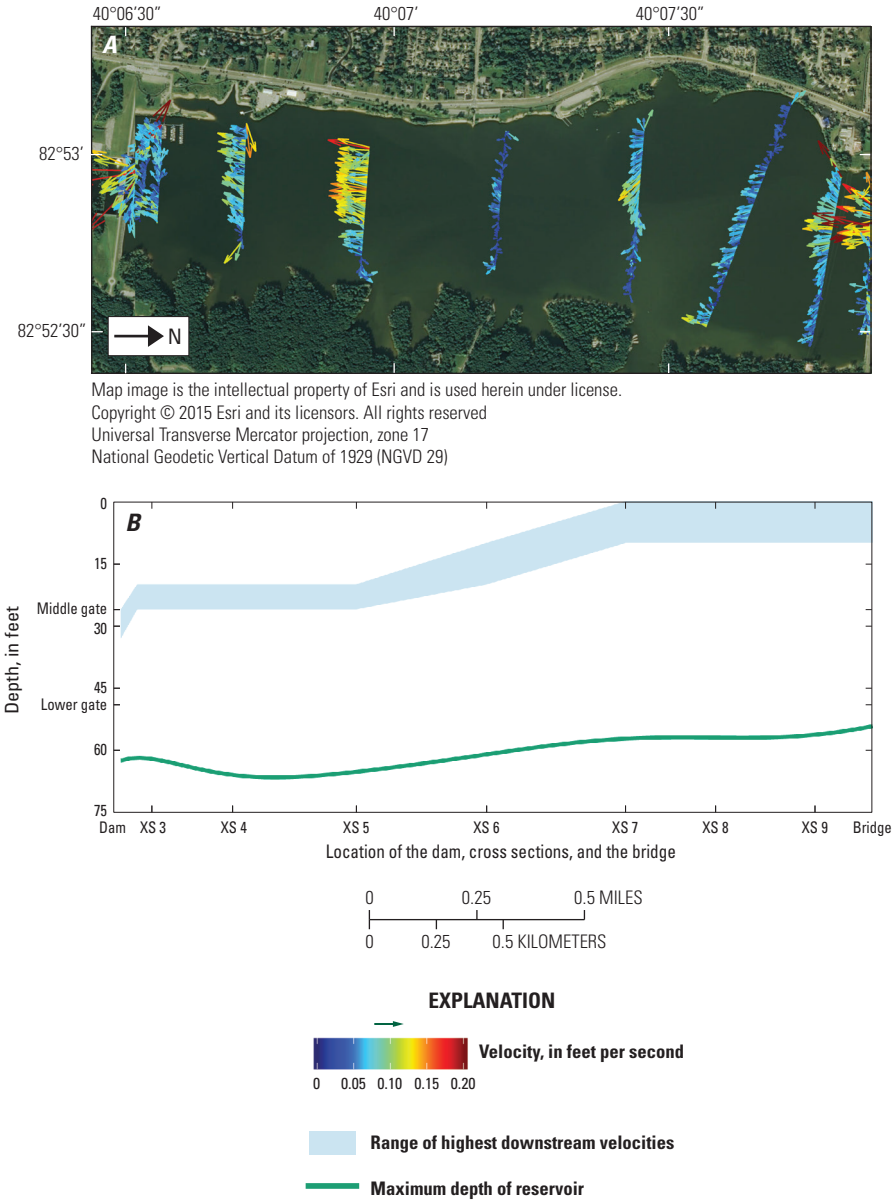

Figure 12. Highest downstream velocity and corresponding depth range at each cross section measured during campaign 1. *A*, highest velocities measured at each cross section during campaign 1 (as plotted in fig. 7 through fig. 11). *B*, the depth range the velocities in *A* were recorded at in reference to the water surface and the reservoir bottom. Mean pool elevations for campaign 1 and 2 are 891.36 and 891.15 ft (NGVD29), respectively.

which for campaign 1 was the depth range from which water was being discharged from the dam (Benjamin Ellsesser, City of Columbus, written commun., 2015).

Similar strong contiguous downstream paths were not present in campaign 2; however, strong downstream flow was observed along the surface near the bridge opening and then seemed to disperse into large slow areas of downstream velocities above and below the layer of high upstream flow discussed in the following section (appendix 1). It is also possible that the inability to measure near-bed flows with an ADCP may be responsible, in part, for the lack of contiguous downstream flow path data in campaign 2 (the ADCP used cannot measure the lower 6 percent of the flow depth due to acoustic interference with the bed).

Additionally, during campaign 2, depths from 10 to 26 ft show upstream flow through every cross section, with flow in the 20 to 26 ft range being particularly high in magnitude (figs. 7 and 8). This layer of high upstream flow was absent in campaign 1 and could result in shear forces that cause an increase in mixing between the depth layers above and below it.

Recirculation in the Upper Study Section

A circulatory pattern was identified in campaign 1 at depths from 0 to 26 ft between the bridge and cross section 6, where some of the water that entered the lower reservoir through the bridge opening followed the west bank and then turned and flowed back upstream along the east bank (figs. 6, 7, and 8). This flow pattern could result in increased cross-reservoir mixing and an increase residency time in the upper study section.

A similar circulation pattern was evident in campaign 2 for depths between 0 and 10 ft, in which water flowed downstream through the bridge and began to recirculate in cross sections 6 and 7 (fig. 6). However, cross sections 8 and 9 show little velocity in either direction and there is little evidence that the same pattern existed at the 10 to 20 ft depths (figs. 6 and 7).

Vertical Velocities

In campaign 1 and campaign 2, vertical velocities at depths less than 15 ft were primarily downward (negative), whereas vertical velocities at depths greater than 15 ft were primarily upward (positive) (fig. 13). At this depth, where upward velocities met downward velocities, there was likely a location of mixing between near-surface water and deeper water throughout both campaigns. Also, the settling of particles would have been slowed by the upward velocities present below 15 ft of depth.

Cross sections 1 through 4 in campaign 2 show distinct vertical stripes. Vertical water velocities are recorded relative to the ADCP, which is assumed to be on a flat surface. As a result, wave action can impart a false vertical velocity component that is added to the true vertical velocity component. After a review of the ADCP's pitch and roll data, it was determined that these stripes were a result of wave action and are therefore considered erroneous.

Water-Quality Data

Changes in water quality in the Hoover Reservoir study reach during August 25 to August 27, 2015, are presented and discussed in this section. The data are presented first as median profiles of each water-quality parameter over the water column for each field campaign. Additionally, contoured sections of water-quality parameters along the centerline of the reservoir (fig. 3, line C, endpoints 1 and 2) are presented, and differences between water-quality distributions with the middle gates operational and with the lower gates operational are discussed. Note that in order to best visualize the subtle differences between water-quality distributions in difference plots, the color-bar scale varies for each figure.

Water-Quality Profiles

Between August 25 and August 27, 2015, the depth of the epilimnion increased by nearly 5 ft (see temperature profiles in fig. 14 where the changes in the epilimnion are delineated for reference). During this period, the air temperature increased by approximately 5.6 °C, winds decreased from 7 miles per hour (mi/h) to 4 mi/h, no precipitation or storm events occurred, there was very little change in the pool elevation (-0.21 ft), and outflow from the reservoir decreased by about 3 percent (fig. 5). It is highly unlikely that any of these changes were substantial enough by themselves to drive the observed deepening of the epilimnion. Large storm events with high winds would be required to erode the thermocline at this depth (approximately 25 ft below the surface). Temperature profile data from the City of Columbus for the month of August 2015 shows that despite winds between 20 ft/s (13.6 mi/h) and 50 ft/s (34 mi/h) on August 10, 11, 12, and 17, the depth of the thermocline (defined by the base of the epilimnion) remained unchanged at a depth of approximately 20 ft. However, the epilimnion did deepen approximately 10 ft in response to the August 3, 2015, storm with winds gusting more than 40 ft/s (27.3 mi/h), but the thermocline was relatively shallow (approximately 7 ft deep) prior to the storm. A shallow thermocline is more susceptible to turbulence generated at the surface of the lake. Surface-generated turbulence weakens through dissipation of energy as depth increases; therefore, the energy or work required to disrupt the thermocline increases with increasing thickness of the epilimnion (Wetzel 2001). For reference, the lower gate was in operation for the first 3 weeks of August 2015 and no gate changes were made until August 21, 2015 (Matt Steele, City of Columbus, oral commun., February 14, 2016).

Based on the lack of response of a relatively deep thermocline (greater than 20 ft) to wind and storm events the first 3 weeks of August 2015, it is likely that the observed deepening

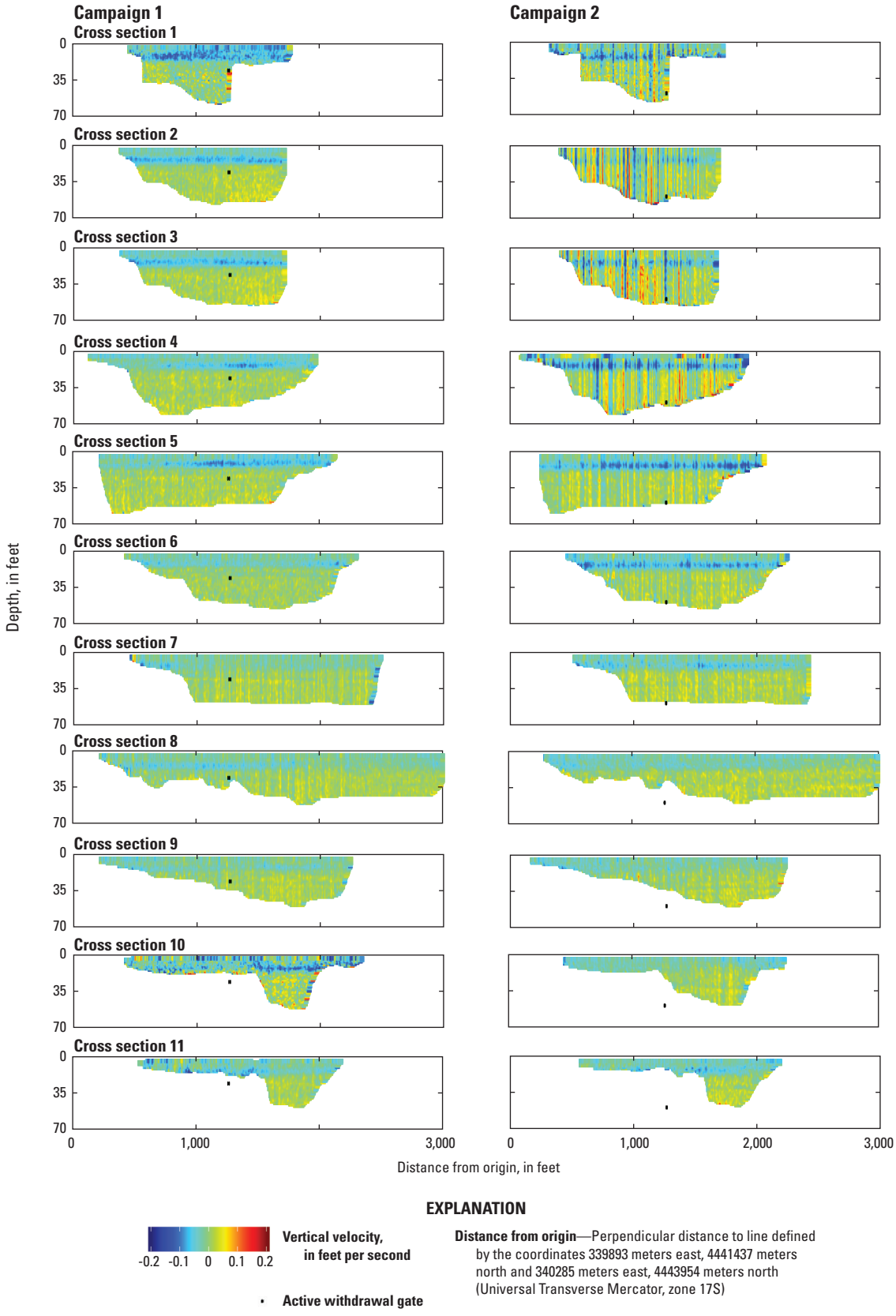

Figure 13. Vertical velocities for campaign 1 and campaign 2. Velocities flowing toward the surface are positive. Mean pool elevations for campaign 1 and 2 are 891.36 and 891.15 feet (National Geodetic Vertical Datum of 1929), respectively. The active withdrawal gate, scaled to actual size and location in the cross section, is shown for each cross section.

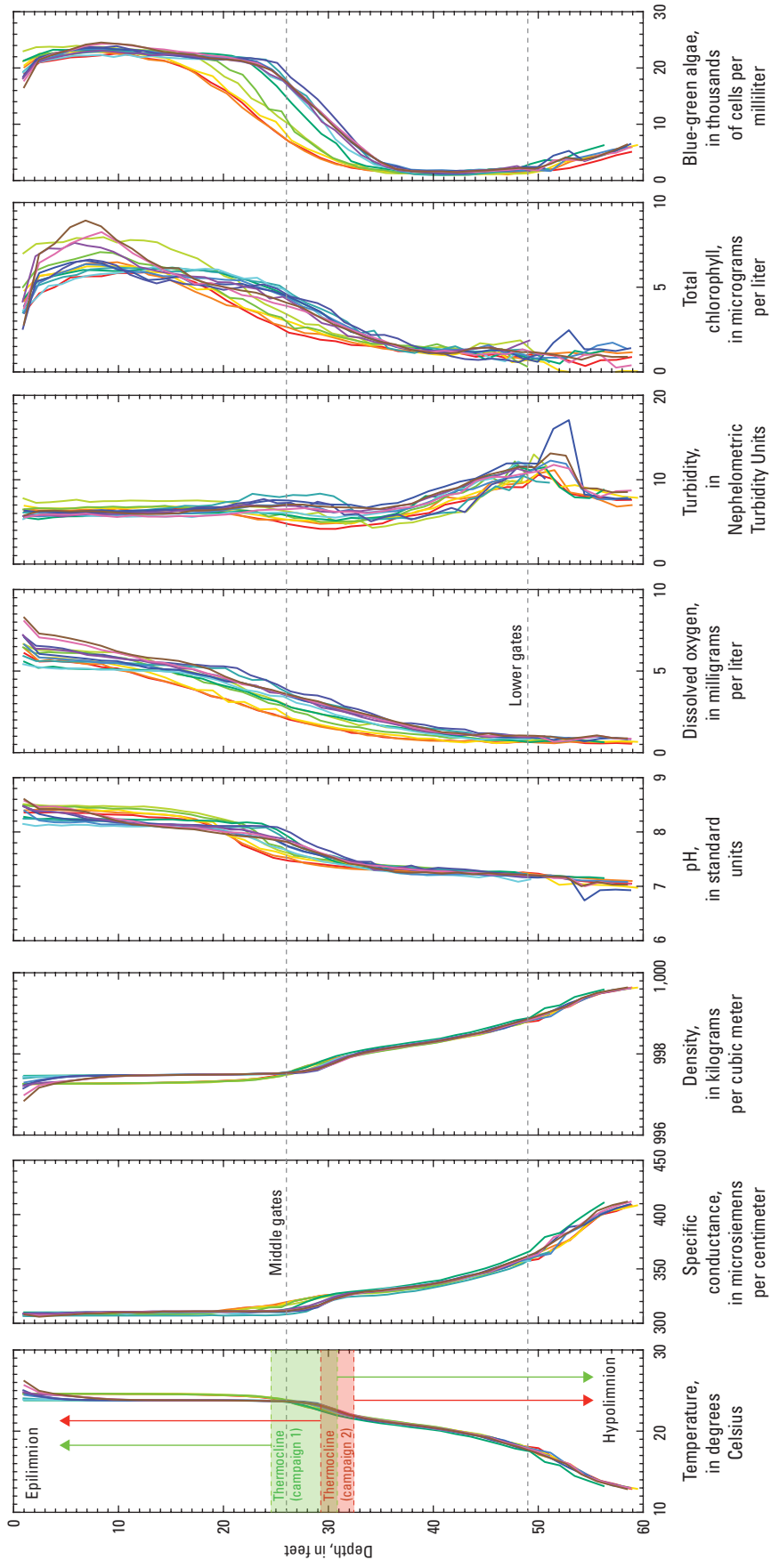

Figure 14. Median profiles of water-quality parameters as a function of depth for 14 surveys using the autonomous underwater vehicle (table 3). Mean pool elevations for campaign 1 and 2 are 891.36 and 891.15 feet (National Geodetic Vertical Datum of 1929), respectively.

of the epilimnion was caused by shifting withdrawals at the dam from the middle gate (August 25, 2015) to the lower gate (August 27, 2015). The approximate depths of these structures during the survey period was 26 ft and 49 ft for the middle and lower gates, respectively (mean pool elevations for campaign 1 and 2 are 891.36 and 891.15 ft [NGVD29], respectively).

At a depth of 26 ft, the middle gates withdrew water from near the base of the epilimnion, whereas the lower gates, at 49 ft, withdrew water from the hypolimnion. Based on the approximate surface area of the reservoir at the 30-ft contour (3.6×10^7 ft^2) and a change in the thermocline depth of 5 ft, the volume required to be exported from the hypolimnion to create such a change in the thermocline (in the absence of mixing) would be approximately 1.8×10^8 cubic feet. At a mean outflow rate of 163 ft^3/s, the volume of water withdrawn from the hypolimnion during the 48 hours between August 25 and August 27, 2015, was approximately 2.8×10^7 cubic feet. This volume of water removed from the hypolimnion would, in the absence of mixing, only produce a lowering of the thermocline by about 0.8 ft. The observed 5-ft change in the depth of the thermocline during 48 hours is more than 6 times greater than can be explained by volumetric exchange; therefore, it is hypothesized that the gate changes induced currents in the reservoir, especially at the depth of the thermocline where the greatest velocities were measured in campaign 2 (fig. 8), which enhanced shear-driven mixing processes at the thermocline and caused the epilimnion to deepen. It should be noted that in the several months prior to August 24, 2015, the lower gates were utilized for withdrawals from the reservoir. The middle gates were activated on August 21, 2015, for the purpose of this study (Matt Steele, City of Columbus, oral commun., February 14, 2016).

Profiles of water-quality parameters show no substantial variation between the east and west surveys (fig. 3, lines E and W) and the centerline survey (fig. 3, line C) (fig. 14). Surveys 4, 5, 7, 8, 11, and 12, which are off-center surveys (lines E and W), have very similar median profiles between the east side of the reservoir and the west side of the reservoir. Although masked in figure 14 by temporal variability and the numerous profiles plotted, these profiles were compared on a one-to-one basis with each other and with the nearest-in-time centerline profile and no substantial differences were observed in any of the measured parameters; therefore, the centerline surveys of water quality seem to be representative of the lower part of Hoover Reservoir and will be used for further comparisons.

Profiles of basic water-quality parameters collected by the automated profiler operated by the City of Columbus show good agreement with the median AUV profiles and better resolve the oxycline and vertical gradient in pH compared to AUV data (figs. 14 and 15). Four representative surveys were chosen: two during campaign 1 on August 25, 2015 (morning and afternoon) and two during campaign 2 on August 27, 2015 (morning and afternoon) for comparison. Profiles 87, 88, 99, and 101 collected by the City of Columbus profiler were the closest in time to the four AUV surveys and were used for comparison. There is good agreement between the median AUV profiles and the City of Columbus profiles for temperature, specific conductance, density, and turbidity (fig. 15). Because of a lag in the response time of dissolved oxygen and the pH sensors on the AUV, the vertical gradients of dissolved oxygen and pH across the thermocline are artificially smoothed, which resulted in apparently weaker dissolved oxygen and pH gradients compared to the City of Columbus profile data. The City of Columbus profiler uses the same sensors but profiles slowly in steps, which allows full equilibration of the sensors at each depth in the profile. The AUV is not able to traverse the water column slow enough to allow the sensors to fully equilibrate and still maintain stability and control. Sensors with faster response times are not currently (2017) commercially available for this AUV.

Finally, there is good general agreement between the profiles for total chlorophyll and blue-green algae concentration (fig. 15); however, differences exist, especially in total chlorophyll, due to differences in the calibration method for the AUV and the City of Columbus's sensors. The AUV sensors for both of these parameters were calibrated with a one-point calibration in deionized water (this method defines the sensor zero concentration point), whereas the City of Columbus used a two-point calibration with deionized water and a 110-µg/L rhodamine WT solution for the chlorophyll sensor, and a single-point deionized water calibration for the phycocyanin sensor. A one-point calibration in deionized water effectively allows the AUV to collect relative, but not absolute, concentrations for these parameters. For this reason, the trends in the median AUV profiles for total chlorophyll and blue-green algae match the City of Columbus profiles, but the magnitudes differ slightly. Despite the differences in magnitudes, the relative concentrations given by the AUV for these two parameters are sufficient to evaluate any change in concentration distributions due to operational gate changes at the dam at Hoover Reservoir.

Water-Quality Sections

The observations in this section are presented by parameter, and for simplicity, two pairs of centerline surveys were used to compare the spatial distribution of water-quality parameters in lower Hoover Reservoir between August 25 and August 27, 2015. The surveys chosen for comparison are surveys 1 and 6 and surveys 3 and 14 (table 3). These paired surveys were chosen to ascertain differences between morning (surveys 1 and 6) and afternoon (surveys 3 and 14) water-quality distributions when dam releases were being made from the middle and lower gates. Difference plots were prepared for the paired surveys to highlight the otherwise subtle changes in water quality arising from these gate changes and other factors. All survey results plotted in this section of the report (figs. 16 through 39) were prepared from data collected along the approximate centerline of the reservoir from point 1 to point 2 (fig. 3, line C). The cross sections in these figures are oriented such that they are viewed looking west (see fig. 3), where the dam is nearest point 1 (left side of figure) and the Smothers Road Bridge is nearest point 2 (right side of figure).

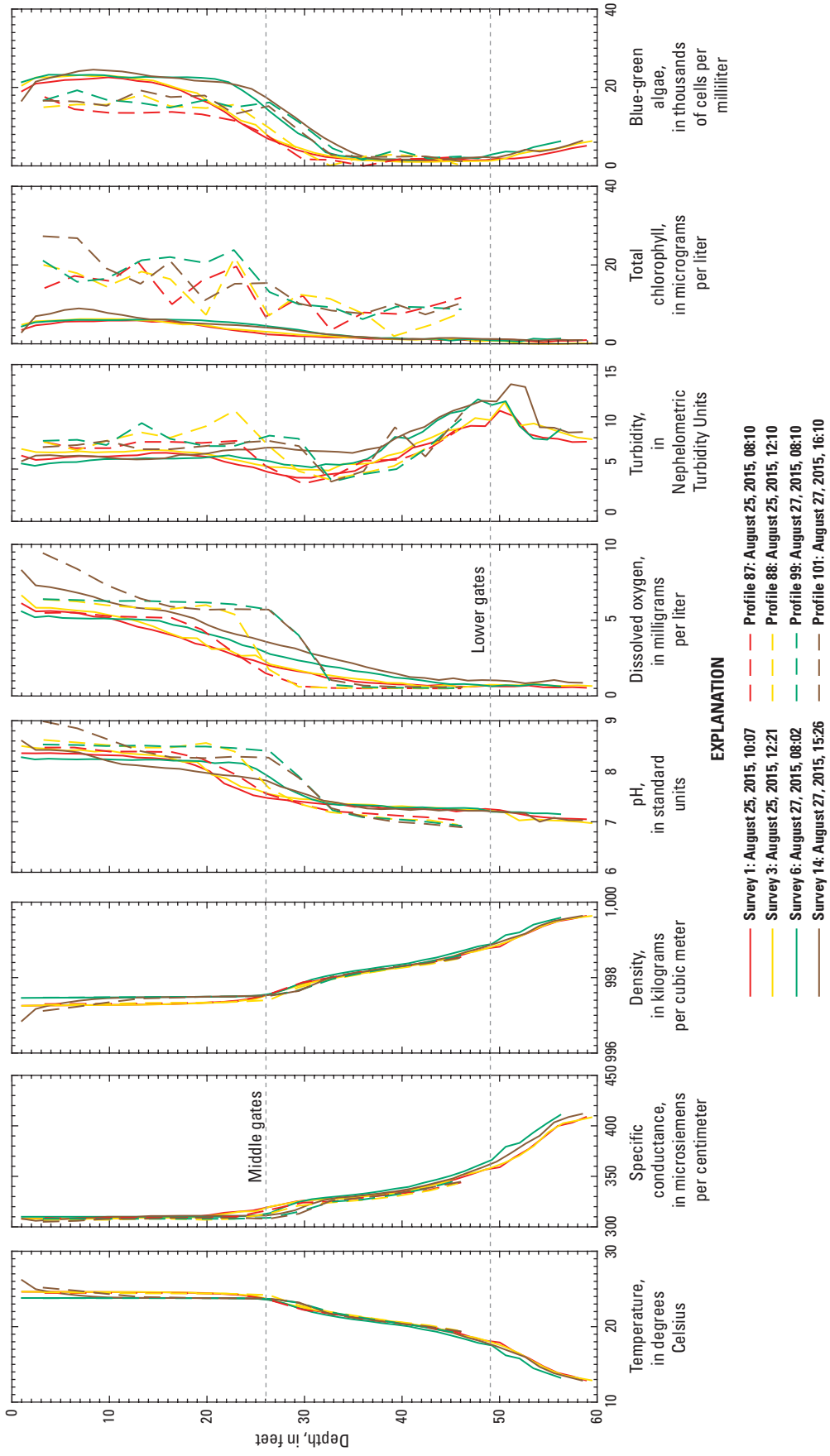

Figure 15. Median profiles of water-quality parameters as a function of depth for four representative surveys using the autonomous underwater vehicle (AUV) compared with the profiles nearest in time to each AUV survey by the automated profiler operated by the City of Columbus, Ohio. Mean pool elevations for campaign 1 and 2 are 891.36 and 891.15 feet (National Geodetic Vertical Datum of 1929), respectively.

Temperature

With the exception of the surface layer (0 to 3 ft below the surface), the epilimnion decreased in temperature and the hypolimnion increased in temperature between August 25 and 27, 2015 (figs. 16, 17, and 18). The epilimnion decreased in temperature by approximately 0.5 to 1 °C between surveys over the full depth of the mixed layer; however, the afternoon surveys show a nearly 2 °C increase in the surface layer (fig. 18), likely due to solar heating and the 5.6 °C increase in air temperature between the surveys. Despite the increase in the surface layer driven by atmospheric forcing, the remainder of the epilimnion cooled. A possible explanation for this decrease in temperature in the epilimnion is enhanced mixing across the thermocline bringing deeper, colder water up from the hypolimnion. Such mixing would also mix warmer, epilimnetic water into the hypolimnion and raise the temperature of the water below the thermocline, which is consistent with what was observed (figs. 17 and 18). Unlike the epilimnion, where the temperature change was approximately uniform over the depth, the changes in the hypolimnion were confined to bands mostly near the thermocline and near depressions in the bed (figs. 17 and 18). This nonuniform distribution is likely an artifact of the linear stratification of the hypolimnion, which suppresses mixing. In density stratified flows, gravitational forces fight to restore equilibrium to a water column disturbed by mixing processes; thus, stratification can inhibit mixing over the full water column or over a stratified region like the hypolimnion. The most significant increase in temperature was in the 25 to 30 ft depth interval where the thermocline deepened. Comparison of the morning surveys (surveys 1 and 6; fig. 17) also reveals a substantial (approximately 1 °C) rise in temperature of the near-bed water, especially within depressions, near the level of the lower gate.

Specific Conductance

The greatest changes in specific conductance between August 25 and 27, 2015, were along the thermocline and at the base of the epilimnion (figs. 19, 20, and 21). As the epilimnion deepened following the change to the lower gates, it seems that higher specific conductance water at the top of the hypolimnion mixed across the thermocline with lower specific conductance water in the epilimnion, which created an overall band of decreased specific conductance along the 25 to 30 ft depth interval. Interestingly, the morning (fig. 20) and afternoon (fig. 21) survey comparisons show this band along the thermocline thickening as one moves upstream away from the dam. Near point 2 (close to the Smothers Road Bridge), the layer of negative change in specific conductance is nearly twice the thickness of that near the dam. This thickness of this layer, combined with the fact that the greatest changes are observed away from the dam and that figure 9 shows the highest velocities in the survey are at the depth of the thermocline and at the Smothers Road Bridge constriction, may indicate that the shear-driven mixing just south of Smothers Road is stronger than mixing near the dam. Such enhanced mixing could, in part, be associated with the constrained, bidirectional flow observed through the Smothers Road Bridge opening, which produces stronger shear at the thermocline (see the "Velocity Data" section).

Density

The density of the water in Hoover Reservoir is controlled primarily by temperature; therefore, it is not surprising that the changes in density observed between August 25 and 27, 2015, closely follow the changes observed in temperature. In general, the epilimnion increased in density (with the exception of the surface layer) and the hypolimnion remained unchanged or decreased in density, with the most substantial changes occurring along the thermocline and in depressions in the bed (figs. 22, 23, and 24). Like temperature, the hypolimnion shows banded changes with little change over much of this layer and the primary changes concentrated near the thermocline and near the bed. Once again, this is likely a result of the linear stratification in the hypolimnion suppressing the mixing. Except for the surface layer on the afternoon survey comparison (fig. 24), the increase in density in epilimnion is relatively uniform over this well-mixed layer.

Dissolved Oxygen

Changes in the dissolved oxygen distribution between campaigns 1 and 2 are primarily constrained to the central part of the water column near the thermocline and within the epilimnion (figs. 15, 25, 26, and 27). Despite the artificial smoothing of the vertical gradients in dissolved oxygen produced by the lag in the response time of the AUV dissolved oxygen sensor, the general changes in dissolved oxygen can be inferred from figures 26 and 27 and subsidized by dissolved oxygen data from the City of Columbus profiler (fig. 15). The mixing associated with the deepening of the epilimnion drives dissolved oxygen deeper into the water column and dissolved oxygen concentrations in the 15 to 33 ft depth interval increased between 2 to 5 milligrams per liter (mg/L) between August 25 and 27, 2015 (figs. 15, 26, and 27). City of Columbus profiles show little to no change during the study period in dissolved oxygen in the hypolimnion below 33 ft; however, AUV data shows a 0 to 1 mg/L increase to a depth of about 40 ft (fig. 15). The difference is due primarily to the sensor response time lag and City of Columbus profiles are a better representation of reality due to the equilibration of their sensors at each depth interval during profiling. It should be noted that the dissolved oxygen in the top 15 to 20 ft of the water column was significantly higher (greater than 2 mg/L) in the afternoon of August 27, 2015, compared to other surveys during the study period. This difference is likely due to oxygen production during photosynthesis in daylight hours, as evidenced by observations of higher concentrations of total chlorophyll and blue-green algae in the afternoon of August 27, 2015 (presented later in this section).

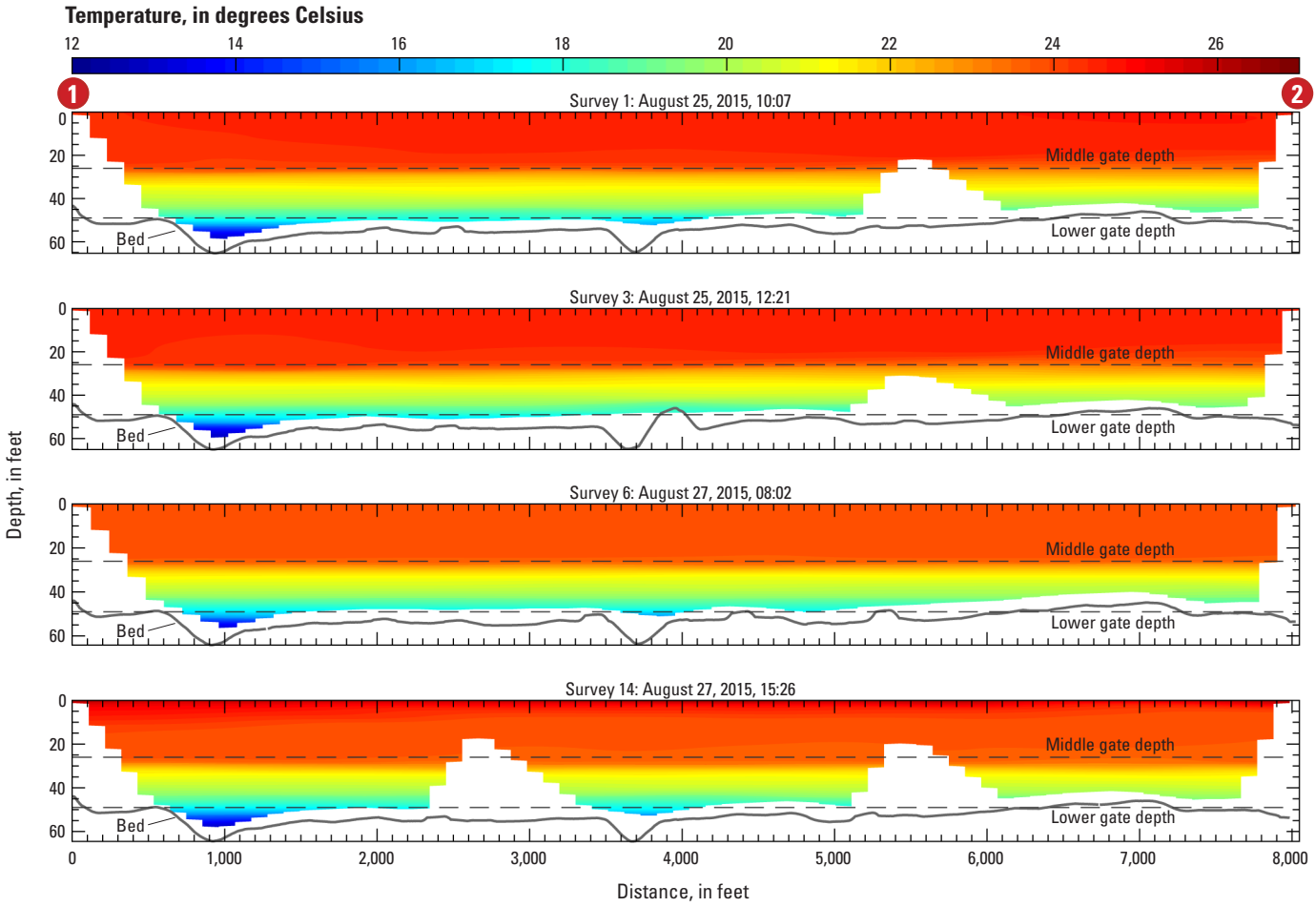

EXPLANATION

[All cross sections are plotted along the approximate centerline of the reservoir from point 1 to point 2 (fig. 3, line C) where the dam is nearest point 1 (left side of figure) and the bridge at Smothers Road is nearest point 2 (right side of the figure). Mean pool elevation for campaign 1 is 891.36. Mean pool elevation for campaign 2 is 891.15 feet. National Geodetic Vertical Datum of 1929]

1 **Numerical marker that provides a reference point (fig. 3)**

Figure 16. Temperature distributions in lower Hoover Reservoir for August 25 (surveys 1 and 3) and August 27, 2015 (surveys 6 and 14). All cross sections plotted are along the approximate centerline of the reservoir from point 1 to point 2 (fig. 3, line C) where the dam is nearest point 1 (left side of figure) and the Smothers Road Bridge is nearest point 2 (right side of figure). Mean pool elevations for campaign 1 and 2 are 891.36 and 891.15 feet (National Geodetic Vertical Datum of 1929), respectively.

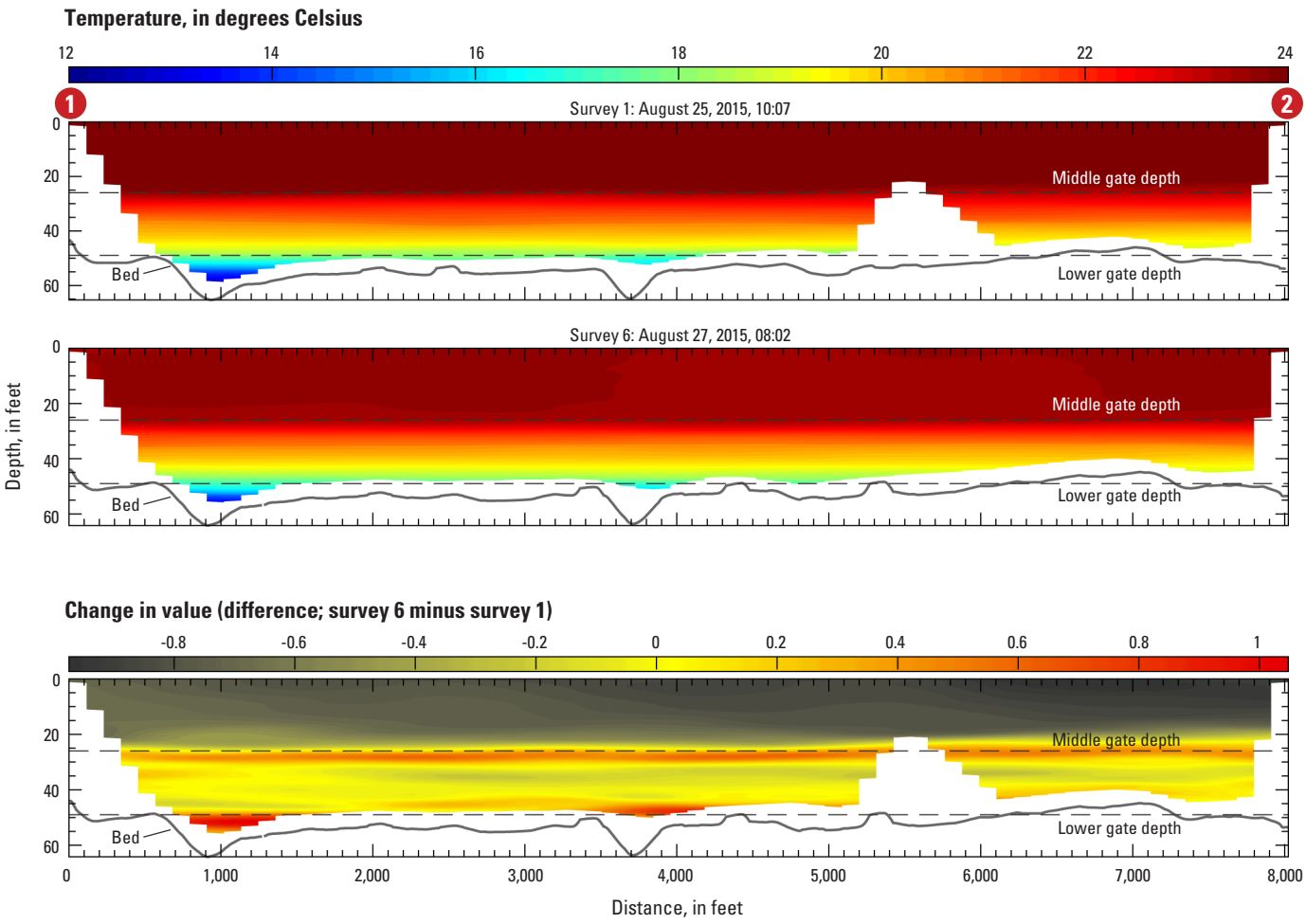

EXPLANATION

[All cross sections are plotted along the approximate centerline of the reservoir from point 1 to point 2 (fig. 3, line C) where the dam is nearest point 1 (left side of figure) and the bridge at Smothers Road is nearest point 2 (right side of the figure). Mean pool elevation for campaign 1 is 891.36. Mean pool elevation for campaign 2 is 891.15 feet. National Geodetic Vertical Datum of 1929]

1 **Numerical marker that provides a reference point (fig. 3)**

Figure 17. Temperature distributions in lower Hoover Reservoir for morning surveys (surveys 1 and 6) on August 25 and August 27, 2015, and their difference (survey 6 minus survey 1). All cross sections plotted are along the approximate centerline of the reservoir from point 1 to point 2 (fig. 3, line C) where the dam is nearest point 1 (left side of figure) and the Smothers Road Bridge is nearest point 2 (right side of figure). Mean pool elevations for campaign 1 and 2 are 891.36 and 891.15 feet (National Geodetic Vertical Datum of 1929), respectively.

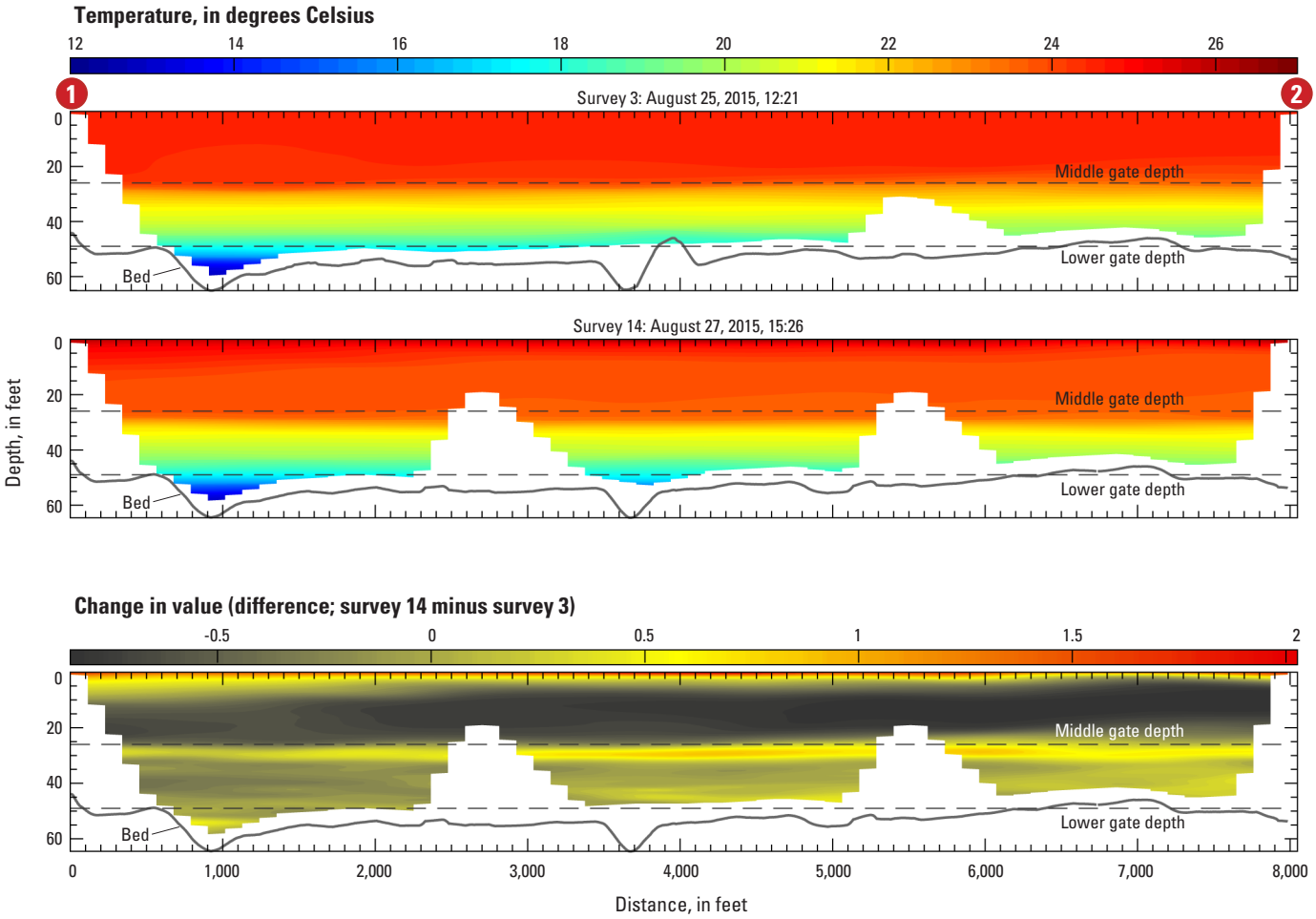

EXPLANATION

[All cross sections are plotted along the approximate centerline of the reservoir from point 1 to point 2 (fig. 3, line C) where the dam is nearest point 1 (left side of figure) and the bridge at Smothers Road is nearest point 2 (right side of the figure). Mean pool elevation for campaign 1 is 891.36. Mean pool elevation for campaign 2 is 891.15 feet. National Geodetic Vertical Datum of 1929]

1 **Numerical marker that provides a reference point (fig. 3)**

Figure 18. Temperature distributions in lower Hoover Reservoir for afternoon surveys (surveys 3 and 14) on August 25 and August 27, 2015, and their difference (survey 14 minus survey 3). All cross sections plotted are along the approximate centerline of the reservoir from point 1 to point 2 (fig. 3, line C) where the dam is nearest point 1 (left side of figure) and the Smothers Road Bridge is nearest point 2 (right side of figure). Mean pool elevations for campaign 1 and 2 are 891.36 and 891.15 feet (National Geodetic Vertical Datum of 1929), respectively.

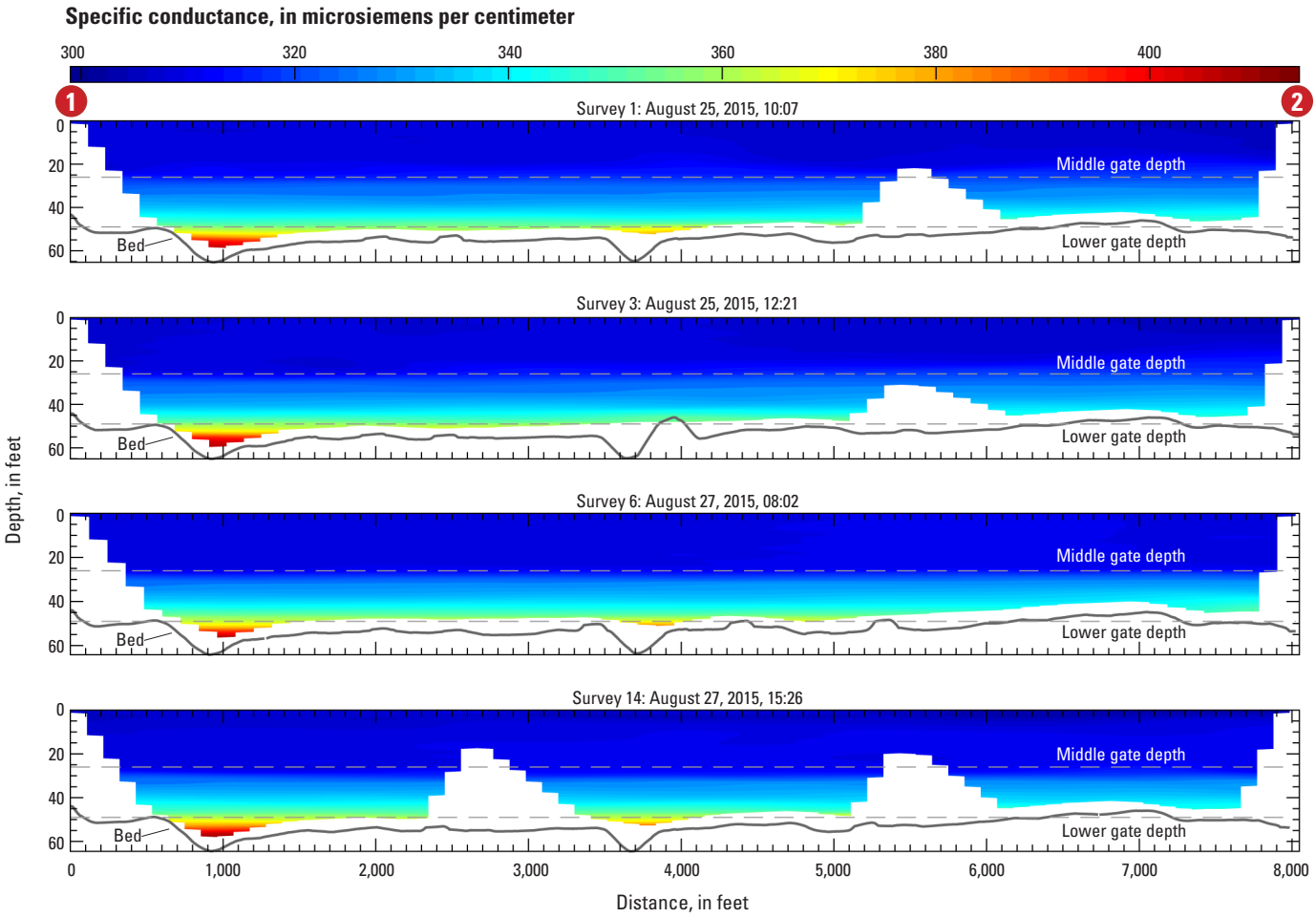

EXPLANATION

[All cross sections are plotted along the approximate centerline of the reservoir from point 1 to point 2 (fig. 3, line C) where the dam is nearest point 1 (left side of figure) and the bridge at Smothers Road is nearest point 2 (right side of the figure). Mean pool elevation for campaign 1 is 891.36. Mean pool elevation for campaign 2 is 891.15 feet. National Geodetic Vertical Datum of 1929]

1 **Numerical marker that provides a reference point (fig. 3)**

Figure 19. Specific conductance distributions in lower Hoover Reservoir for August 25 (surveys 1 and 3) and August 27, 2015 (surveys 6 and 14). All cross sections plotted are along the approximate centerline of the reservoir from point 1 to point 2 (fig. 3, line C) where the dam is nearest point 1 (left side of figure) and the Smothers Road Bridge is nearest point 2 (right side of figure). Mean pool elevations for campaign 1 and 2 are 891.36 and 891.15 feet (National Geodetic Vertical Datum of 1929), respectively.

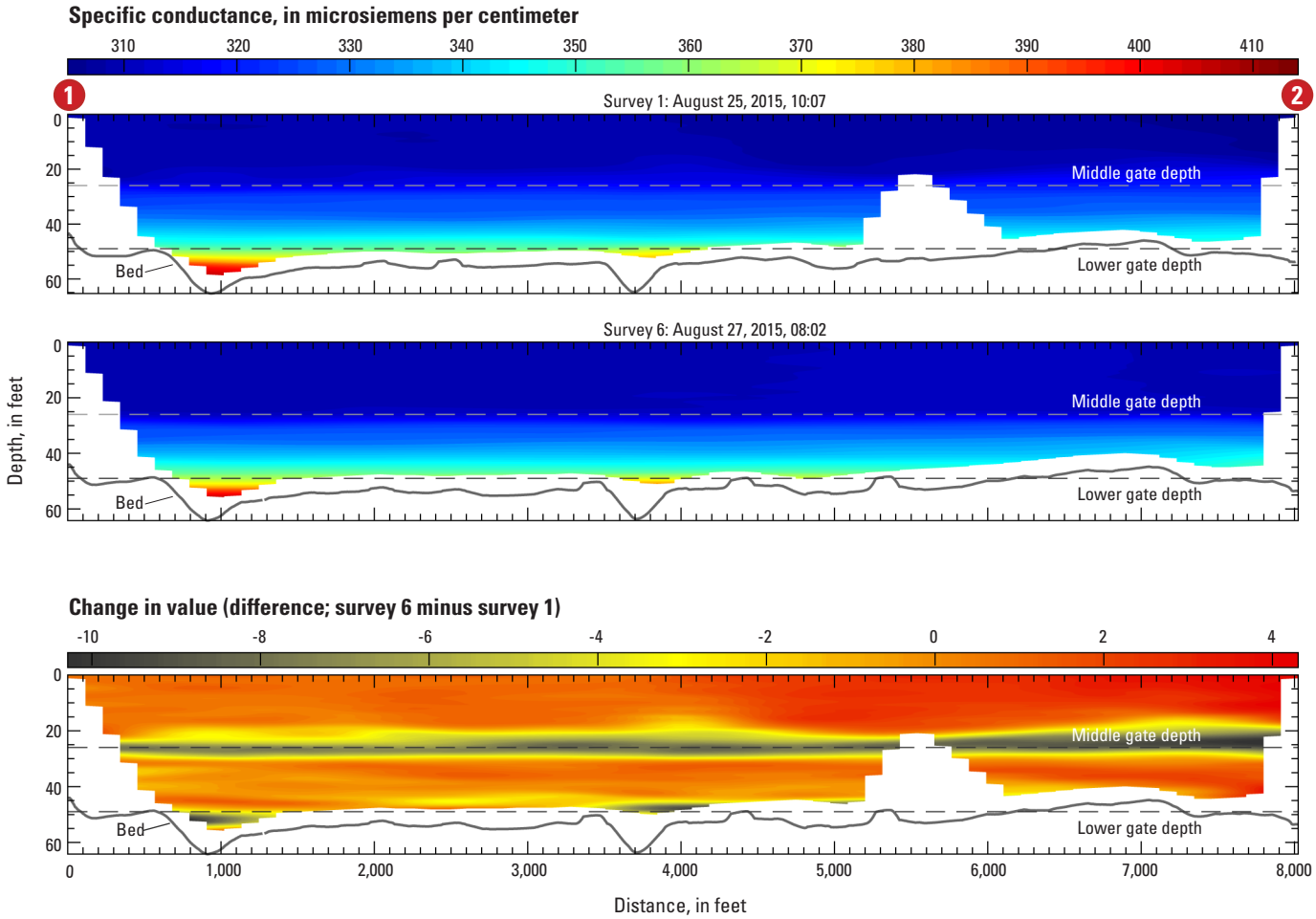

EXPLANATION

[All cross sections are plotted along the approximate centerline of the reservoir from point 1 to point 2 (fig. 3, line C) where the dam is nearest point 1 (left side of figure) and the bridge at Smothers Road is nearest point 2 (right side of the figure). Mean pool elevation for campaign 1 is 891.36. Mean pool elevation for campaign 2 is 891.15 feet. National Geodetic Vertical Datum of 1929]

1 **Numerical marker that provides a reference point (fig. 3)**

Figure 20. Specific conductance distributions in lower Hoover Reservoir for morning surveys (surveys 1 and 6) on August 25 and August 27, 2015, and their difference (survey 6 minus survey 1). All cross sections plotted are along the approximate centerline of the reservoir from point 1 to point 2 (fig. 3, line C) where the dam is nearest point 1 (left side of figure) and the Smothers Road Bridge is nearest point 2 (right side of figure). Mean pool elevations for campaign 1 and 2 are 891.36 and 891.15 feet (National Geodetic Vertical Datum of 1929), respectively.

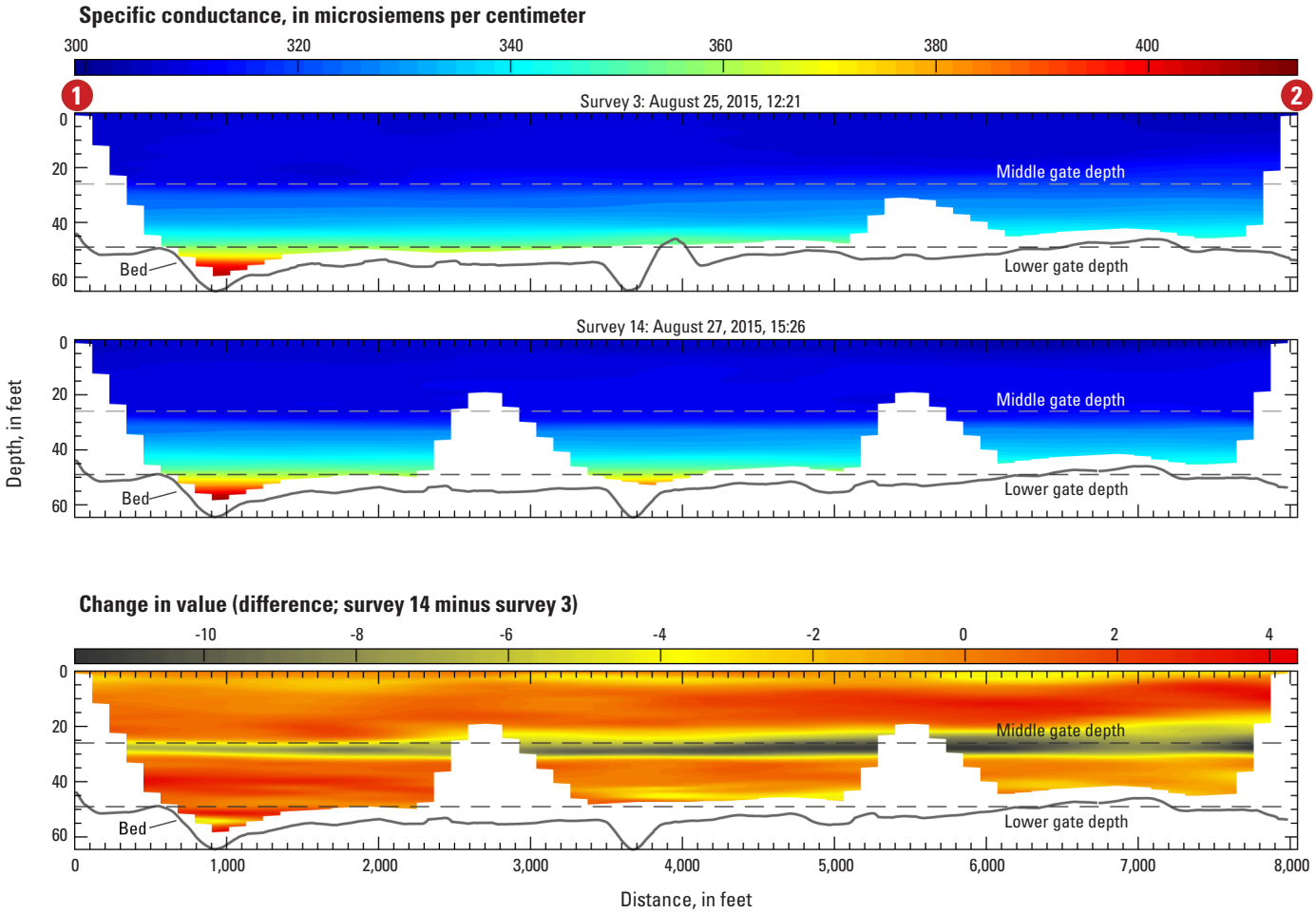

EXPLANATION

[All cross sections are plotted along the approximate centerline of the reservoir from point 1 to point 2 (fig. 3, line C) where the dam is nearest point 1 (left side of figure) and the bridge at Smothers Road is nearest point 2 (right side of the figure). Mean pool elevation for campaign 1 is 891.36. Mean pool elevation for campaign 2 is 891.15 feet. National Geodetic Vertical Datum of 1929]

1 **Numerical marker that provides a reference point (fig. 3)**

Figure 21. Specific conductance distributions in lower Hoover Reservoir for afternoon surveys (surveys 3 and 14) on August 25 and August 27, 2015, and their difference (survey 14 minus survey 3). All cross sections plotted are along the approximate centerline of the reservoir from point 1 to point 2 (fig. 3, line C) where the dam is nearest point 1 (left side of figure) and the Smothers Road Bridge is nearest point 2 (right side of figure). Mean pool elevations for campaign 1 and 2 are 891.36 and 891.15 feet (National Geodetic Vertical Datum of 1929), respectively.

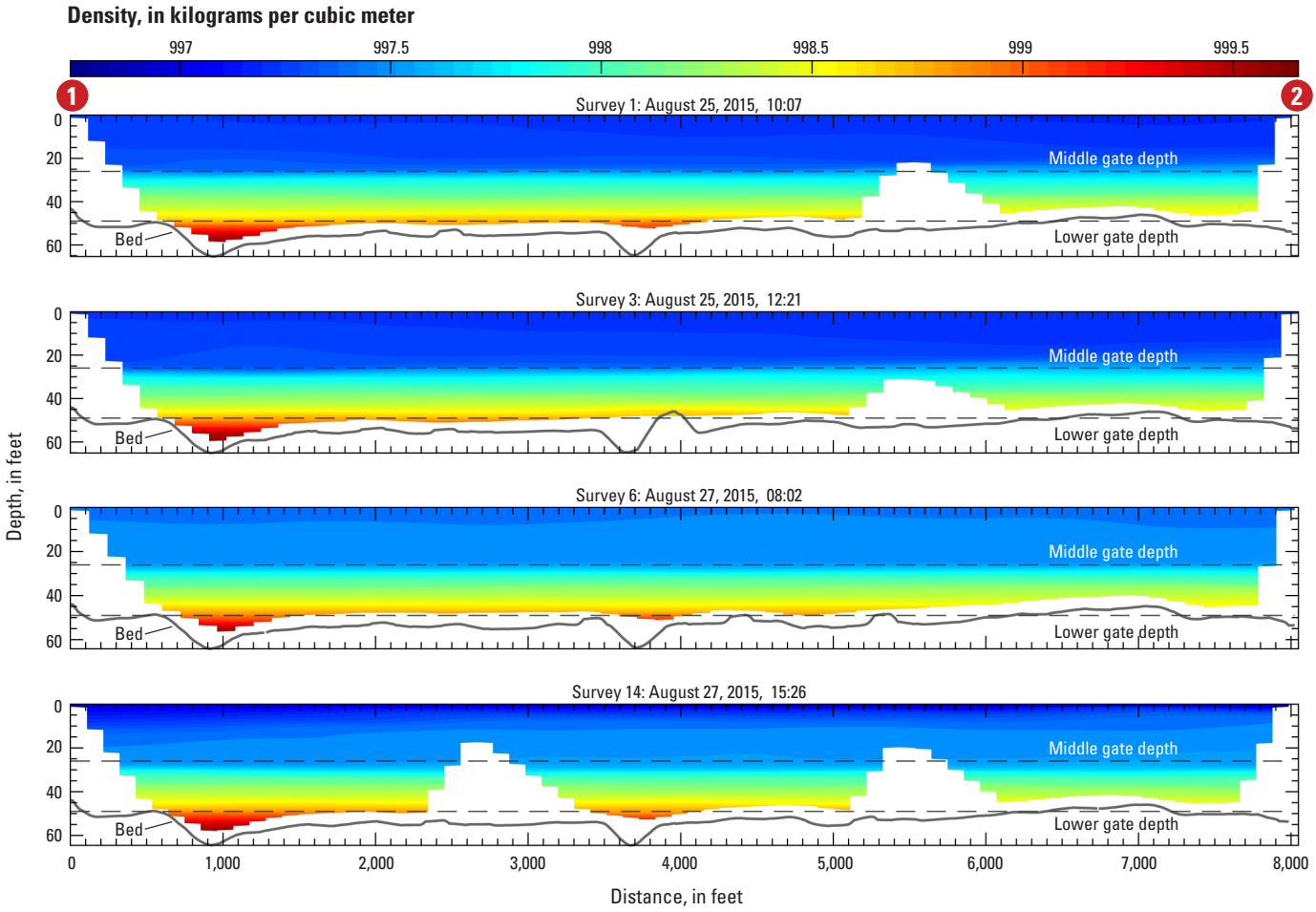

EXPLANATION

[All cross sections are plotted along the approximate centerline of the reservoir from point 1 to point 2 (fig. 3, line C) where the dam is nearest point 1 (left side of figure) and the bridge at Smothers Road is nearest point 2 (right side of the figure). Mean pool elevation for campaign 1 is 891.36. Mean pool elevation for campaign 2 is 891.15 feet. National Geodetic Vertical Datum of 1929]

1 **Numerical marker that provides a reference point (fig. 3)**

Figure 22. Density distributions in lower Hoover Reservoir for August 25 (surveys 1 and 3) and August 27, 2015 (surveys 6 and 14). All cross sections plotted are along the approximate centerline of the reservoir from point 1 to point 2 (fig. 3, line C) where the dam is nearest point 1 (left side of figure) and the Smothers Road Bridge is nearest point 2 (right side of figure). Mean pool elevations for campaign 1 and 2 are 891.36 and 891.15 feet (National Geodetic Vertical Datum of 1929), respectively.

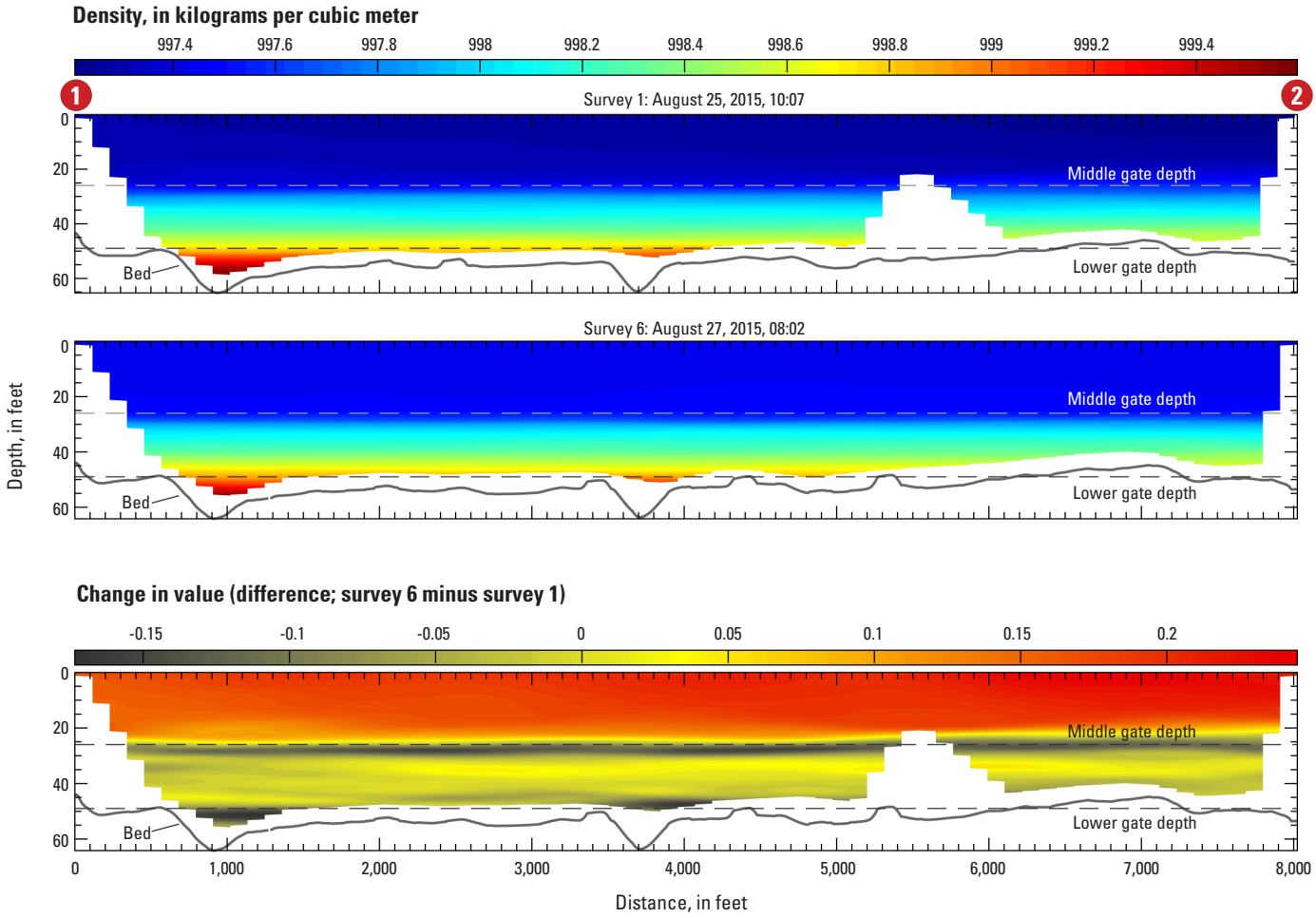

EXPLANATION

[All cross sections are plotted along the approximate centerline of the reservoir from point 1 to point 2 (fig. 3, line C) where the dam is nearest point 1 (left side of figure) and the bridge at Smothers Road is nearest point 2 (right side of the figure). Mean pool elevation for campaign 1 is 891.36. Mean pool elevation for campaign 2 is 891.15 feet. National Geodetic Vertical Datum of 1929]

1 **Numerical marker that provides a reference point (fig. 3)**

Figure 23. Density distributions in lower Hoover Reservoir for morning surveys (surveys 1 and 6) on August 25 and August 27, 2015, and their difference (survey 6 minus survey 1). All cross sections plotted are along the approximate centerline of the reservoir from point 1 to point 2 (fig. 3, line C) where the dam is nearest point 1 (left side of figure) and the Smothers Road Bridge is nearest point 2 (right side of figure). Mean pool elevations for campaign 1 and 2 are 891.36 and 891.15 feet (National Geodetic Vertical Datum of 1929), respectively.

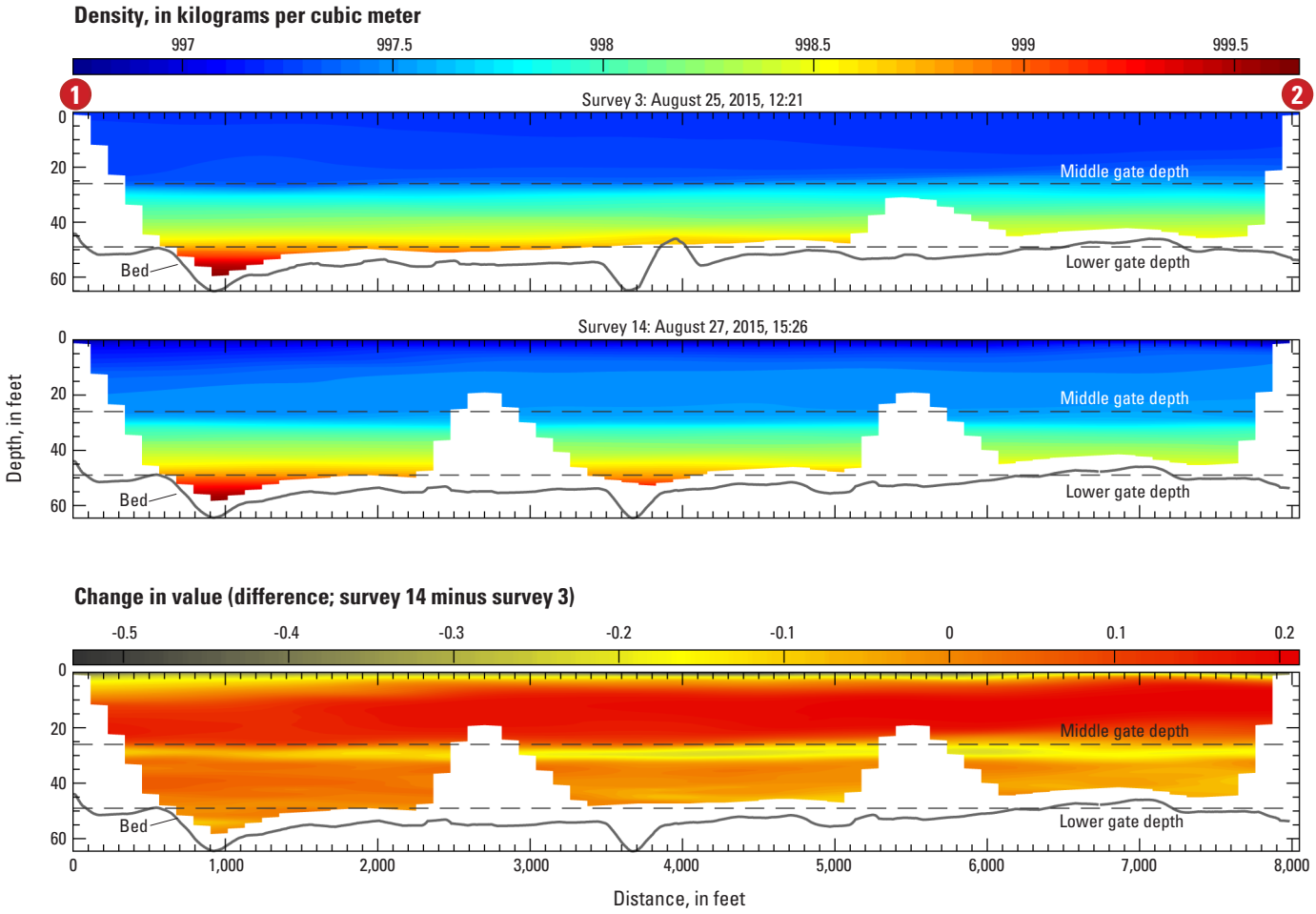

EXPLANATION

[All cross sections are plotted along the approximate centerline of the reservoir from point 1 to point 2 (fig. 3, line C) where the dam is nearest point 1 (left side of figure) and the bridge at Smothers Road is nearest point 2 (right side of the figure). Mean pool elevation for campaign 1 is 891.36. Mean pool elevation for campaign 2 is 891.15 feet. National Geodetic Vertical Datum of 1929]

1 **Numerical marker that provides a reference point (fig. 3)**

Figure 24. Density distributions in Lower Hoover Reservoir for afternoon surveys (surveys 3 and 14) on August 25 and August 27, 2015, and their difference (survey 14 – survey 3). All cross sections plotted are along the approximate centerline of the reservoir from point 1 to point 2 (fig. 3, line C) where the dam is nearest point 1 (left side of figure) and the Smothers Road Bridge is nearest point 2 (right side of figure). Mean pool elevations for campaign 1 and 2 are 891.36 and 891.15 feet (National Geodetic Vertical Datum of 1929), respectively.

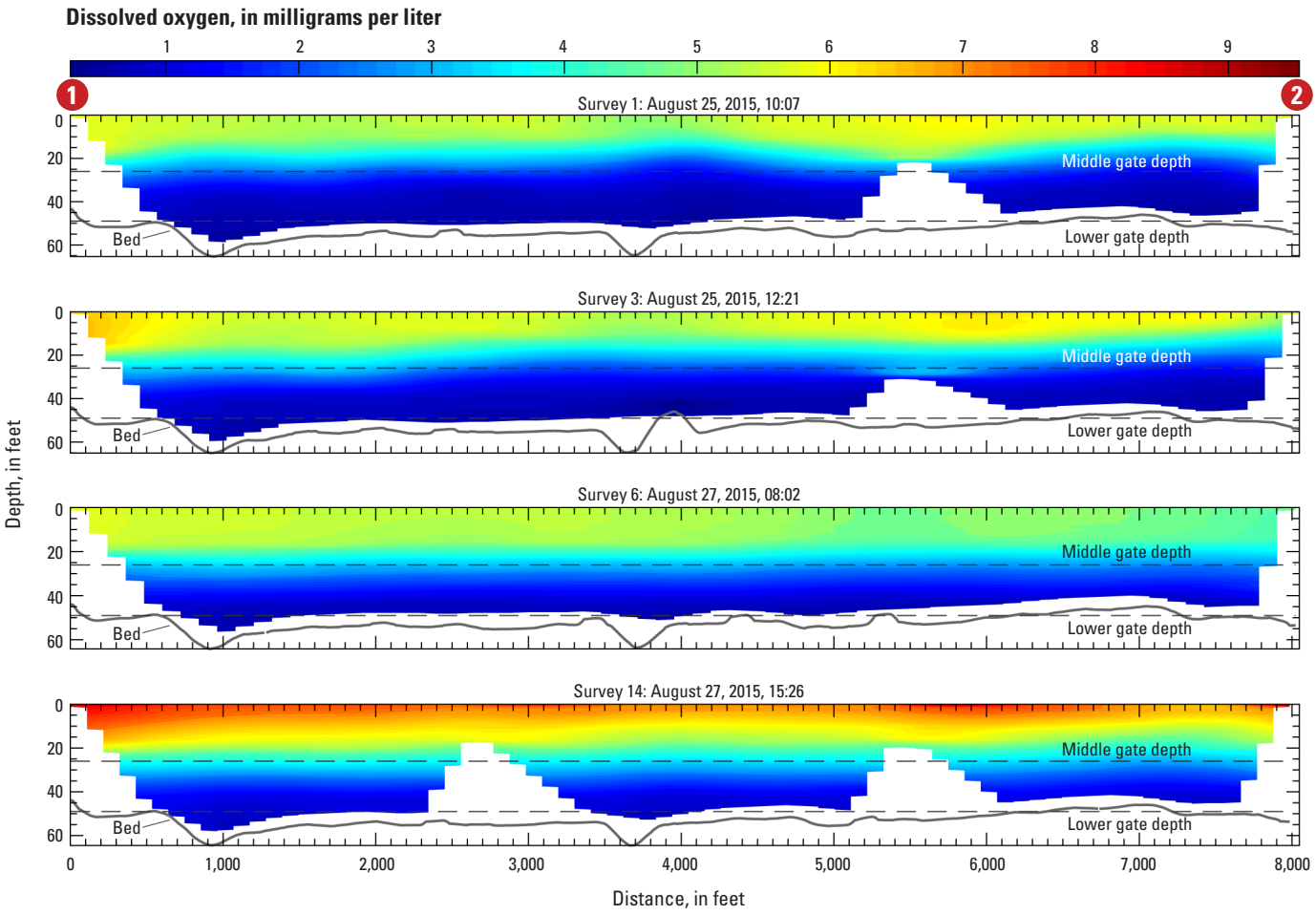

EXPLANATION

[All cross sections are plotted along the approximate centerline of the reservoir from point 1 to point 2 (fig. 3, line C) where the dam is nearest point 1 (left side of figure) and the bridge at Smothers Road is nearest point 2 (right side of the figure). Mean pool elevation for campaign 1 is 891.36. Mean pool elevation for campaign 2 is 891.15 feet. National Geodetic Vertical Datum of 1929]

1 **Numerical marker that provides a reference point (fig. 3)**

Figure 25. Dissolved oxygen distributions in lower Hoover Reservoir for August 25 (surveys 1 and 3) and August 27, 2015 (surveys 6 and 14). All cross sections plotted are along the approximate centerline of the reservoir from point 1 to point 2 (fig. 3, line C) where the dam is nearest point 1 (left side of figure) and the Smothers Road Bridge is nearest point 2 (right side of figure). Mean pool elevations for campaign 1 and 2 are 891.36 and 891.15 feet (National Geodetic Vertical Datum of 1929), respectively.

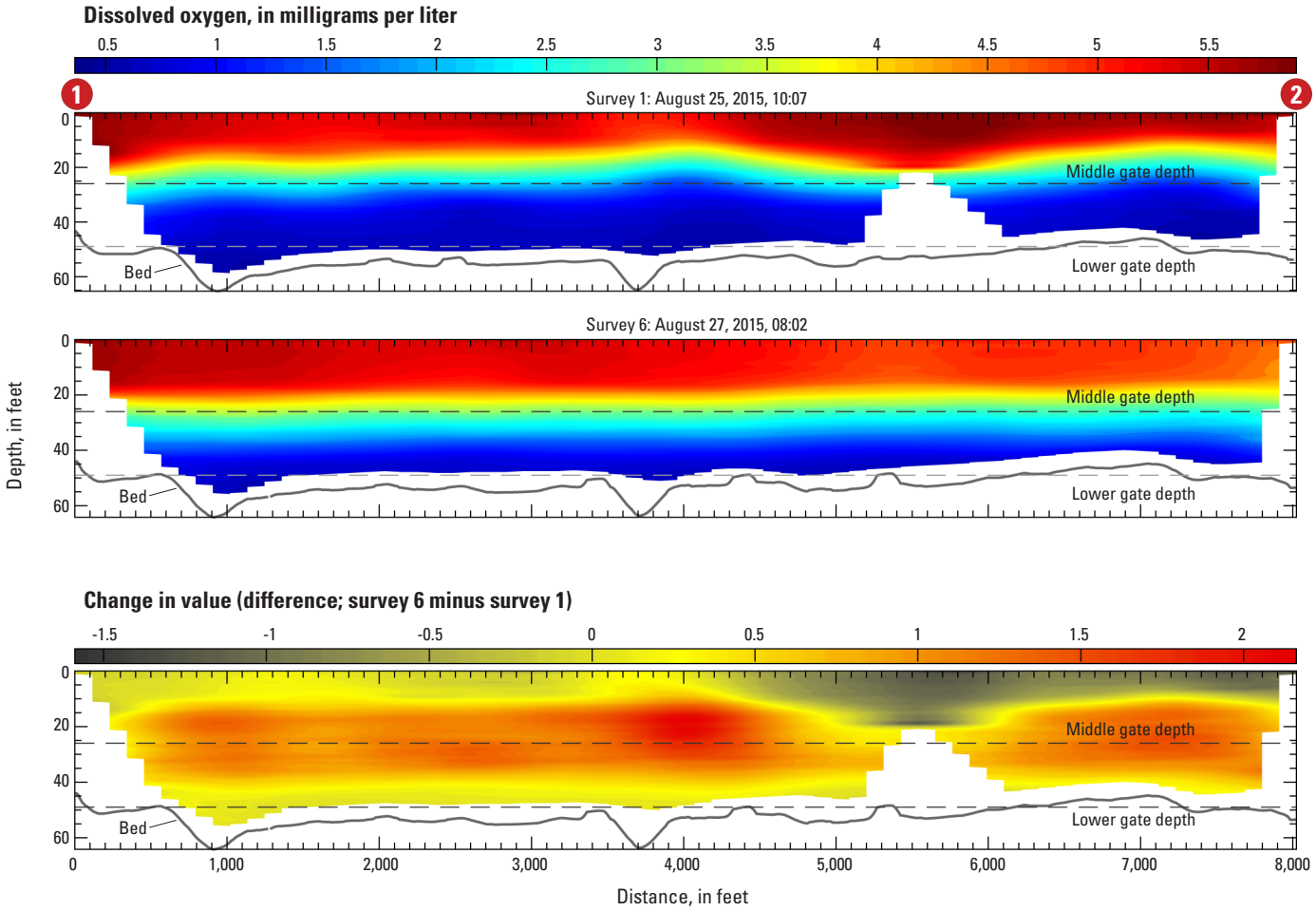

Figure 26. Dissolved oxygen distributions in lower Hoover Reservoir for morning surveys (surveys 1 and 6) on August 25 and August 27, 2015, and their difference (survey 6 minus survey 1). All cross sections plotted are along the approximate centerline of the reservoir from point 1 to point 2 (fig. 3, line C) where the dam is nearest point 1 (left side of figure) and the Smothers Road Bridge is nearest point 2 (right side of figure). Mean pool elevations for campaign 1 and 2 are 891.36 and 891.15 feet (National Geodetic Vertical Datum of 1929), respectively.

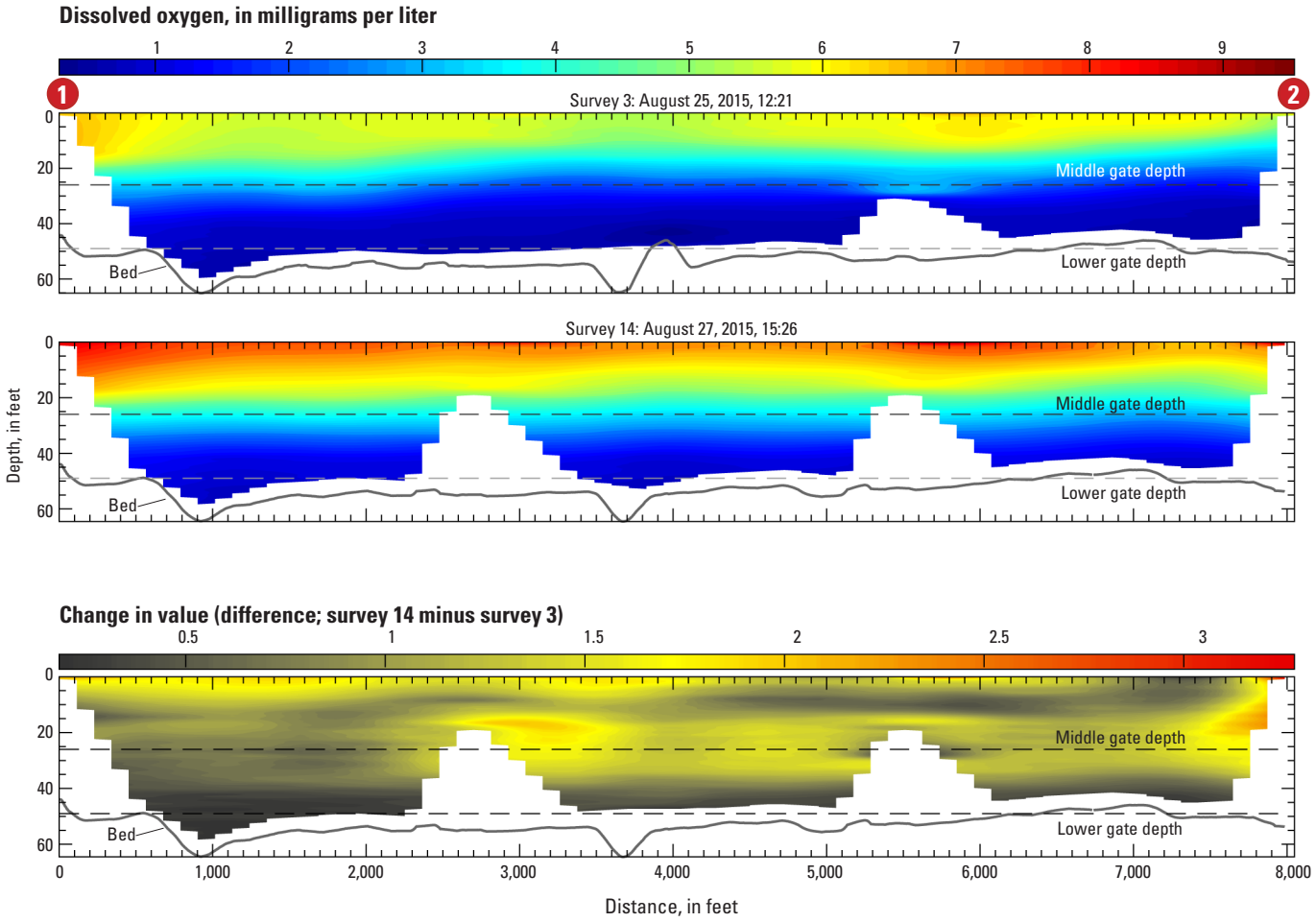

EXPLANATION

[All cross sections are plotted along the approximate centerline of the reservoir from point 1 to point 2 (fig. 3, line C) where the dam is nearest point 1 (left side of figure) and the bridge at Smothers Road is nearest point 2 (right side of the figure). Mean pool elevation for campaign 1 is 891.36. Mean pool elevation for campaign 2 is 891.15 feet. National Geodetic Vertical Datum of 1929]

1 **Numerical marker that provides a reference point (fig. 3)**

Figure 27. Dissolved oxygen distributions in lower Hoover Reservoir for afternoon surveys (surveys 3 and 14) on August 25 and August 27, 2015, and their difference (survey 14 minus survey 3). All cross sections plotted are along the approximate centerline of the reservoir from point 1 to point 2 (fig. 3, line C) where the dam is nearest point 1 (left side of figure) and the Smothers Road Bridge is nearest point 2 (right side of figure). Mean pool elevations for campaign 1 and 2 are 891.36 and 891.15 feet (National Geodetic Vertical Datum of 1929), respectively.

Turbidity

Turbidity generally increased in the hypolimnion between August 25 and 27, 2015 (figs. 15, 28, 29, and 30). A region of low turbidity water (2 to 4 nephelometric turbidity units) can be seen in figure 28 within the central hypolimnion (30 to 45 ft deep) which progressively increases in turbidity throughout the two campaigns until only a small part of this lower turbidity water mass is evident near the dam in survey 14. Some of the changes in the hypolimnion during the study period (figs. 29 and 30) are within this region in the central hypolimnion; however, most of the greatest changes occurred around the depth of the thermocline (25 to 30 ft deep) and around the depth of the lower intake gate (approximately 49 ft deep). The increase near the thermocline may be associated with the deepening of the epilimnion and mixing of more turbid, deep water across the thermocline into the epilimnion (consistent with mixing of other parameters such as specific conductance). The increase in turbidity near the depth of lower intake gate and peak in the turbidity concentration at this depth (figs. 14 and 15) could result from a turbidity current created by plunging of turbid inflows to the reservoir or turbulent resuspension of bed sediments (the highest turbidities were observed just above the bed in both campaigns). There were some changes in near-bed turbidity between campaigns, but the changes were not consistent between morning and afternoon surveys. Because the near-bed turbidity plume spans the whole lower part of Hoover Reservoir, resuspension is likely not localized to the area near the lower intake gates and may be occurring at key locations throughout the lower reach such as the constrained flow through the Smothers Road Bridge opening. Because near-bed velocities are difficult to measure accurately with an ADCP, especially at large depths, the potential for resuspension of sediment by currents induced by the lower gates remains unclear. Future work could test this hypothesis using an uplooking ADCP and a turbidity sensor deployed on the bed of the lake (perhaps more than one to determine if there is a continuous density current in the reservoir or resuspension in the lower reach).

pH

The distributions of pH in lower Hoover Reservoir on August 25 and 27, 2015, show a substantial reduction in pH of 1 to 1.5 standard units between the epilimnion and the hypolimnion (figs. 14, 31, 32, 33). The pH changes sharply at the thermocline and therefore the deepening of the thermocline from August 25 to August 27, 2015, created a noted increase in the pH of about 0.4 to 0.8 standard units between 20 to 30 ft depth for the morning and afternoon surveys (figs. 32 and 33). There was little change in pH below about 35 ft deep. In the epilimnion, pH generally decreased by less than 0.5 standard units between August 25 and 27, 2015 (figs. 32 and 33) as a result of mixing of hypolimnetic water across the thermocline, except for the surface layer in the afternoon surveys, which showed a small increase in pH of less than 0.2 standard units at several locations in the lower reach (fig. 33). The high pH of the epilimnion is likely due to the photosynthetic productivity of the algal biomass, which is primarily constrained to the epilimnion (see "Total Chlorophyll" and "Blue-Green Algae" sections). As algae uptake carbon dioxide and convert sunlight into energy through photosynthesis, the pH increases. Areas in the epilimnion that showed a pH increase near the water surface in the afternoon surveys when productivity is high (fig. 33) are correlated with higher concentrations of total chlorophyll, which reinforces the link between the distributions of pH and algal biomass.

Total Chlorophyll

Total chlorophyll concentrations generally increased along the thermocline and "hot spots" in the epilimnion between August 25 and 27, 2015, but showed little to no change in the hypolimnion below about 35 ft (figs. 14, 34, 35, and 36). Increases along the thermocline between about 20 to 35 ft deep are driven primarily by deepening of the epilimnion. Mixing of hypolimnetic water across the thermocline is likely to transport nutrients into the nutrient-limited epilimnion and increase productivity and algal biomass. The increase in total chlorophyll in survey 14 may be due, in part, to the enhanced mixing across the thermocline driven by operational gate changes. Finally, chlorophyll concentrations typically peaked between 5 and 10 ft below the water surface (figs. 14, 35, and 36). Such a distribution is not uncommon (Walsby, 1987; Mur and others, 1999) and is due to the active positioning of the algae with gas vesicles (such as cyanobacteria or blue-green algae) to optimize their positon in the water column to utilize sunlight from above and nutrients from below.

Blue-Green Algae

Deepening of the epilimnion associated with changing the intakes from the middle to the lower gates significantly increased the blue-green algae concentrations between 20 to 30 ft deep (figs. 14, 37, 38, 39). Below approximately 35 ft depth, there was little to no change in the blue-green algae concentration. In the epilimnion above about 20 ft depth, there was a decrease in the concentration in some areas (figs. 38 and 39), but the changes were small and may have a temporal influence associated with comparing surveys that are not exactly at the same time of the morning or afternoon (the concentration distribution changes throughout the day). Although it is not as pronounced as total chlorophyll, the blue-green algae concentration distribution peaks at about 5–10 ft below the water surface (figs. 14, 38, and 39) likely due to active positioning.

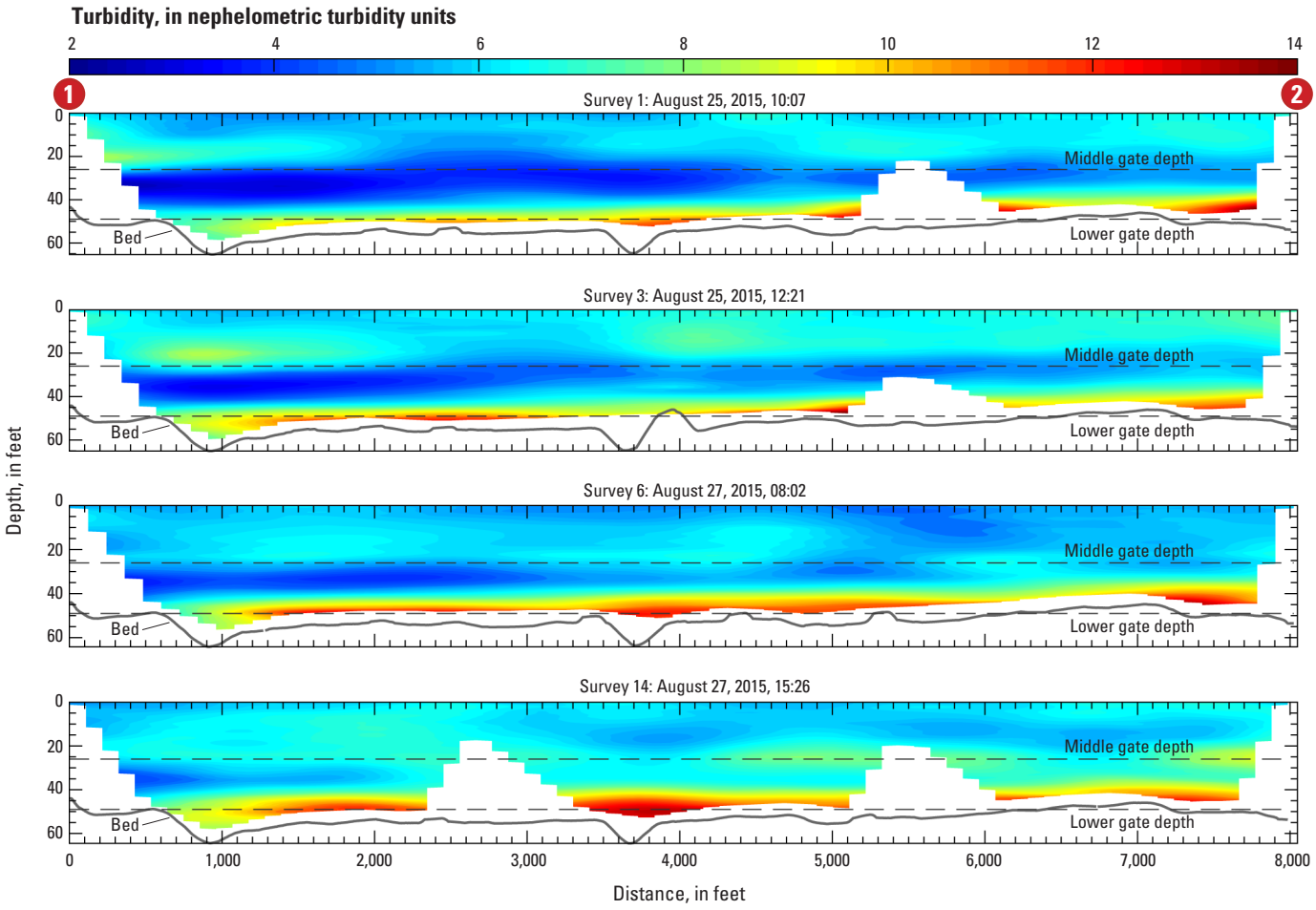

EXPLANATION

[All cross sections are plotted along the approximate centerline of the reservoir from point 1 to point 2 (fig. 3, line C) where the dam is nearest point 1 (left side of figure) and the bridge at Smothers Road is nearest point 2 (right side of the figure). Mean pool elevation for campaign 1 is 891.36. Mean pool elevation for campaign 2 is 891.15 feet. National Geodetic Vertical Datum of 1929]

1 **Numerical marker that provides a reference point (fig. 3)**

Figure 28. Turbidity distributions in lower Hoover Reservoir for August 25 (surveys 1 and 3) and August 27, 2015 (surveys 6 and 14). All cross sections plotted are along the approximate centerline of the reservoir from point 1 to point 2 (fig. 3, line C) where the dam is nearest point 1 (left side of figure) and the Smothers Road Bridge is nearest point 2 (right side of figure). Mean pool elevations for campaign 1 and 2 are 891.36 and 891.15 feet (National Geodetic Vertical Datum of 1929), respectively.

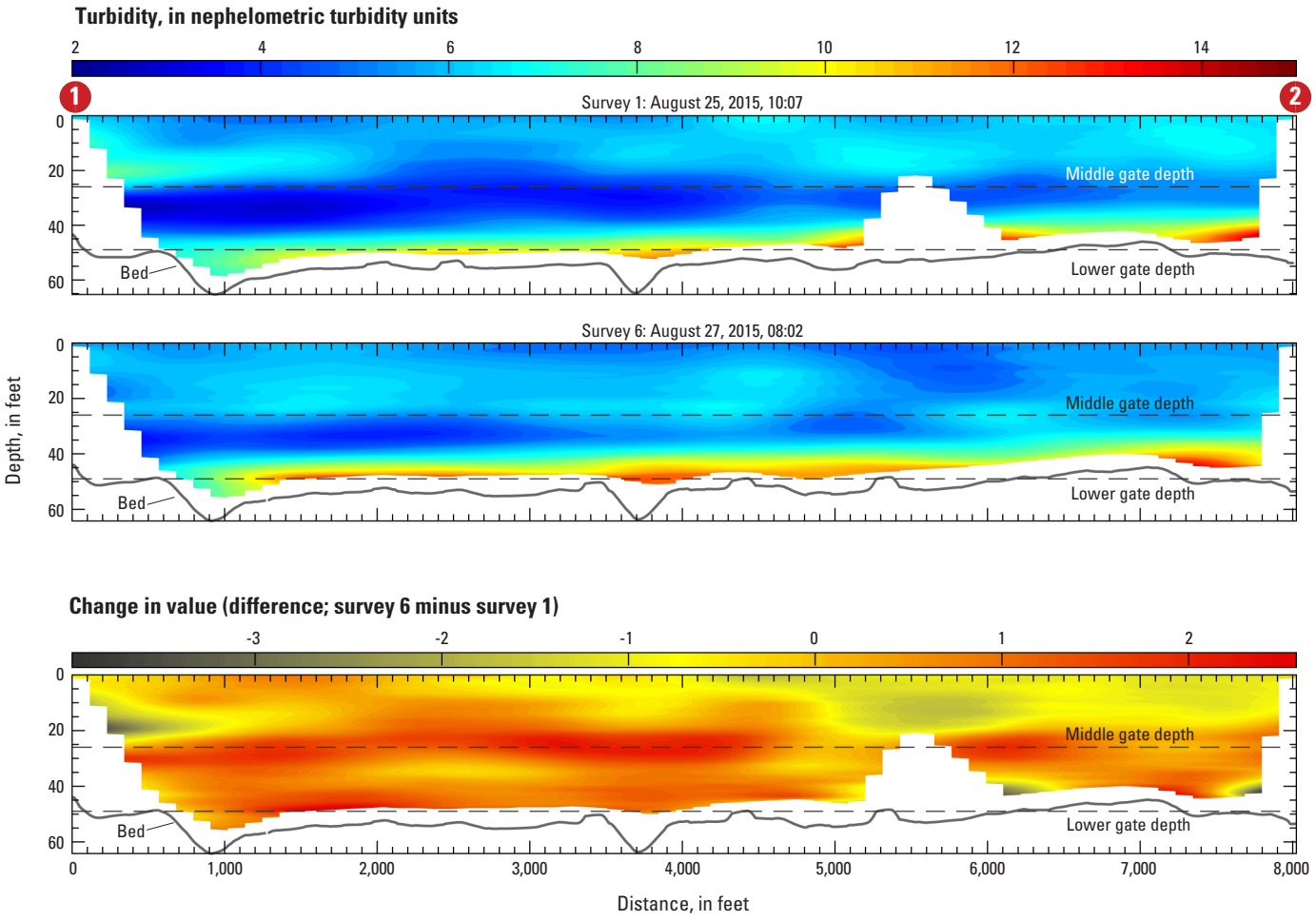

EXPLANATION

[All cross sections are plotted along the approximate centerline of the reservoir from point 1 to point 2 (fig. 3, line C) where the dam is nearest point 1 (left side of figure) and the bridge at Smothers Road is nearest point 2 (right side of the figure). Mean pool elevation for campaign 1 is 891.36. Mean pool elevation for campaign 2 is 891.15 feet. National Geodetic Vertical Datum of 1929]

1 **Numerical marker that provides a reference point (fig. 3)**

Figure 29. Turbidity distributions in lower Hoover Reservoir for morning surveys (surveys 1 and 6) on August 25 and August 27, 2015, and their difference (survey 6 minus survey 1). All cross sections plotted are along the approximate centerline of the reservoir from point 1 to point 2 (fig. 3, line C) where the dam is nearest point 1 (left side of figure) and the Smothers Road Bridge is nearest point 2 (right side of figure). Mean pool elevations for campaign 1 and 2 are 891.36 and 891.15 feet (National Geodetic Vertical Datum of 1929), respectively.

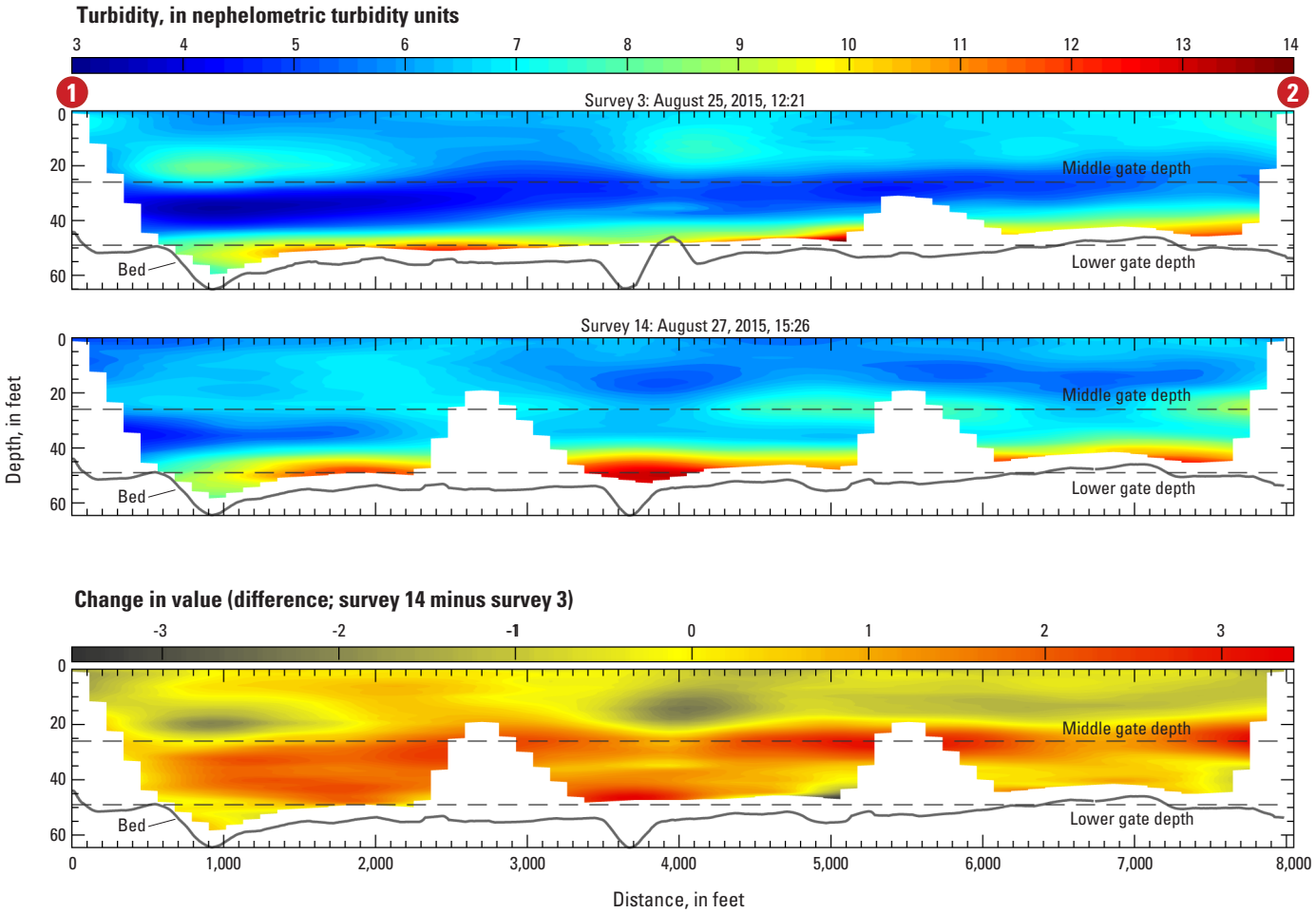

Figure 30. Turbidity distributions in lower Hoover Reservoir for afternoon surveys (surveys 3 and 14) on August 25 and August 27, 2015, and their difference (survey 14 minus survey 3). All cross sections plotted are along the approximate centerline of the reservoir from point 1 to point 2 (fig. 3, line C) where the dam is nearest point 1 (left side of figure) and the Smothers Road Bridge is nearest point 2 (right side of figure). Mean pool elevations for campaign 1 and 2 are 891.36 and 891.15 feet (National Geodetic Vertical Datum of 1929), respectively.

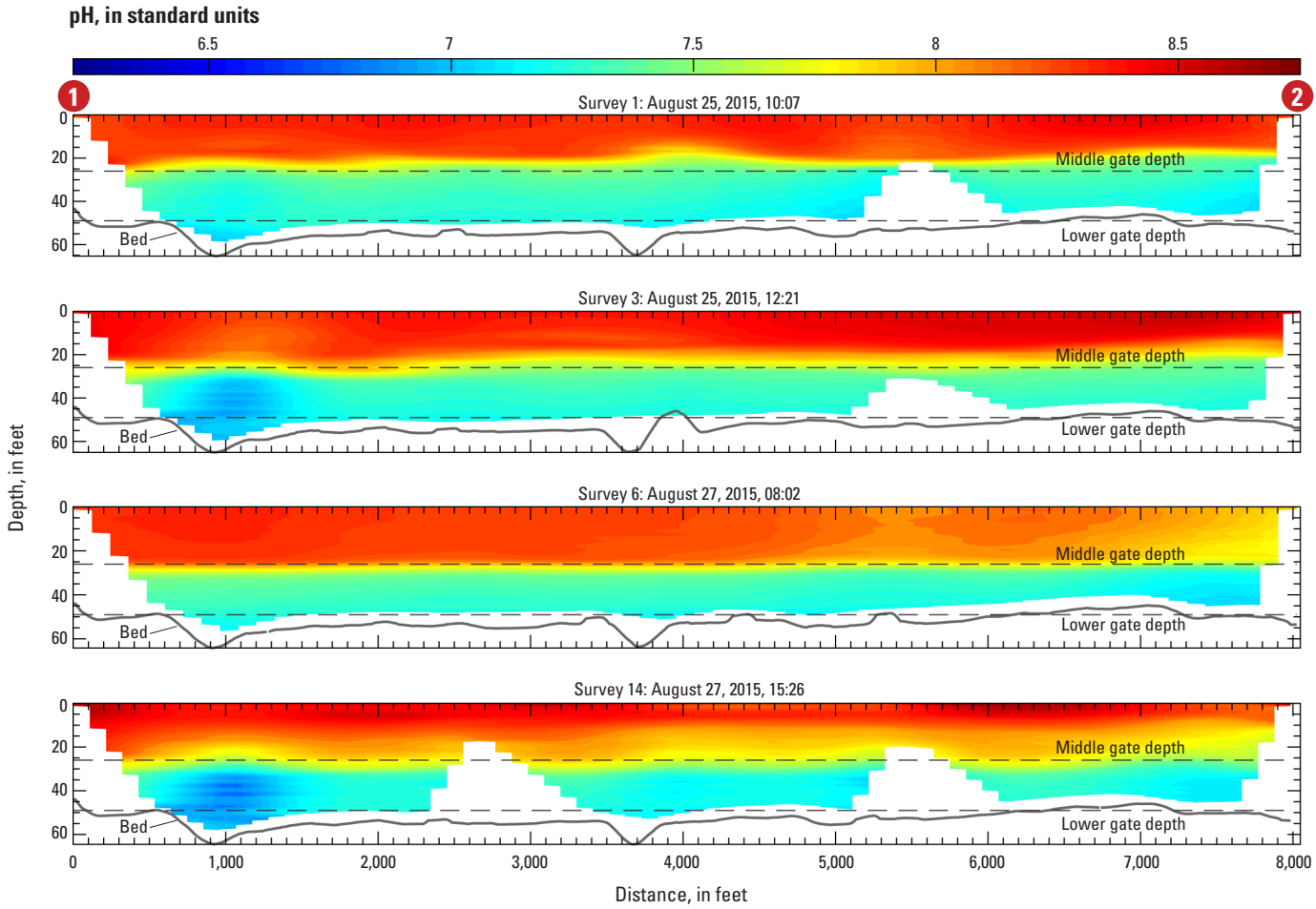

EXPLANATION

[All cross sections are plotted along the approximate centerline of the reservoir from point 1 to point 2 (fig. 3, line C) where the dam is nearest point 1 (left side of figure) and the bridge at Smothers Road is nearest point 2 (right side of the figure). Mean pool elevation for campaign 1 is 891.36. Mean pool elevation for campaign 2 is 891.15 feet. National Geodetic Vertical Datum of 1929]

1 **Numerical marker that provides a reference point (fig. 3)**

Figure 31. pH distributions in lower Hoover Reservoir for August 25 (surveys 1 and 3) and August 27, 2015 (surveys 6 and 14). All cross sections plotted are along the approximate centerline of the reservoir from point 1 to point 2 (fig. 3, line C) where the dam is nearest point 1 (left side of figure) and the Smothers Road Bridge is nearest point 2 (right side of figure). Mean pool elevations for campaign 1 and 2 are 891.36 and 891.15 feet (National Geodetic Vertical Datum of 1929), respectively.

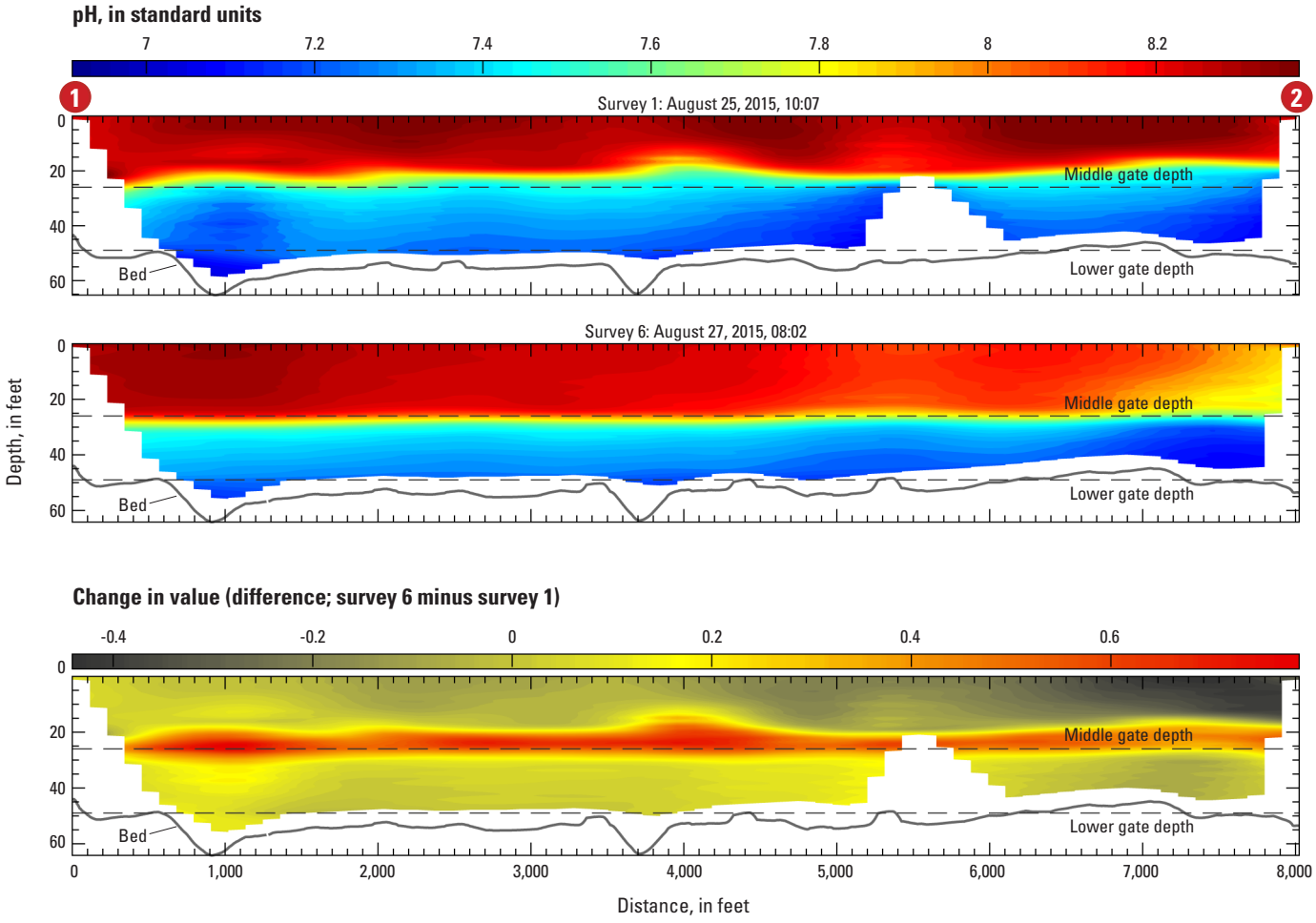

EXPLANATION

[All cross sections are plotted along the approximate centerline of the reservoir from point 1 to point 2 (fig. 3, line C) where the dam is nearest point 1 (left side of figure) and the bridge at Smothers Road is nearest point 2 (right side of the figure). Mean pool elevation for campaign 1 is 891.36. Mean pool elevation for campaign 2 is 891.15 feet. National Geodetic Vertical Datum of 1929]

1 **Numerical marker that provides a reference point (fig. 3)**

Figure 32. pH distributions in lower Hoover Reservoir for morning surveys (surveys 1 and 6) on August 25 and August 27, 2015, and their difference (survey 6 minus survey 1). All cross sections plotted are along the approximate centerline of the reservoir from point 1 to point 2 (fig. 3, line C) where the dam is nearest point 1 (left side of figure) and the Smothers Road Bridge is nearest point 2 (right side of figure). Mean pool elevations for campaign 1 and 2 are 891.36 and 891.15 feet (National Geodetic Vertical Datum of 1929), respectively.

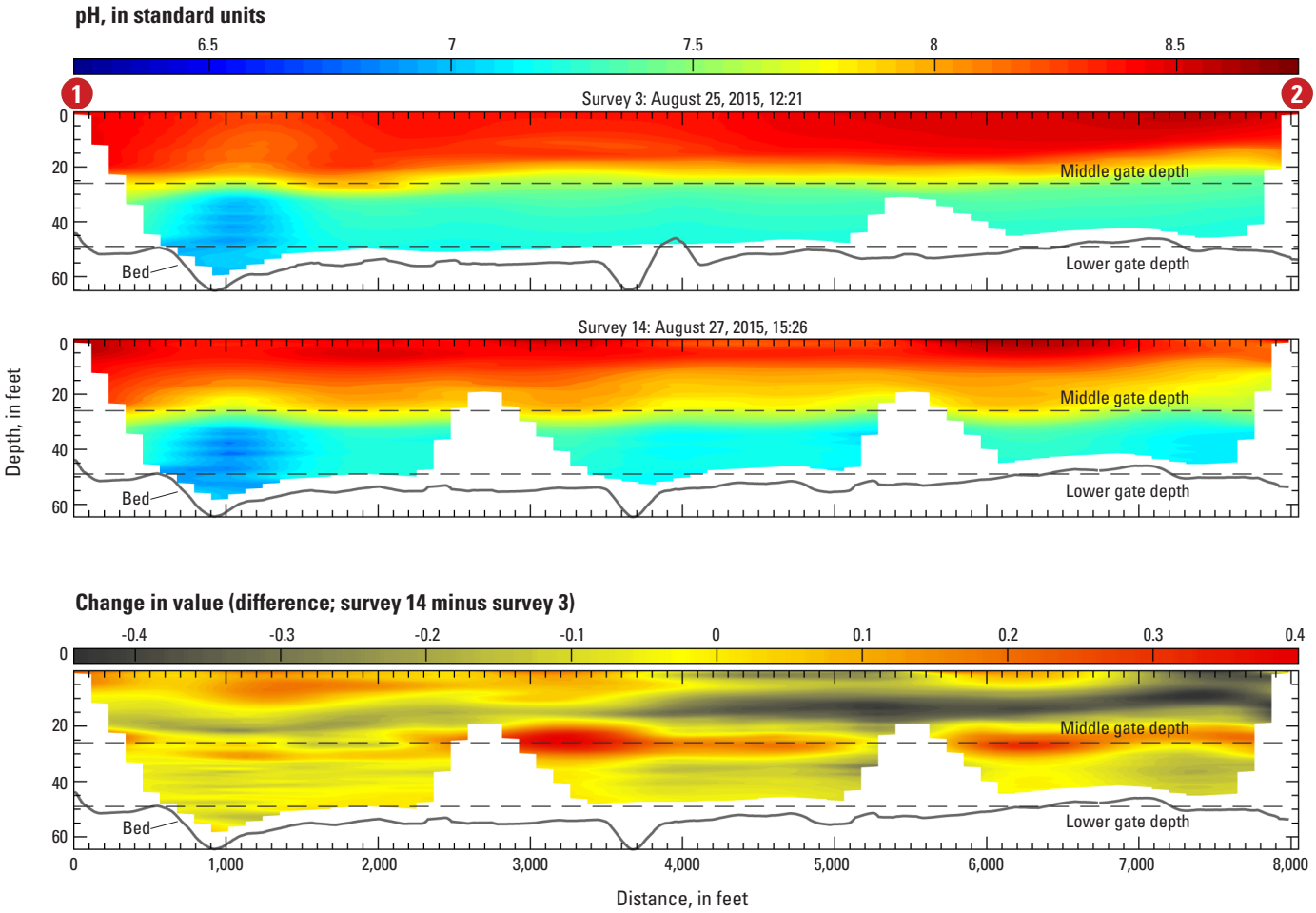

EXPLANATION

[All cross sections are plotted along the approximate centerline of the reservoir from point 1 to point 2 (fig. 3, line C) where the dam is nearest point 1 (left side of figure) and the bridge at Smothers Road is nearest point 2 (right side of the figure). Mean pool elevation for campaign 1 is 891.36. Mean pool elevation for campaign 2 is 891.15 feet. National Geodetic Vertical Datum of 1929]

1 **Numerical marker that provides a reference point (fig. 3)**

Figure 33. pH distributions in lower Hoover Reservoir for afternoon surveys (surveys 3 and 14) on August 25 and August 27, 2015, and their difference (survey 14 minus survey 3). All cross sections plotted are along the approximate centerline of the reservoir from point 1 to point 2 (fig. 3, line C) where the dam is nearest point 1 (left side of figure) and the Smothers Road Bridge is nearest point 2 (right side of figure). Mean pool elevations for campaign 1 and 2 are 891.36 and 891.15 feet (National Geodetic Vertical Datum of 1929), respectively.

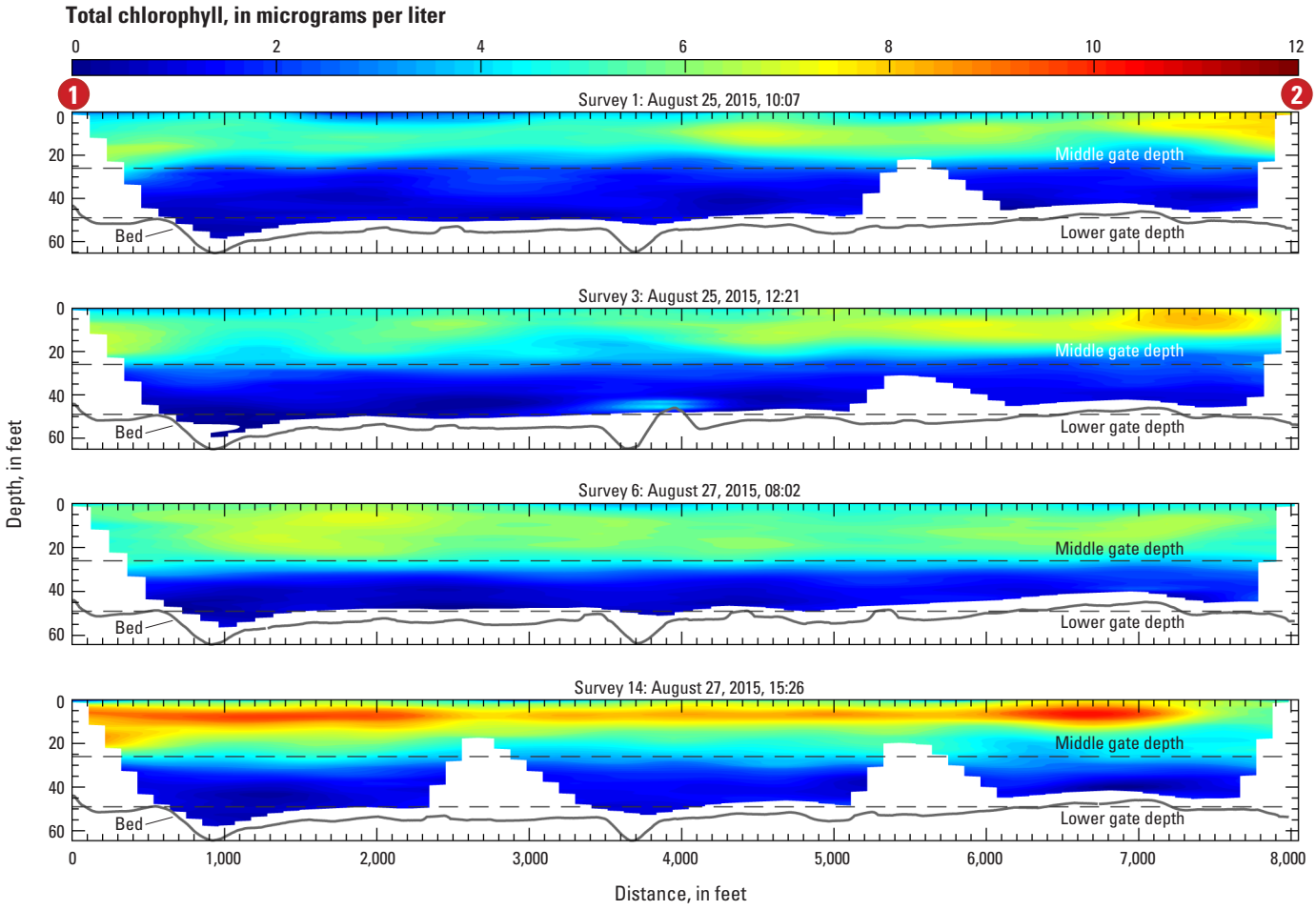

EXPLANATION

[All cross sections are plotted along the approximate centerline of the reservoir from point 1 to point 2 (fig. 3, line C) where the dam is nearest point 1 (left side of figure) and the bridge at Smothers Road is nearest point 2 (right side of the figure). Mean pool elevation for campaign 1 is 891.36. Mean pool elevation for campaign 2 is 891.15 feet. National Geodetic Vertical Datum of 1929]

1 **Numerical marker that provides a reference point (fig. 3)**

Figure 34. Total chlorophyll distributions (relative) in lower Hoover Reservoir for August 25 (surveys 1 and 3) and August 27, 2015 (surveys 6 and 14). All cross sections plotted are along the approximate centerline of the reservoir from point 1 to point 2 (fig. 3, line C) where the dam is nearest point 1 (left side of figure) and the Smothers Road Bridge is nearest point 2 (right side of figure). Mean pool elevations for campaign 1 and 2 are 891.36 and 891.15 feet (National Geodetic Vertical Datum of 1929), respectively.

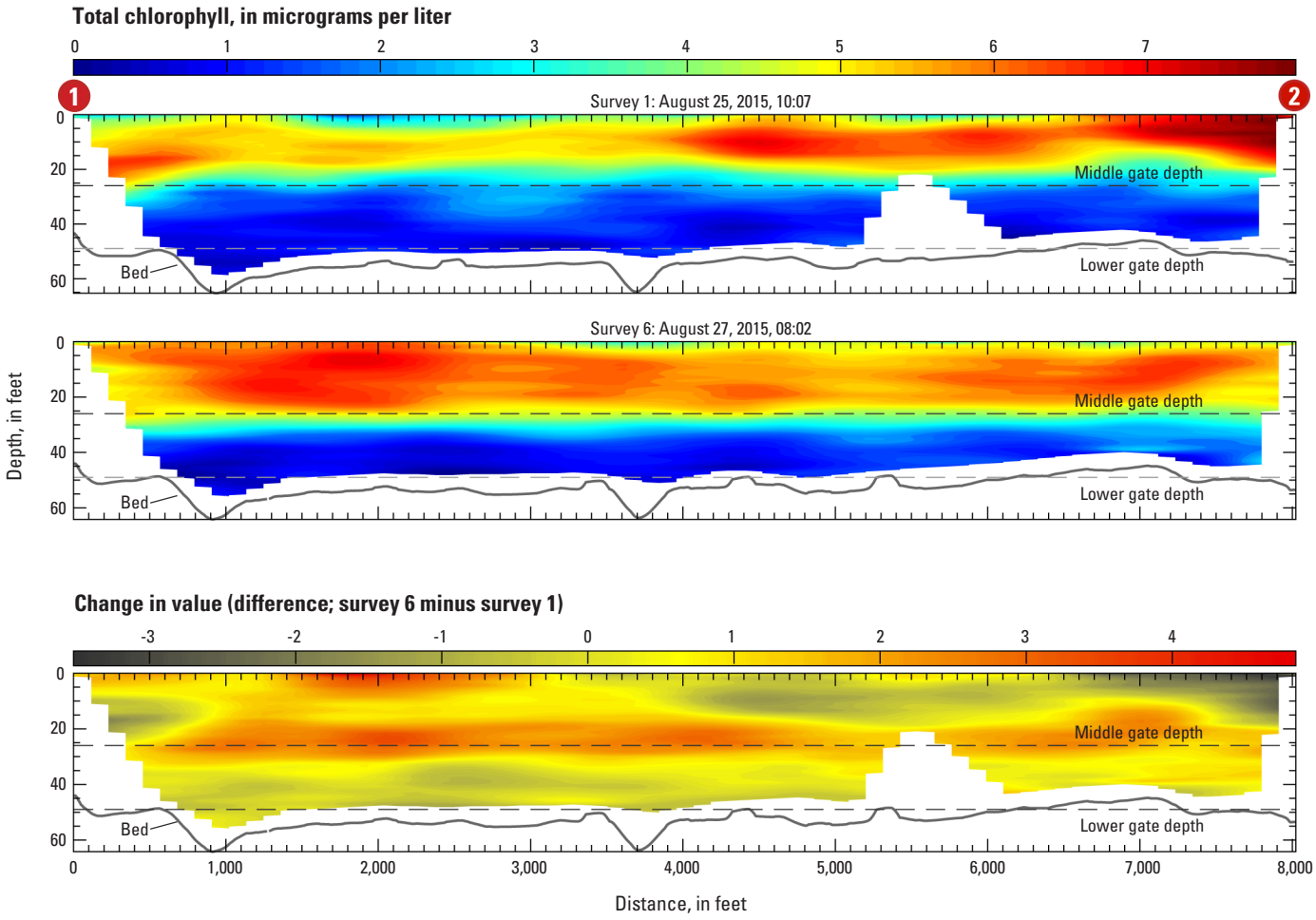

EXPLANATION

[All cross sections are plotted along the approximate centerline of the reservoir from point 1 to point 2 (fig. 3, line C) where the dam is nearest point 1 (left side of figure) and the bridge at Smothers Road is nearest point 2 (right side of the figure). Mean pool elevation for campaign 1 is 891.36. Mean pool elevation for campaign 2 is 891.15 feet. National Geodetic Vertical Datum of 1929]

1 **Numerical marker that provides a reference point (fig. 3)**

Figure 35. Total chlorophyll distributions (relative) in lower Hoover Reservoir for morning surveys (surveys 1 and 6) on August 25 and August 27, 2015, and their difference (survey 6 minus survey 1). All cross sections plotted are along the approximate centerline of the reservoir from point 1 to point 2 (fig. 3, line C) where the dam is nearest point 1 (left side of figure) and the Smothers Road Bridge is nearest point 2 (right side of figure). Mean pool elevations for campaign 1 and 2 are 891.36 and 891.15 feet (National Geodetic Vertical Datum of 1929), respectively.

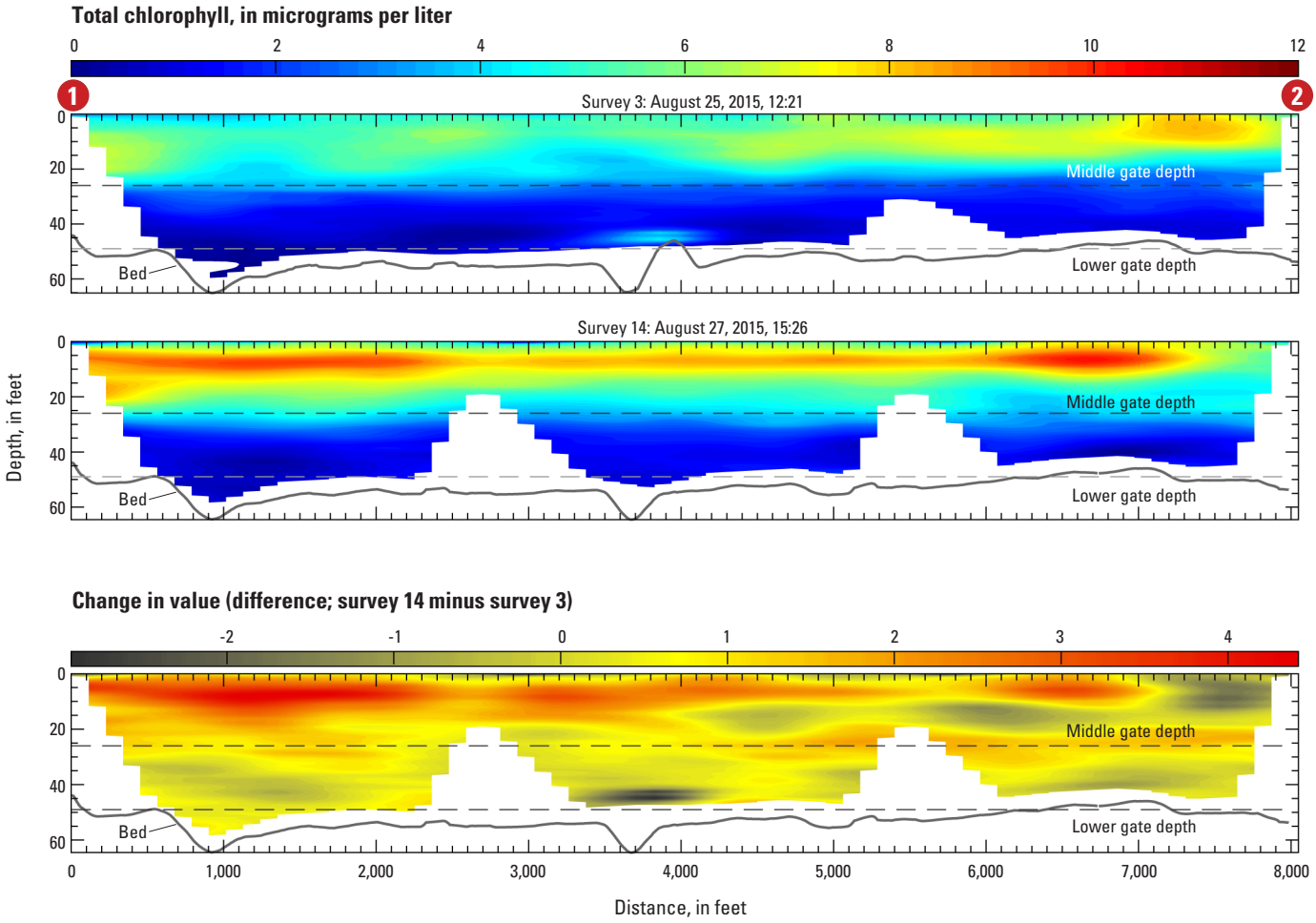

Figure 36. Total chlorophyll distributions (relative) in lower Hoover Reservoir for afternoon surveys (surveys 3 and 14) on August 25 and August 27, 2015, and their difference (survey 14 minus survey 3). All cross sections plotted are along the approximate centerline of the reservoir from point 1 to point 2 (fig. 3, line C) where the dam is nearest point 1 (left side of figure) and the Smothers Road Bridge is nearest point 2 (right side of figure). Mean pool elevations for campaign 1 and 2 are 891.36 and 891.15 feet (National Geodetic Vertical Datum of 1929), respectively.

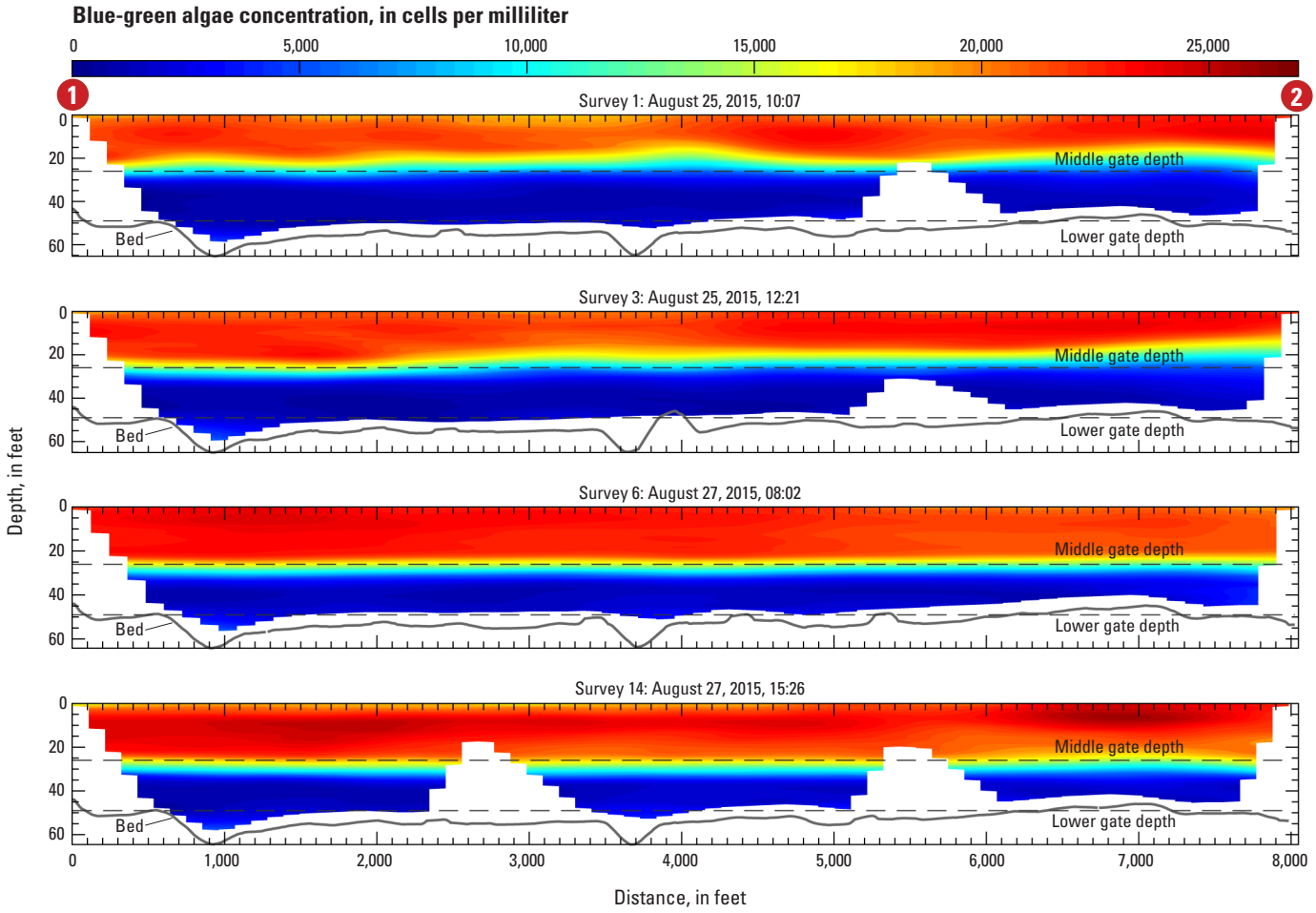

EXPLANATION

[All cross sections are plotted along the approximate centerline of the reservoir from point 1 to point 2 (fig. 3, line C) where the dam is nearest point 1 (left side of figure) and the bridge at Smothers Road is nearest point 2 (right side of the figure). Mean pool elevation for campaign 1 is 891.36. Mean pool elevation for campaign 2 is 891.15 feet. National Geodetic Vertical Datum of 1929]

1 **Numerical marker that provides a reference point (fig. 3)**

Figure 37. Blue-green algae distributions (relative) in lower Hoover Reservoir for August 25 (surveys 1 and 3) and August 27, 2015 (surveys 6 and 14). All cross sections plotted are along the approximate centerline of the reservoir from point 1 to point 2 (fig. 3, line C) where the dam is nearest point 1 (left side of figure) and the Smothers Road Bridge is nearest point 2 (right side of figure). Mean pool elevations for campaign 1 and 2 are 891.36 and 891.15 feet (National Geodetic Vertical Datum of 1929), respectively.

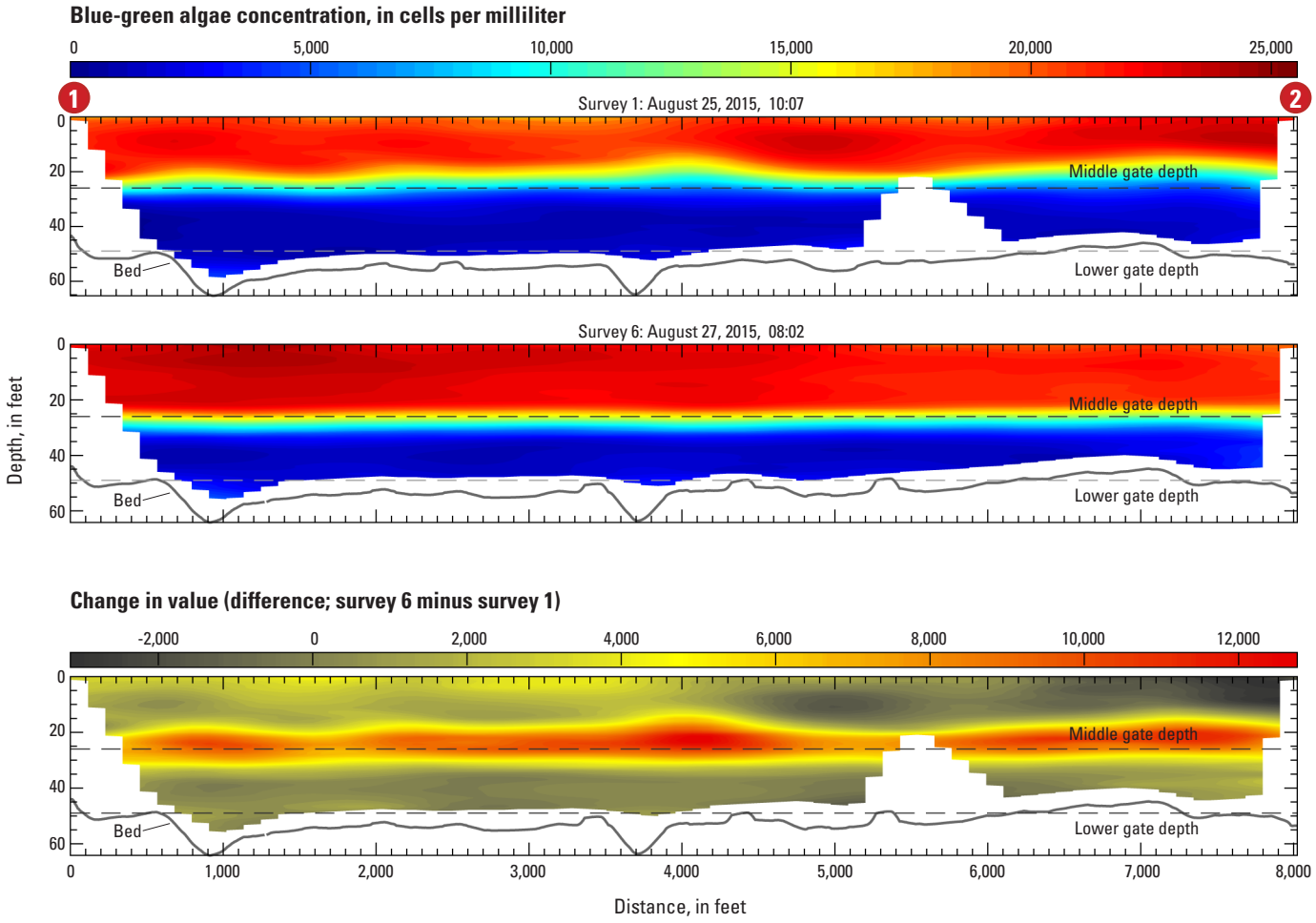

Figure 38. Blue-green algae distributions (relative) in lower Hoover Reservoir for morning surveys (surveys 1 and 6) on August 25 and August 27, 2015, and their difference (survey 6 minus survey 1). All cross sections plotted are along the approximate centerline of the reservoir from point 1 to point 2 (fig. 3, line C) where the dam is nearest point 1 (left side of figure) and the Smothers Road Bridge is nearest point 2 (right side of figure). Mean pool elevations for campaign 1 and 2 are 891.36 and 891.15 feet (National Geodetic Vertical Datum of 1929), respectively.

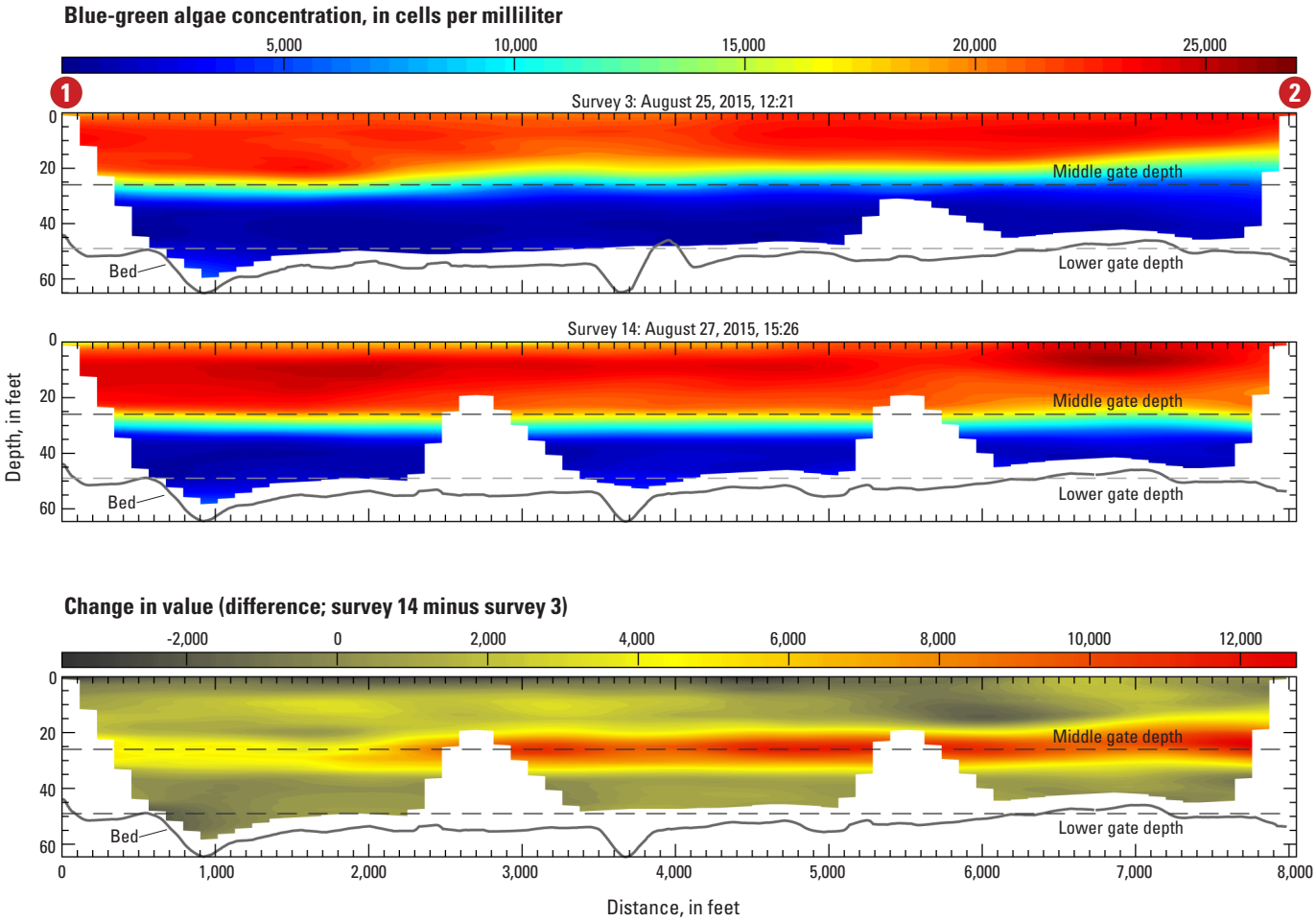

EXPLANATION

[All cross sections are plotted along the approximate centerline of the reservoir from point 1 to point 2 (fig. 3, line C) where the dam is nearest point 1 (left side of figure) and the bridge at Smothers Road is nearest point 2 (right side of the figure). Mean pool elevation for campaign 1 is 891.36. Mean pool elevation for campaign 2 is 891.15 feet. National Geodetic Vertical Datum of 1929]

1 **Numerical marker that provides a reference point (fig. 3)**

Figure 39. Blue-green algae distributions (relative) in lower Hoover Reservoir for afternoon surveys (surveys 3 and 14) on August 25 and August 27, 2015, and their difference (survey 14 minus survey 3). All cross sections plotted are along the approximate centerline of the reservoir from point 1 to point 2 (fig. 3, line C) where the dam is nearest point 1 (left side of figure) and the Smothers Road Bridge is nearest point 2 (right side of figure). Mean pool elevations for campaign 1 and 2 are 891.36 and 891.15 feet (National Geodetic Vertical Datum of 1929), respectively.

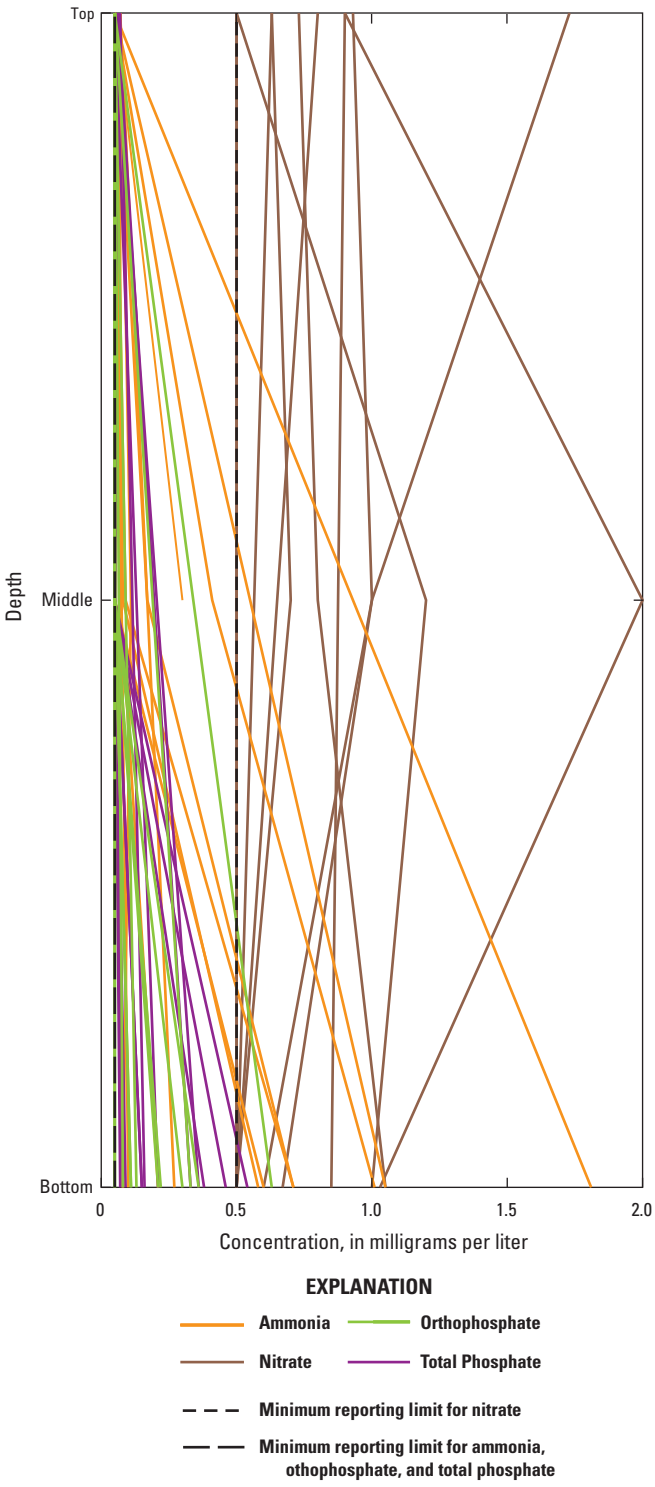

Figure 40. Nutrient profiles for ammonia, nitrate, orthophosphate, and total phosphate reported at relative depths by the City of Columbus, Ohio, during the summer and early fall of 2014, 2015, and 2016.

Nutrient Data

Although no nutrient data were collected during the USGS synoptic surveys on August 24–28, 2015, nutrient data collected by the City of Columbus during the summers of 2014–16 can provide some insight into nutrient distributions in Hoover Reservoir and implications for the results of the present study (Benjamin Ellsesser, City of Columbus, unpub. data, September 23, 2016). Of the four nutrient parameters that the City of Columbus sampled during the 2014, 2015, and 2016 summers, ammonia, orthophosphate, and total phosphate consistently had lower concentrations near the surface than near the bottom of the reservoir (fig. 40). Nitrate was more inconsistent in the shape of its profiles and was more likely, compared to the other nutrients, to have lower concentrations at the bottom than near the surface. These trends can be explained by several potential processes. First, with higher algae populations in the epilimnion than in the hypolimnion, nutrient consumption near the surface was higher than near the bottom, which leads to the lower concentrations of orthophosphate and total phosphate near the surface. Second, because of the lower dissolved oxygen in the hypolimnion, nitrate was converted to ammonia below the thermocline where dissolved oxygen concentrations were lower. This conversion could explain why ammonia had increasing concentrations with depth and why nitrate showed several instances where concentrations were higher near the top than the bottom.

The higher concentrations of nutrients deeper in the reservoir indicate that by releasing water from the lower gate, more nutrients were likely discharged downstream. Also, the increase in mixing across the thermocline that was observed during campaign 2 would likely cause an increase in nutrient concentration in the epilimnion and thus decrease the amount of nutrients in the hypolimnion. In the short term, mixing of nutrients into the epilimnion, especially phosphorous, which fuels algal growth, could lead to increased algae blooms.

Conclusions

Hoover Reservoir, a key water supply for the City of Columbus, Ohio, had a series of taste and odor problems over the past few years. These taste and odor problems, caused by the compounds geosmin and 2-methylisoborneol, are thought to have been caused by cyanobacteria blooms when the reservoir turned over in autumn. In an effort to reduce the phosphorus available for cyanobacteria blooms at fall turnover, the City of Columbus began experimenting with the dam's selective withdrawal system, changing the gate from the middle to the lower gate, in hopes of removing excess phosphorus from the hypolimnion, which is released from bottom sediments during summer anoxic conditions.

The U.S. Geological Survey completed two campaigns to assess distributions of water quality and water velocity in the lower part of Hoover Reservoir to provide information on

the changes to reservoir dynamics caused by changing dam operations. The first campaign was done while water was being withdrawn from a mid-level gate and the second while water was being withdrawn from a low-level gate. Circulation patterns were assessed using velocity data measured with an acoustic Doppler current profiler (ADCP) and water-quality parameters were assessed using water-quality data collected with an autonomous underwater vehicle (AUV) equipped with a suite of water-quality sensors. Along with the water-quality and water-velocity data, meteorological, inflow and outflow discharges, and independent water-quality data were compiled to monitor changes in other parameters that affect reservoir behavior. Monthly nutrient data, collected by the City of Columbus, were also analyzed for trends in concentration during periods of expected stratification. Interpretations of the processes in the reservoir during operation of the two different gates are based on the spatiotemporal variations observed in this dataset.

The meteorological data indicate that the period leading up to and through data collection was cooler and received more precipitation than is typical for the late August period. Winds, inflows, and outflows from the reservoir were all variable for the period leading up to and through the data collection period, August 24–28, 2015 . These unusual and variable conditions contribute to uncertainty in determining the cause(s) of observed water-quality and velocity patterns.

Velocity patterns within the reservoir were complex, with flow changing direction and magnitude frequently throughout the study section. Despite the complexity, some patterns that may affect reservoir circulation and mixing were observed:

- In the first campaign, two contiguous paths of downstream flow were identified. These paths were perhaps the most direct route of transport through the study section.
- In campaign 1 and possibly in campaign 2, evidence of a circulatory pattern that would increase residency time and cross-reservoir mixing was observed in the upper study section.
- In campaign 2, contiguous upstream flow was observed along several depth planes. This layer may cause shear-induced mixing between it and adjacent depth layers.
- Vertical velocities at depths less than 15 ft were primarily downward (negative), whereas vertical velocities at depths greater than 15 ft were primarily upward (positive) in campaign 1 and campaign 2. The convergence of these vertical fluxes was near the base of the epilimnion where there was likely shear-induced mixing. Furthermore, the upward velocities near the bottom would slow the settling of particles.

The water-quality mapping showed a stratified reservoir with a well-defined epilimnion, thermocline, and hypolimnion. Some distinct differences in water-quality distributions that are thought to result from changing withdrawal depths were observed. When changed to the lower gate, the epilimnion deepened by approximately 5 feet. Also, in all of the water-quality parameters mapped, the data are consistent with increased mixing across the thermocline except for chlorophyll and blue-green algae, where concentrations were constrained to the epilimnion. Evidence in campaign 2 of high velocities at the base of the epilimnion just above the thermocline indicates the deepening of the epilimnion through enhanced mixing may have resulted from shear-driven mixing at the thermocline. If the changes in water-quality distributions presented herein are repeatable and result primarily from changes in gate depths (an assumption that must be proven with additional surveys), these results indicate that varying the gate depths may allow for limited management of the outflow water quality and the water-quality distribution in the lower part of the reservoir.

An increase in turbidity in the hypolimnion between the two surveys with different gate configurations was of particular interest to this study. Increasing turbidity in the hypolimnion combined with the withdrawal from the lower gate may indicate an increase in the amount of nutrients and sediment being released downstream. Although it is possible the increase in turbidity could be due to currents induced by the activation of the lower withdrawal gate, it is not possible to discern with the current dataset whether the increase in turbidity is caused by sediment resuspension by near-bed currents, by an increase in advection of water in the hypolimnion (allowing sediments to remain in suspension longer in the hypolimnion), or by turbidity currents from the inflow. Further research is required to determine the correlation between near-bed currents, turbidity, and continuity of currents between the inflow and the dam, which may include the use of uplooking ADCPs in combination with turbidity meters.

There is considerable uncertainty as to which processes are affecting change in the reservoir during gate changes because the hydrodynamics of the reservoir were complex, nutrients were not directly measured during the study, and the equipment used could not measure near-bottom velocities and water quality. This uncertainty could be reduced with a similar, but more robust, study that includes (1) nutrient measurement during the study, (2) summer-long deployment of uplooking ADCPs and turbidity sensors, and (3) two campaigns done while water is being withdrawn from the middle gate, followed by changing to the lower gate and waiting a week for the reservoir to fully react to the change, then doing another two campaigns while water is being withdrawn from the lower gate. Such a study could supplement the present study in a few ways: (1) direct measurement of nutrients would identify the direct effect of gate changes on nutrient concentrations, (2) the source of the increased turbidity in the hypolimnion could be better understood, (3) it would allow comparison with this study and could indicate how consistent these dynamics are across years, and (4) repeat surveys would allow more insight to what changes can be attributed to variable meteorological and flow conditions and which are a result of changes to the withdrawal gates.

Based on the results of the two surveys, it seems that when compared to withdrawing water through the middle gate, withdrawing water through the lower gate increases vertical mixing and causes a deepening of the thermocline throughout the lower part of Hoover Reservoir. This increased mixing is thought to be caused by shear between a layer of upstream flow near the thermocline and adjacent depth layers. The increase in mixing across the thermocline likely provides algal populations confined to the epilimnion with key nutrients, including phosphorous, that would otherwise be confined to, and may settle in, the hypolimnion. Following this theory, the immediate response of the reservoir to activation of the lower gate may be an increase in algal populations resulting from the increased flux of nutrients across the thermocline into the epilimnion; however, such practices may, in time, reduce the accumulation of nutrients in the hypolimnion, making sustained blooms driven by the autumn turnover (like that in 2013/2014) less common. However, because nutrient concentrations were not directly measured as a part of this synoptic study and a limited amount of data are available for analysis, such theories cannot be conclusively affirmed and additional data are required to confirm this hypothesis.

References Cited

American Water Works Association, 2010, Algae—Source to treatment (1st ed.): American Water Works Association Manual of Water Supply Practices M57, p. 350–355.

Arenschield, L., 2015, Smelly, foul-tasting water? Columbus treating for algae again: The Columbus Dispatch, accessed April 15, 2016, at http://www.dispatch.com/content/stories/local/2015/07/09/Algae-causing-taste-and-smell-issues-in-water.html.

Blevins, A., 2014, City of Columbus annual report: accessed April 25, 2016, at https://columbus.gov/uploadedFiles/Columbus/Elected_Officials/City_Council/Annual_Reports/2014%20City%20of%20Columbus%20Annual%20Report.pdf.

City of Columbus Public Utilities, 2016, Historical info for water supply and source management: accessed April 25, 2016, at https://www.columbus.gov/Templates/Detail.aspx?id=16077.

City of Columbus Water Protection, 2016, Water distribution system: accessed April 25, 2016, at https://www.columbus.gov/Templates/Detail.aspx?id=36944.

Graham, J.L., Loftin, K.A., Ziegler, A.C., and Meyer, M.T., 2008, Cyanobacteria in lakes and reservoirs—Toxin and taste-and-odor sampling guidelines (ver. 1.0): U.S. Geological Survey Techniques of Water-Resources Investigations, book 9, chap. A7, section 7.5, accessed July 12, 2016, at http://pubs.water.usgs.gov/twri9A/.

Horne, A.J., and Goldman, C.R., 1994, Limnology (2d ed.): New York, McGraw-Hill Co., 576 p.

Hunt, S., 2014, Toxic algae in Hoover Reservoir cost city $723,000: The Columbus Dispatch, accessed April 15, 2016, at http://www.dispatch.com/content/stories/local/2014/02/03/toxic-algae-in-hoover-cost-city-723000.html.

Hutchinson, G.E., 1957, A treatise on limnology—Volume I. Geography, physics, and chemistry: New York, John Wiley and Sons, 1015 p.

Imberger, J., and Hamblin, P.F., 1982, Dynamics of lakes, reservoirs, and cooling ponds: Annual Review Fluid Mechanics, v. 14, p. 153–187, accessed April 14, 2016, at http://www.annualreviews.org/doi/abs/10.1146/annurev.fl.14.010182.001101.

Jackson, P.R., 2013, Circulation, mixing, and transport in nearshore Lake Erie in the vicinity of Villa Angela Beach and Euclid Creek, Cleveland, Ohio, September 11–12, 2012: U.S. Geological Survey Scientific Investigations Report 2013–5198, 34 p.

Jackson, P.R., and Dupre, D.H., 2016, Three-dimensional point measurements of basic water-quality parameters in Hoover Reservoir near Westerville, Ohio, August 25 and 27, 2015: U.S. Geological Survey data release, accessed September 1, 2016, at http://dx.doi.org/10.5066/F70863D8.

Mur, L.R., Skulberg, O.M., and Utkilen, H., 1999, Cyanobacteria in the environment, chap. 2 *of* Chorus, I., and Bartram, J., ed., Toxic cyanobacteria in water—A guide to their public health consequences, monitoring and management: London, United Kingdom, E & FN Spon, p. 14–40.

Narciso, D., 2014, Algae update—Fixing bad-tasting drinking water already expensive: The Columbus Dispatch, accessed April 15, 2016, at http://www.dispatch.com/content/stories/local/2014/05/10/algae-update.html.

Nürnberg, G.K., 2007, Lake responses to long-term hypolimnetic withdrawal treatments: Lake and Reservoir Management, v. 23, p. 388–409.

National Oceanic and Atmospheric Administration, 2016, Quality controlled local climatological data, Columbus Port Columbus International Airport, OH US GHCND:USW00014821: accessed May 26, 2016, at https://www.ncdc.noaa.gov/cdo-web/datasets/GHCND/stations/GHCND:USW00014821/detail.

National Weather Service, 2015, Columbus climate normals: accessed April 4, 2016, at http://www.weather.gov/iln/climate_normals_cmh#.

Ohio Department of Natural Resources, 2010, Hoover Reservoir: accessed March 2, 2016, at http://wildlife.ohiodnr.gov/hooverreservoir#tabr2.

Ohio Environmental Protection Agency, 2001, Land use and land cover 2000–2002: 319 Grant Project #01 (h)EPA-06, Statewide Land Use Classification and Validation in Ohio, accessed March 28, 2016, at http://wwwapp.epa.ohio.gov/dsw/nps/NPSMP/photos/LULC_County.pdf.

Parsons, D.R., Jackson, P.R., Czuba, J.A., Engel, F.L., Rhoads, B.L., Oberg, K.A., Best, J.L., Mueller, D.S., Johnson, K.K., and Riley, J.D., 2013, Velocity Mapping Toolbox (VMT)—A processing and visualization suite for moving-vessel ADCP measurements: Earth Surface Processes and Landforms, v. 38, p. 1244–1260.

R Core Team, 2016, R: The R Project for Statistical Computing, v. 3.2.5, accessed March 1, 2016, at https://www.R-project.org/.

Standard Methods Online, 2016, Standard methods for the examination of water and wastewater: accessed September 26, 2016, at http://standardmethods.org.

Teledyne RD Instruments, 2014, WinRiver II Version 2.16.

U.S. Geological Survey, 2015a, National Water Information System, USGS 03228300 Big Walnut Creek at Sunbury: U.S. Geological Survey database, accessed October 21, 2015, at http://nwis.waterdata.usgs.gov/nwis/dv?site_no=03228300.

U.S. Geological Survey, 2015b, National Water Information System, USGS 03228400 Hoover Reservoir at Central College: U.S. Geological Survey database, accessed October 21, 2015, at http://nwis.waterdata.usgs.gov/nwis/dv?site_no=03228400.

U.S. Geological Survey, 2015c, National Water Information System, USGS 03228500 Big Walnut Creek at Central College: U.S. Geological Survey database, accessed October 21, 2015, at http://nwis.waterdata.usgs.gov/nwis/dv?site_no=03228500.

U.S. Geological Survey, 2016, The StreamStats program for Ohio: accessed March 28, 2016, at http://water.usgs.gov/osw/streamstats/ohio.html.

Vonins, B.L., 2017, Survey of velocity and bathymetry in Hoover Reservoir, ADCP source data, Columbus, OH (August, 2015): U.S. Geological Survey data release, accessed March 31, 2017, at https://doi.org/10.5066/F75X271K.

Walsby, A.E., 1987, Mechanisms of buoyancy regulation by planktonic cyanobacteria with gas vesicles, in Fay, P., and Van Baalen, C., eds., Cyanobacteria—A comprehensive review: Elsevier, Amsterdam, p. 377–414.

Wetzel, R.G., 2001, Limnology—Lake and river ecosystems: San Diego, California, Academic Press, 1006 p.

Appendix 1. Cross-Section Profiles

This appendix contains contour plots of streamwise velocity at each cross section during campaign 1 and campaign 2. Cross sections are plotted looking downstream with positive velocities going into the page. A moving average of five horizontal and five vertical cells was used for smoothing purposes.

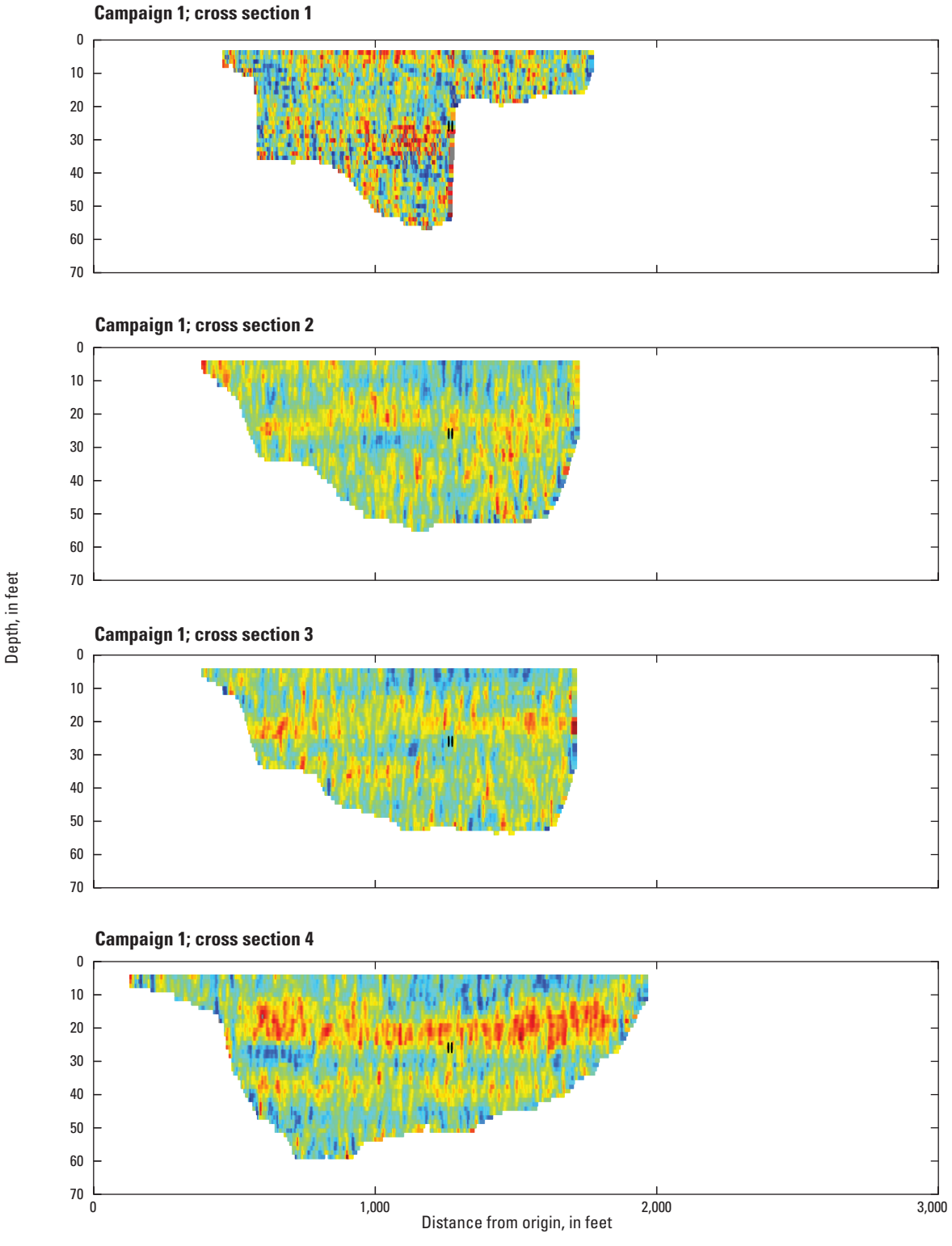
Campaign 1; cross section 1
Campaign 1; cross section 2
Campaign 1; cross section 3
Campaign 1; cross section 4
Depth, in feet
0
10
20
30
40
50
60
70
0
1,000
2,000
3,000
Distance from origin, in feet
EXPLANATION
-0.2 -0.1 0 0.1 0.2
Streamwise velocity, in feet per second
Active withdrawal gate
Distance from origin—Perpendicular distance to line defined by the coordinates 1115134 feet east, 14571644 feet north, and 1116421 feet east, 14579902 feet north (Universal Transverse Mercator, zone 17S)

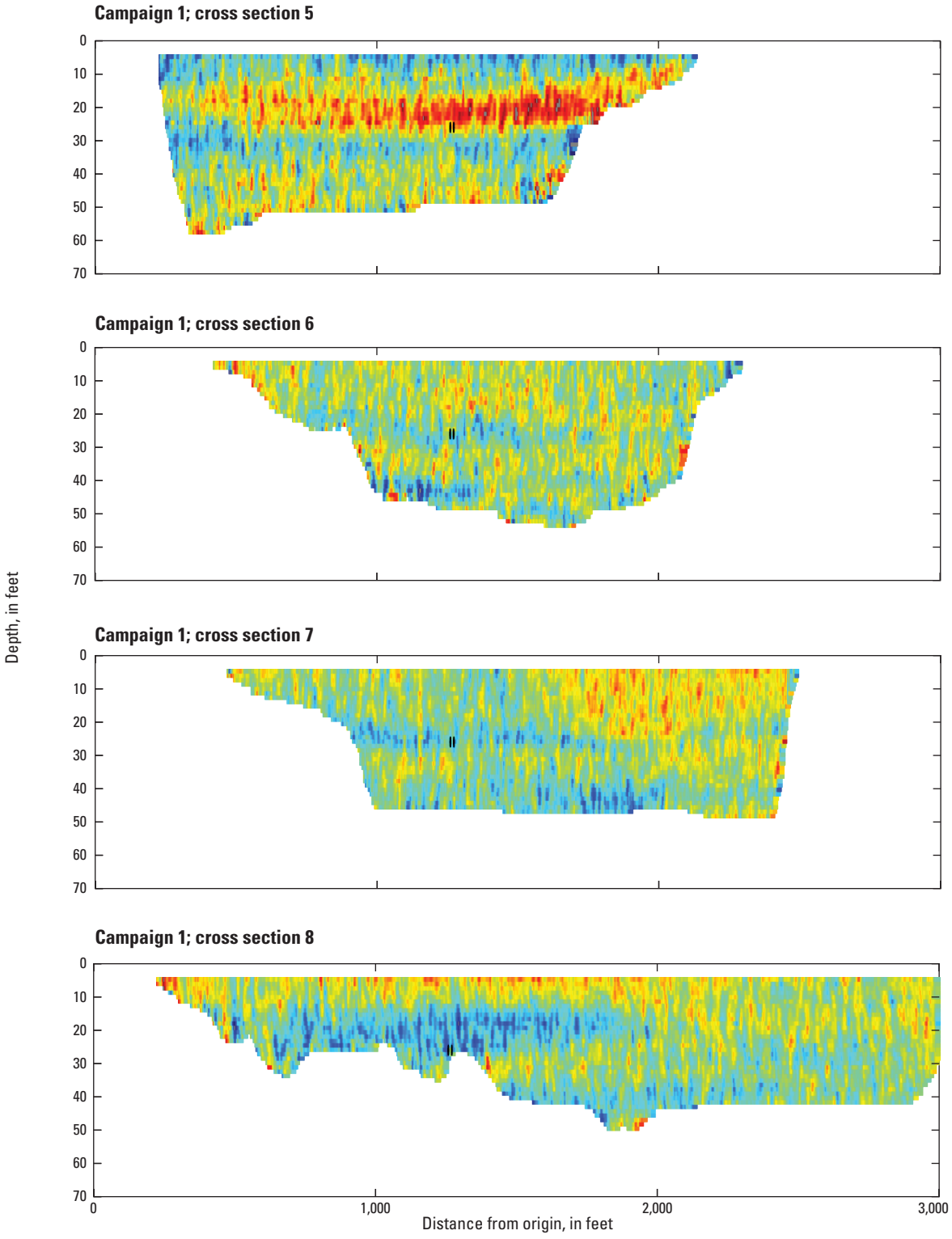
Campaign 1; cross section 5
Campaign 1; cross section 6
Campaign 1; cross section 7
Campaign 1; cross section 8
Depth, in feet
0
10
20
30
40
50
60
70
0
1,000
2,000
3,000
Distance from origin, in feet
EXPLANATION
-0.2 -0.1 0 0.1 0.2
Streamwise velocity, in feet per second
Active withdrawal gate
Distance from origin—Perpendicular distance to line defined by the coordinates 1115134 feet east, 14571644 feet north, and 1116421 feet east, 14579902 feet north (Universal Transverse Mercator, zone 17S)

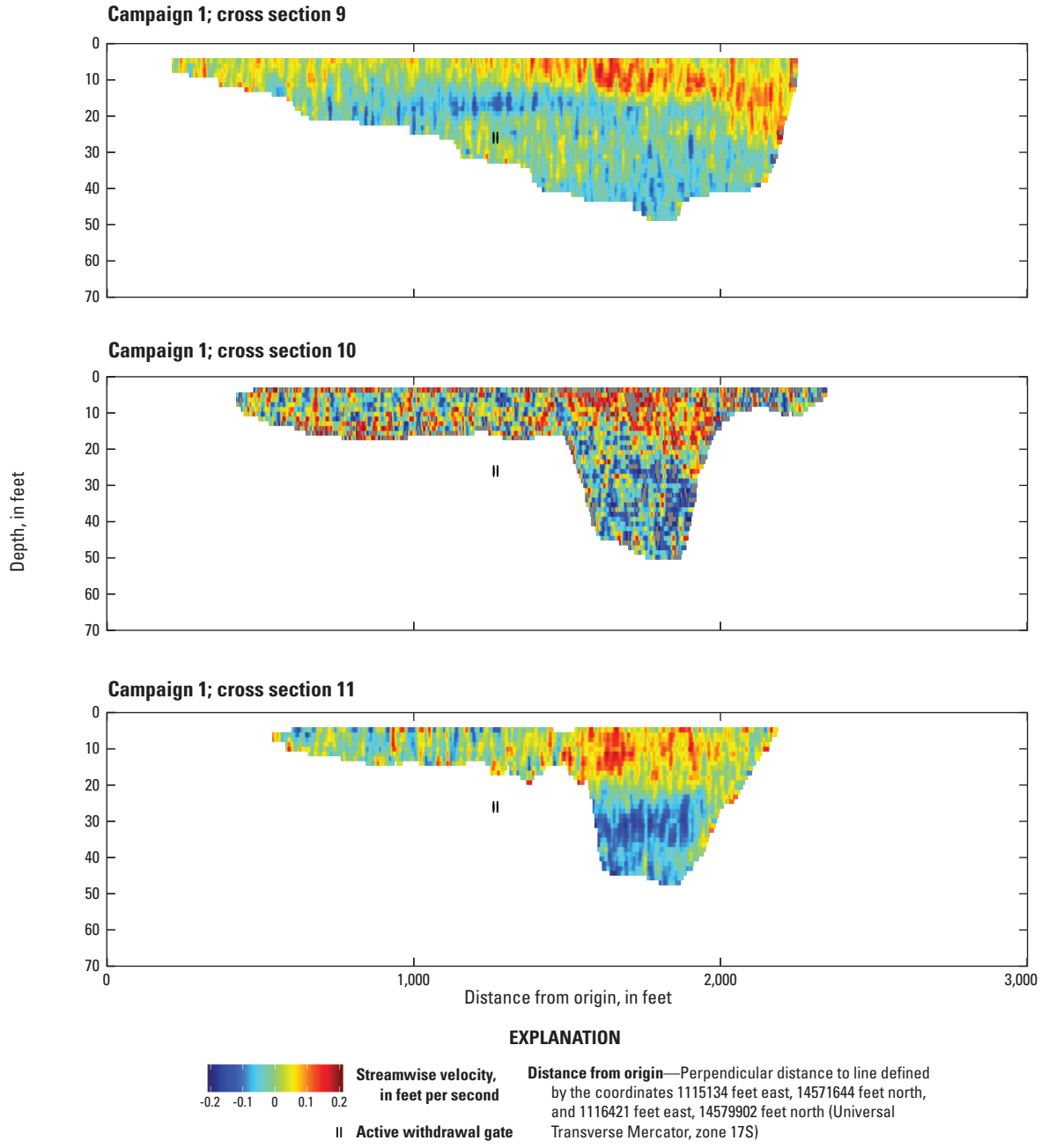
Campaign 1; cross section 9
Campaign 1; cross section 10
Campaign 1; cross section 11
Depth, in feet
0
10
20
30
40
50
60
70
0
1,000
2,000
3,000
Distance from origin, in feet
EXPLANATION
-0.2 -0.1 0 0.1 0.2
Streamwise velocity, in feet per second
Active withdrawal gate
Distance from origin—Perpendicular distance to line defined by the coordinates 1115134 feet east, 14571644 feet north, and 1116421 feet east, 14579902 feet north (Universal Transverse Mercator, zone 17S)

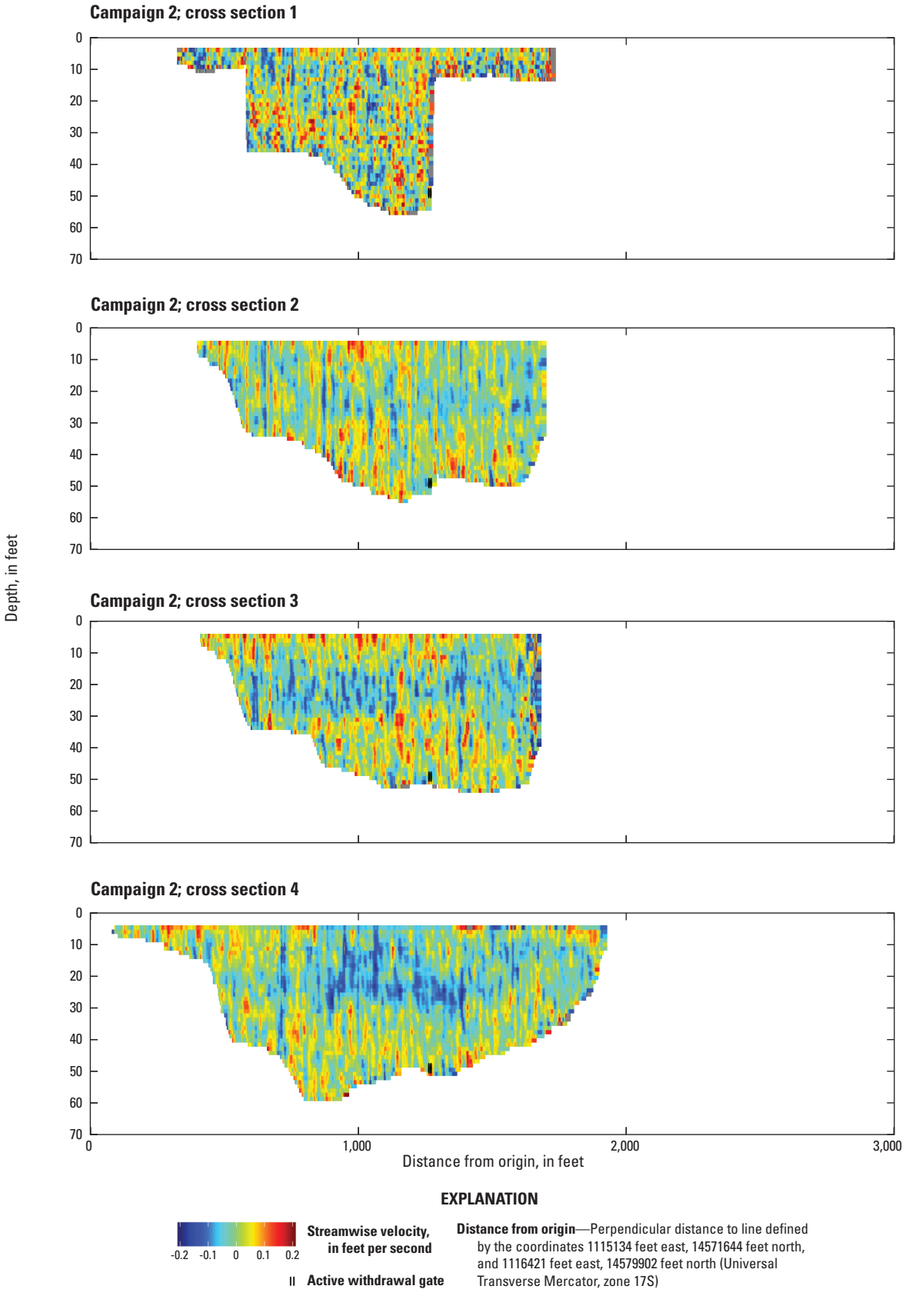
Campaign 2; cross section 1
Campaign 2; cross section 2
Campaign 2; cross section 3
Campaign 2; cross section 4
0
10
20
30
40
50
60
70
Depth, in feet
0
1,000
2,000
3,000
Distance from origin, in feet
EXPLANATION
-0.2 -0.1 0 0.1 0.2
Streamwise velocity, in feet per second
Active withdrawal gate
Distance from origin—Perpendicular distance to line defined by the coordinates 1115134 feet east, 14571644 feet north, and 1116421 feet east, 14579902 feet north (Universal Transverse Mercator, zone 17S)

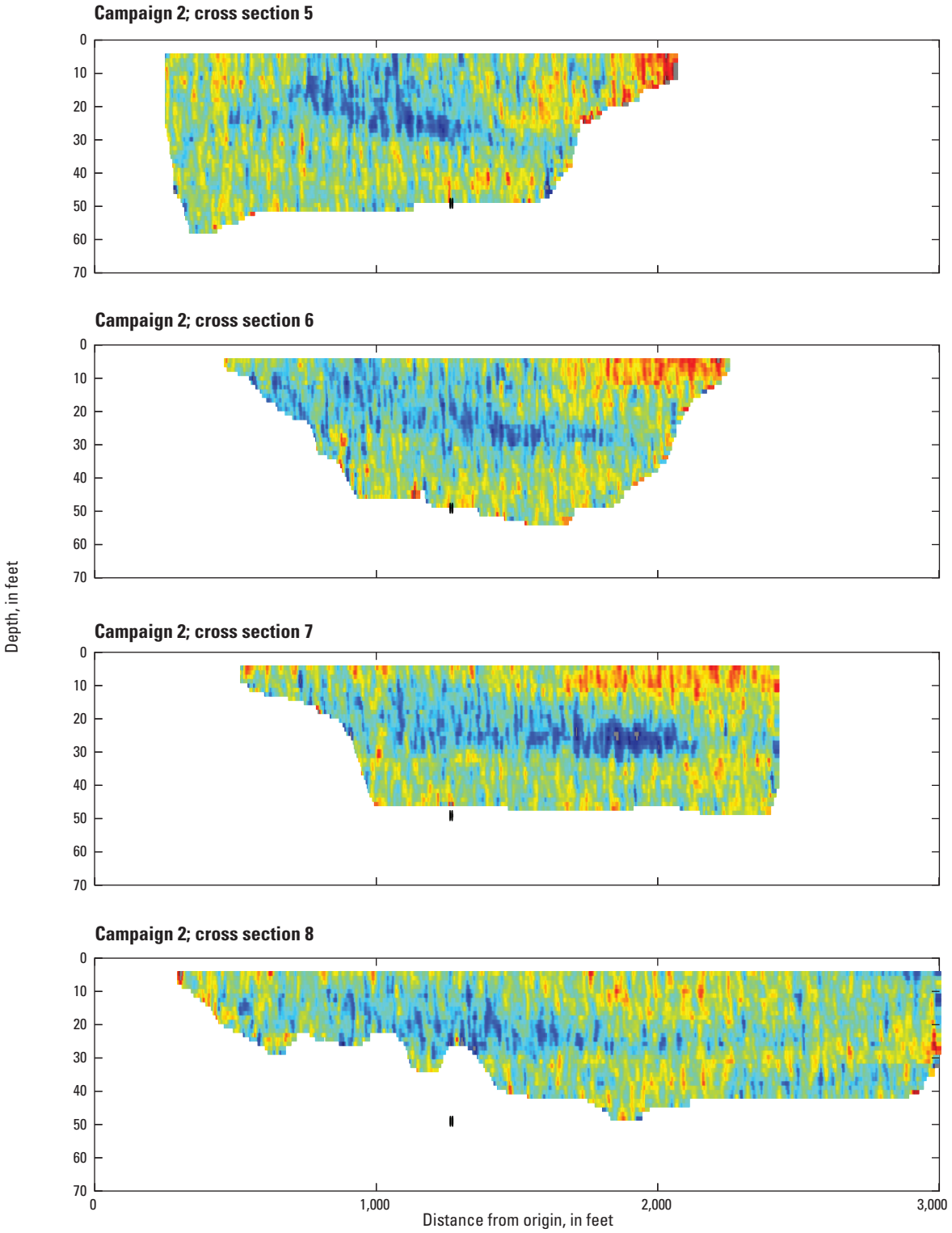
Campaign 2; cross section 5
Campaign 2; cross section 6
Campaign 2; cross section 7
Campaign 2; cross section 8
Depth, in feet
0
10
20
30
40
50
60
70
0
1,000
2,000
3,000
Distance from origin, in feet
EXPLANATION
-0.2 -0.1 0 0.1 0.2
Streamwise velocity, in feet per second
Active withdrawal gate
Distance from origin—Perpendicular distance to line defined by the coordinates 1115134 feet east, 14571644 feet north, and 1116421 feet east, 14579902 feet north (Universal Transverse Mercator, zone 17S)

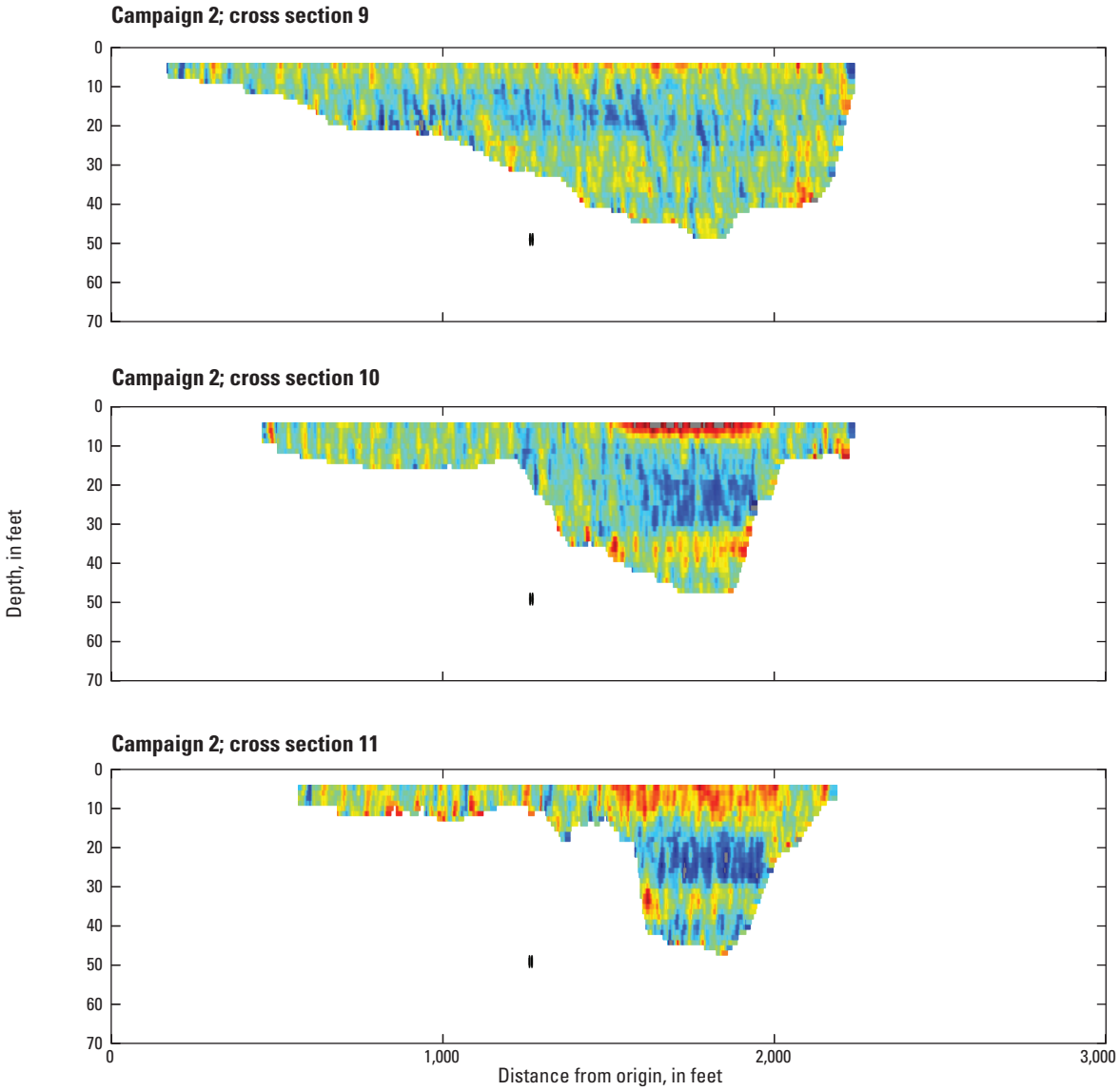
Campaign 2; cross section 9
Campaign 2; cross section 10
Campaign 2; cross section 11
Depth, in feet
0
10
20
30
40
50
60
70
0
1,000
2,000
3,000
Distance from origin, in feet
EXPLANATION
-0.2 -0.1 0 0.1 0.2
Streamwise velocity, in feet per second
Active withdrawal gate
Distance from origin—Perpendicular distance to line defined by the coordinates 1115134 feet east, 14571644 feet north, and 1116421 feet east, 14579902 feet north (Universal Transverse Mercator, zone 17S)

Publishing support provided by:
Madison and Rolla Publishing Service Center

For additional information concerning this publication, contact:
Director, USGS Ohio Water Science Center
6460 Busch Blvd. STE 100
Columbus, OH 43229-1737
(614) 430–7700

Or visit the Ohio Water Science Center website at:
https://oh.water.usgs.gov

USGS

Vonins and Jackson—**Response of Currents and Water Quality to Changes in Dam Operations in Hoover Reservoir, Columbus, Ohio**—SIR 2017–5027

ISSN 2328-0328 (online)
https://doi.org/10.3133/sir20175027